DESTRESS

Demonstration of soft stimulation treatments of geothermal reservoirs

# Deliverable 6.5: Optimization of the business case, based on optimized reservoir management and operation

## WP 6: Intelligent Tools Controlling Performance and Environment

| | |
|---|---|
| **Lead Beneficiary** | 6 – TUD |
| **Type** | ☑ R - report, document etc. ☑ OTHER - software, technical diagram etc.<br>☐ DEM - demonstrator, pilot etc. ☐ E - ethics<br>☐ DEC - website, patent filing etc. |
| **Status** | ☑ Draft<br>☑ WP manager accepted<br>☑ Project coordinator accepted |
| **Dissemination level** | ☑ PU - Public<br>☐ CO - Confidential: only for members of the consortium |
| **Contributors** | ☐ 1-GFZ ☐ 5-GES ☐ 9-GTL ☐ 13-SNU ☐ 17-UU<br>☐ 2-ENB ☑ 6-TNO ☐ 10-UoS ☐ 14-KIC<br>☐ 3-ESG ☐ 7-ETH ☑ 11-TUD ☐ 15-ECW<br>☐ 4-UoG ☐ 8-GTN ☐ 12-NEX ☐ 16-WES |
| **Creation date** | 26.02.2020 |
| **Last change** | 26.02.2020 |
| **Version** | 01 |
| **Due date** | 29.02.2020 |
| **Submission date** | 28.02.2020 |

This project has received funding from the European Union's Horizon 2020 research and innovation programme under grant agreement No 691728

# Optimization of the business case, based on optimized reservoir management and operation

## Authors

Sanaz Saeid (TUDelft)

Christian Bos (TNO)

Nima Gholizadeh Doonechaly (TUDelft)

## Publication Date

28.02.2020

## Abstract

Task 6.5 of the DESTRESS project aims at developing workflows for optimization of the business case, based on closed loop reservoir management. The specific approaches developed in previous WPs provide the basis to develop optimized strategies and field development concepts for improved geothermal energy recovery in enhanced geothermal systems and thus improved technical and economic performance.

Both the underlying (simplified) reservoir models and the optimization tool target decision makers to plan their reservoir operational strategies proactively while aiming at optimized business case. The developing workflow in this task is generic and should, in principle, be able to be applied on any enhanced geothermal systems. Therefore the choice of application site is insignificant. In this task, we are taking the Westland (Triassic) geothermal field as a basis for these studies due to availability of field data and models.

In this task two main models has developed:

1. A Thermo-Hydro-Mechanical (THM) reservoir model
2. Economic model

The THM model allows us to look into fault reactivation/slip at different reservoir realizations and taking into account various well placement scenarios (relative to faults). Besides, sensitivity analysis will provide good insight on fault slips under various physical parameters and operational options.

The economic model imports the time-series of the THM model for each case simulated (rates, pressures, temperatures, SCU value per fault) and converts that into economic time-series and Key Performance Indicators (KPI). This is done under a range of assumptions related to planning, surface equipment, revenue and costs. It also defines an acceptance norm for the areal % of the fault that is allowed to have a SCU-value above 1. The economic life of the case is constrained by economics: subject to a user-defined minimum number of injection/production years, the geothermal doublet is closed-in as soon as a maximum number of user-defined consecutive years with a negative Net Cash Flow has been reached. The economic model allows economic uncertainties to be modelled using the Monte Carlo sampling process (tariffs, capex, opex, subsidies, etc.), resulting in output distributions for the various KPIs. To compare the different cases simulated, an objective function can be formulated. In this study, the mean of the NPV output distribution is chosen, conditional on some user-defined slip tendency/ fault reactivation risk acceptance norm. The comparison of the objective function of all cases identified which cases are likely to be economic and meet the fault reactivation risk acceptance norm.

# Table of Content

# 1. Introduction

Decision making is an important part of the execution of any project, including enhanced geothermal systems. To make it right it is important to define a reliable representative business case which includes both surface and subsurface uncertainties.

In this project, Work Package 6 (WP6) is responsible for "Intelligent tools controlling performance and environment". As part of WP6, TUD and TNO have collaborated during 2019-2020 on developing a method and tool to optimize operational activities of a geothermal doublet, with the objective to maximize the discounted heat sales value from a geothermal doublet, given the reservoir properties and given constraints such as the risk of induced seismicity caused by fault reactivation.

In this task two main models has developed:

1. A Thermo-Hydro-Mechanical (THM) reservoir model
2. Economic model

Trias Westland geothermal project in the Netherlands has been chosen as the application field study. The Trias Westland geothermal project is a partnership between Flora Holland, HVC, Westland Infra and the Municipality of Westland. It is the first geothermal project in the Netherlands that will drill as deep as the Trias layer, situated at a depth of 4 kilometers (http://www.triaswestland.nl/, sd). In February 2018 after drilling and coring to Trias layer at a depth of 4 km, it has concluded that this location turned out not to be suitable for cost-effective heat extraction. The core showed very low permeability. The layer above - the Delft sandstone – has better permeability and turn out to be economically more attractive.

In this task several realization of the reservoir permeability within Westland fault architecture system will be presented. For each realization the possibility of fault reactivation under different operational conditions will be studied. The cases with lower chance of reactivation of faults will be selected for economic analysis.

The economic analysis is aimed at better understanding of how the risk of fault reactivation can be managed by operational variables (such as the location of wells with respect to the faults, and the injection and production rate), and how this operational management impacts on the economics of the doublet. For the various reservoir descriptions (notably the value of the reservoir permeability) there is a trade-off between on the one hand injection rate (and therefore production rate), and on the other hand the risk of fault reactivation. For a better economic performance, higher rates are obviously desired, but they tend to coincide with a higher risk of fault reactivation. The comparison of the projected economic performance of alternative reservoir management plans can then be done depending on the acceptance norm assumed for the risk of fault reactivation. In this sense, the economics are optimized under the constraint of some tolerance norm for the risk of fault reactivation.

# 2. Thermo-Hydro-Mechanical reservoir model

## 2.1 Model description

A 3D thermo-hydro-mechanical model is built using COMSOL Multiphysics solver based on which, the mass, momentum and energy conservation equations are solved numerically for porous media (both rock matrix and faults). Mechanical effects are investigated using linear elasticity. Flow in both the rock matrix as well as the faults are formulated based on Darcy’s law.

The model consists of a rectangular block with the side length of 2.5km representing the reservoir as well as two confining layers on the top and bottom of the reservoir layer (Figure 1). The top layer of the reservoir is available from data whereas there is no clear/sharp boundary as the bottom layer. Therefore reservoir layer thickness is set as 180m and the thickness of the confining layers varies over the extend of the reservoir with minimum thickness of 100m. The spatial coordinates of the block corner points are set in such a way that the block orientation is consistent with the direction of the in-situ principal stresses extracted from offset well data.

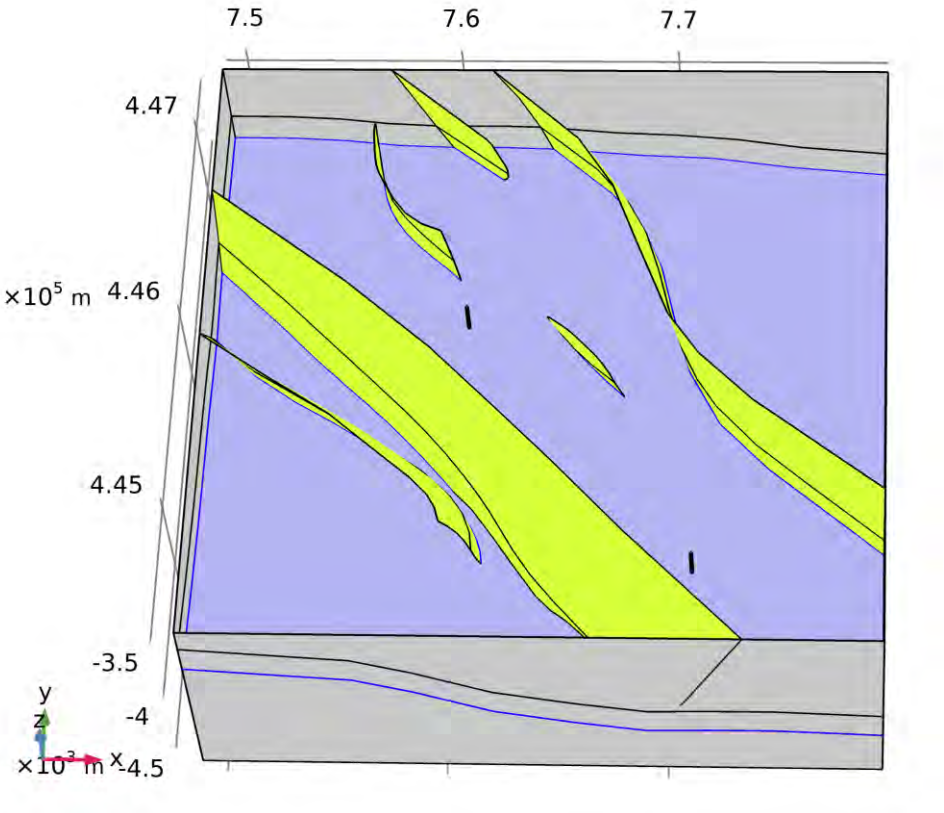


Figure 1. model geometry in comsol for Westland Trias geothermal field

The present faults in the reservoir domain are first converted to CAD surfaces and then discretely implemented in the model with zero thickness in order to improve the computational efficiency. Therefore, the faults are considered as 2D objects in the model whereas the fault thickness is taken into account in the mathematical formulation. The vertical extend of the faults are set to be equal to the extent of the confining layers on the top and bottom of the reservoir layer. The fault thickness is assumed to be 20m and fault permeability is set to 50 mD. Six normal faults exist in Westland Trias field which named from F1 to F6 (Figure 2).

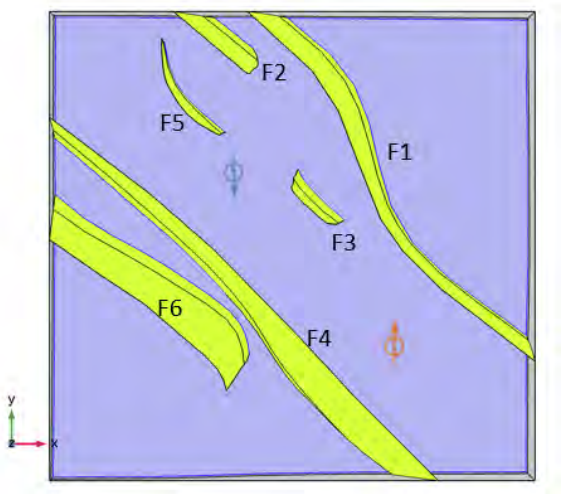


Figure 2. Westland fault system and wells location. Injection and production wells are indicated by blue and red arrows.

The stress boundary condition is first initialized to the principal stress values extracted from available data as follows: vertical stress of 90.23MPa, minimum horizontal stress of 57.2MPa and maximum horizontal stress of 72.8MPa. The injection and production wells are also implemented in the model explicitly. Initially injection well planned 230m from F5, 430m from F3, and 480m from F4. Production well placed in almost equal distance of 550m from F1 and F4 (Figure 2). A heat flux of 0.065W/m$^2$ is applied at the bottom of the model. A skin factor of -4 is also assumed for the injection well to demonstrate stimulation.

In order to improve the computational efficiency, the balance equations are solved with direct solver using segregated approach. The reservoir parameters are set according to the extracted data from publicly available sources from offset wells, from the literature or made assumptions[1].

## 2.2 Governing equations

Modelling deep geothermal systems involves solving nonlinear conductive-convective heat flow occurring in a complicated and disproportionate geometry. To model this geothermal reservoir in the most computational efficient way, the reservoir model is decomposed in 3 parts; a 3D THM model in porous media, a 2D heat and fluid flow model in fault and a 1D heat and fluid flow model inside wellbores. The 1D model has not been coupled directly to reservoir for the sake of computational time.

The fault can be considered as a 2D object in modelling since its thickness, comparing to the fault surface is very small and negligible. The main fluid flows alongside the fault surface, therefore a fault can be considered simply as a 2D object inside the model. In the other hand a wellbore is a highly slender cylinder consisting of an inner pipe carrying the fluid, surrounded by a cemented grout and soil mass. Such geometry exhibits a unique and challenging numerical problem. If a standard 3D finite element (finite volume or finite difference) formulation is utilized to model heat flow in the wellbore and the surrounding soil mass, meshes with an enormous number of finite elements will be needed, resulting in unrealistic computational time (Saeid et al., 2015). To decrease the computational demands a pseudo-3D model is considered for wellbore modelling. This model is capable of simulating heat flow in a multicomponent domain using a 1D line element (Al-Khoury, 2011; Saeid et al., 2013).

[1] THE MEASURED DATA FROM THE RECENTLY DRILLED WELL INTO THE TARGET FORMATION HAS JUST BEEN RECEIVED FROM THE COMPANY AND THE CHARACTERIZATION OF THE DATA AS WELL AS THE ADJUSTMENTS OF THE NUMERICAL MODEL'S PARAMETERS ARE CURRENTLY UNDERGOING.

### 2.2.1. Heat and fluid flow in the reservoir

Heat and fluid flow in a this reservoir can be explained by Energy Balance and Darcy equations as:

$$\rho C \frac{\partial T}{\partial t} + \rho_f C_f \mathbf{q} \nabla T - \nabla(\lambda \nabla T) = 0 \quad (1)$$

where T (K) is the temperature, ρ is the mass density (kg/m3), c (J/kg.K) is the specific heat capacity, λ (W/m.K) is the thermal conductivity, and **q** (m/s) is the Darcy velocity. The suffix *f* refers to the pore fluid and *s* to the solid matrix. The thermal conductivity and the volumetric heat capacity are described in terms of a local volume average, as

$$\lambda = (1-\varphi)\lambda_s 1 + \varphi\lambda_f \quad (2)$$

$$\rho C = (1-\varphi)\,\rho_s C_s + \varphi \rho_f C_f \quad (3)$$

The fluid flow in the reservoir can be expressed as

$$\varphi \frac{\partial \rho_f}{\partial t} + \nabla.\left(\rho_f\, \mathbf{q}\right) = 0 \quad (4)$$

Where q (m/s) defines by Darcy's law as:

$$\mathbf{q} = -\frac{k}{\mu}\left(\nabla P - \rho_f \mathbf{g} \nabla z\right) \quad (5)$$

in which k is the intrinsic permeability ($m^2$) of the porous medium, μ (Pa.s) is the fluid dynamic viscosity, **g** ($m/s^2$) is the gravity vector, and $P$ is the hydraulic pressure (Pa).

The geothermal fluid density and viscosity variation with temperature are based on the exponential functions for the geothermal fluid in the Soultz-sous-Forêts EGS, as described in the following functions according to (Magnenet Vincent and Fond, 2014):

$$\boldsymbol{\rho_T} = 1070 \times exp(-3\{1.3224 \times 10^{-4}(T-293.15) + 43315 \times 10^{-7}(T-293.15)^2 + 2.49962 \times 10^{-10}(T-293.15)^3\}) \quad (6)$$

$$\boldsymbol{\mu_T} = 1.934 \times 10^{-4} + 61.7 \times 10^{-6} \times exp\{-0.02395 \times (T-406.4)\} \quad (7)$$

where $\rho_T$ and $\mu_T$ are the density and viscosity at temperature $T$ respectively. All other fluid properties are assumed to be constant with the specific heat capacity, thermal conductivity, density (at surface) and compressibility set at 3800 (J/(kg.K)), 0.69 (W/(m.K)), 1070 ($kg/m^3$) and $4.5\times10^{-10}$(1/Pa) respectively.

### 2.2.2. Heat and fluid flow in the fault

In this paper, fault is considered as a 2D object since the fluid flow mainly passes through fault surface, while the dimension and amount of flow passing through the normal axis to the fault surface is small and negligible. Fluid flow in the fault is described as:

$$V_F = -\frac{k_F}{\mu}\nabla P_F \quad (8)$$

$$d_F \frac{\partial(\varepsilon\rho)}{\partial t} + \nabla.(d_F \rho V_F) = d_F Q_m \quad (9)$$

In which $V_F$ (m/s) is fluid velocity inside the fault. ε is the Fault porosity, $k_F$ is fault permeability, and $d_F$ (m) is fault thickness. $Q_m$ is the source or sink term.

### 2.2.3. Heat and fluid flow in the wellbore

In order to have a computationally efficient model, the wellbores and their surrounding material (cement) are considered as 1D objects so that a significant reduction in the number of mesh elements and consequently on computational time occurs.

The mass flow inside the wellbore can simply be considered as a 1D flow, since no flow is occurring perpendicular to wellbore axis. The flow pattern can also be considered as homogeneous along the pipe because of the slenderness of the wellbore compared to its length. The mass flow inside the wellbore and the incompressible fluid can be described using the conservation of mass equation:

$$\frac{\partial A\rho_f}{\partial t} + \frac{\partial}{\partial z}(A\rho_f u) = 0 \tag{10}$$

where $A = \pi d_i^2/4$ (m²) is the cross sectional area of the pipe, $d_i$ (m) is the inner pipe diameter, $\rho_f$ (kg/m³) is the density, and $u$ (m/s) is the fluid velocity.

The pressure drop along the wellbore ($\Delta P^w$) can be described as (Livescu et al., 2010) :

$$\Delta P^w = \Delta P_h^w + \Delta P_a^w + \Delta P_f^w \tag{11}$$

in which, $\Delta P_h^w$ is the hydrostatic pressure loss, $\Delta P_a^w$ is the pressure loss due to acceleration, and $\Delta P_f^w$ is the pressure loss due to frictional effects. The pressure loss due to acceleration in a typical reservoir simulation problem is smaller than the heat loss due to gravitation and friction (Livescu et al., 2010). These terms are defined as (Livescu et al., 2010):

$$\Delta P_h^w = -\rho g\, h\, sin\,\theta \tag{12}$$

$$\Delta P_a^w = -\rho_f \frac{\partial u}{\partial t} - \rho_f \frac{\partial^2 u}{\partial z^2} \tag{13}$$

$$\Delta P_f^w = -\frac{1}{2} f_D \frac{\rho_f}{d} |u|\, u \tag{14}$$

where $P$ (N/m²) stands for pressure, superscript $w$ stands for well, $g$ (m/s²) is the gravitational acceleration, $\theta$ is the wellbore inclination angle from the ground surface, and $f_D$ is the Darcy friction factor.

The Darcy friction factor, $f_D$, is a dimensionless quantity used for the description of friction losses in pipe flow as well as open channel flow. It is a function of the Reynolds number and the surface roughness divided by the hydraulic pipe diameter. Churchill's relation (Churchill, 1977), which is valid for the entire range of laminar flow, turbulent flow, and the transient region in between (Lin et al., 1991), has been used to describe friction in pipes:

$$f_D = 8\left[\left(\frac{8}{\mathrm{Re}}\right)^{12} + (c_A + c_B)^{-1.5}\right]^{1/12} \tag{15}$$

in which $C_A$ and $C_B$ are defined as

$$C_A = \left[ -2.457 \ln\left( \left( \frac{7}{\mathrm{Re}} \right)^{0.9} + 0.27 \left( \frac{e}{d} \right) \right) \right]^{16}$$
$$C_B = \left( \frac{37530}{\mathrm{Re}} \right)^{16} \quad (16)$$

*e* (m) is the tubing surface roughness, *d* (m) is the tubing diameter, and Re is the Reynolds number. Eq (15) shows that the Darcy friction factor is also a function of the fluid properties, through the Reynolds number, defined as:

$$\mathrm{Re} = \frac{\rho u d}{\mu} \quad (17)$$

For a low Reynolds number (laminar flow, Re < 2000), the friction factor is independent from surface roughness and given by 64/Re (Brill and Mukherjee, 1999). In this paper the Haaland equation (Haaland, 1983), which is commonly used for oil wells is used. This formula considers both small and large relative roughness of wells for a wide range of Reynolds numbers (4000 <Re< 1.1e8) (COMSOL Multiphysics, 2017):

$$\sqrt{\frac{1}{f_D}} = -1.8\, log_{10}\left( \left( \frac{e/d}{3.7} \right)^{1.11} + \left( \frac{6.9}{Re} \right) \right) \quad (18)$$

Heat flow in a wellbore is conductive-convective and arises from the flow of a working fluid running through an inner pipe (tubing), and the thermal interaction between the wellbore components and the surrounding soil mass, plus heat created by friction. It can be all formulated on a 1D heat flow model. In this model, preservation in the equation is made of the involved physical and thermal properties of the pipe components, such as: the cross sectional areas; the thermal conductivities of the surrounding soil mass and the inner pipe materials; and the fluid thermal properties and flow rate. The 1D representation, implies that the variation of the temperature is along its axis, and that no temperature variation exists in its radial direction. The latter condition is reasonably valid because of the slenderness of the wellbore, where the radial variation of temperature is negligible. Nevertheless, heat fluxes normal to the contact surfaces along the vertical axis are fully considered, and included explicitly in the mathematical model (Saeid et al., 2013). Hence, the heat transfer inside the wellbore can be defined as:

$$\rho_f A c_{pf} \frac{\partial T_i}{\partial t} + \rho_f A c_{pf} ue.\nabla T_i = \nabla.(A\lambda_f \nabla T_i) + Q_{friction} + Q_{wall} \quad (19)$$

in which $T_i$ describes the temperature in the working fluid, $Q_{friction}$ (W/m) is the heat created by the friction inside the well and $Q_{wall}$ (W/m) describes the heat loss/gain to the surroundings. They are described as

$$Q_{friction} = \frac{1}{2} f_D \frac{\rho A}{d_h} |u| u^2 \quad (20)$$

$$Q_{wall} = (b_{fs}) z (T_s - T_f) \quad (21)$$

$$Z = \pi d \quad (22)$$

where the subscript *f* represents the geothermal fluid and subscript s represent surrounding soil mass, $b_{fs}$ (W/m$^2$K) is the reciprocal of the thermal resistance between the fluid and the soil (Saeid et al., 2013). *Z* (m) is the contact surface area (perimeter) between the injection well pipe and the surrounding soil formation. Other parameters are similar to those described earlier.

### 2.2.4. Mechanical model

In the solid mechanics model, the physical descriptions are based on the laws for the balance of forces and the constitutive relations that relate the stresses to strains. The stress field acts as a load on the fracture aperture. The deformed aperture of the fracture follows the linear elasticity behaviour of a spring as explained in the Hooke's law as

$$f_s = -\gamma(u - u_0) \quad (23)$$

where fs is a force/unit area, u is the displacement deforming the spring, and ϒ is the stiffness matrix. u is an optional offset, which describes the stress-free state of the spring (Lepillier et al., 2019). The stiffness is a function of the fracture material properties and the fracture width (aperture) df. The stiffness in the normal direction is computed based on a state of plane strain as

$$\Upsilon_n = \frac{E\,(1-\nu)}{d_f(1+\nu)(1-\nu)} \quad (24)$$

where $\Upsilon_n$ is the normal stiffness, E is the Young's modulus and v is the Poisson's ratio.

## 2.3 Fault stability

Injection and production in geothermal fields change reservoir pressure and temperature and consequently stress regime. It is known that microseismisity in geothermal fields results from stress regime disturbance which caused by hydrothermal activities. During such processes overpressure causes a reduction of effective stresses along pre-existing faults and fractures that may reactivate them (Jeanne et al., 2014).

In this work Mohr–Coulomb criterion has used to describe maximum compressive stresses at failure. To indicate fault slip, Shear Capacity Utilization (SCU) parameter is used (Wassing et al., 2017). SCU is a measure of the proximity to failure and is defined as

$$SCU = \frac{\tau}{\tau_{max}} \quad (25)$$

where τ is the shear stress on the fault and $\tau_{max}$ is the maximum shear stress that a fault can bear before it fails. And defined by:

$$\tau_{max} = C + \sigma_n f \quad (26)$$

Where C is fault cohesion and f is friction coefficient and $б_n$ is the effective normal stress on fault. To consider the extreme case fault cohesion is assumed to be zero. Friction coefficient of 0.6 is assumed here which is a typical value for faults in sandstones (Wassing et al., 2017).

The utilized mechanical model in this task does not include stress release due to rupture, hence does not include seismic event nucleation. Instead in this model we have stress build up in time, which in reality represent the worst case.

Zobak and Gorelick showed that there is a relationship between the fault size and the seismic magnitude that can happen based on fault slip. Their findings show that the seismic magnitude for

small faults (<~300m) in small and negligible (Zoback and Gorelick, 2012). Therefore, we can conclude that the change of stress on fault 5 and 3 (F5 and F3) due to operational activities is not of importance. Conversely analysis of the stress field over fault 4 in very important.

To analyses the effect of operation activities on fault stabilities, in this project, we look to areal SCU%. Which shows the areal percentage of the fault which pass the criterion of SCU>1. SCU itself cannot indicate if the faults will slip or not. The integral of the areas with SCU>1 over the fault surface plays important role in the indication of fault slip.

Since areal coverage of SCU>1 is rather qualitative parameter, hence in this study we kept it as a KPI in economic model (details in section 3)

## 2.4 Sensitivity analysis on various reservoir realizations

In this task several realization of the reservoir permeability within Westland fault architecture system will be presented. For each realization the possibility of fault reactivation under different operational conditions will be studied. The cases with lower chance of reactivation of faults will be selected for economic analysis.

The temperature logs in the drilled well in Trias Westland show that reservoir has higher thermal gradient (0.0375 to 0.04 oC/m) comparing to average thermal gradient of the Netherlands (0.0313 oC/m) subsurface. This may resulted due to high permeability of faults in this region that facilitated the flow of hot fluid from deeper depths to this layer.

This induce the idea of drilling on the fault or closer to faults might be helpful in terms of having the better flow and controlling of pressure, knowing reservoir permeability is very low in Trias Westland.

Various realization were generated by combining a set of well locations and reservoir permeabilities. 5 permeabilities have been considered for this study: 0.05mD, 0.5mD, 5mD, 50mD, and 500mD. 4 well locations were considered in this project as shown in Figure 3. In the middle of faults, near fault 4, on fault 4, and Tuned middle. The “Tuned Middle” is the case where both injection and production wells tried to be placed exactly in the middle of faults. In total 20 realization as a combination of 5 reservoir permeabilities and 4 well locations has generated.

Within each realization several sensitivity analysis on injection production flow rate, well distance, injection temperature, Kv/Kh ratio, and skin factor has been carried out. The results show that injection-production flow rate and well placement relative to faults, in combination with reservoir permeability are the major parameters which effect SCU values and reservoir lifetime.

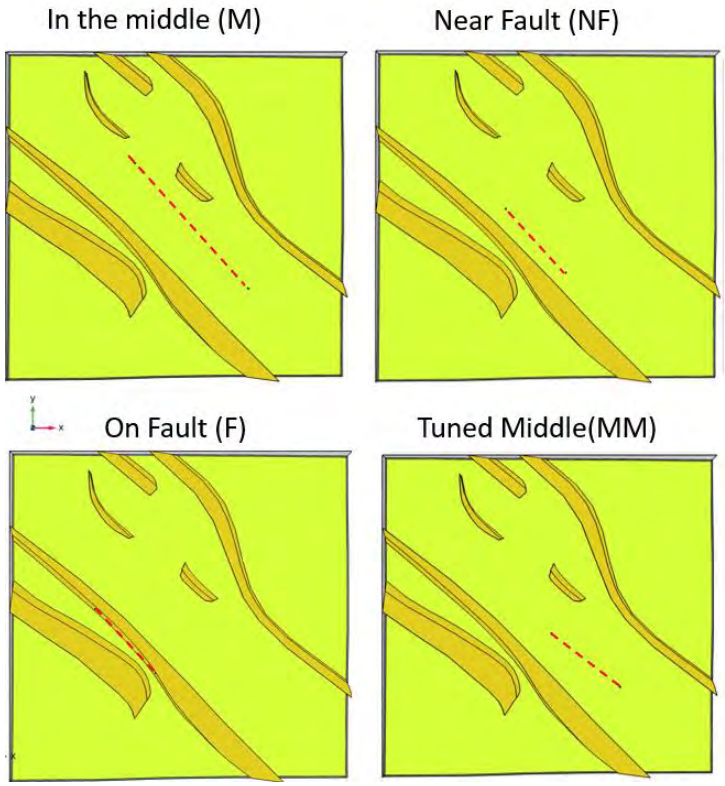


Figure 3. different well location which considered for this study

### 2.4.1. Well placement

When the reservoirs permeability is very low (e.g. 0.05 mD) the case may not be economic due to the high injection and production pressures and hence the high pump power and pump costs. This could be mitigated by changing the well locations and place them closer to fault which in this case has higher permeability (50 mD). However, as the wells place closer to the fault (Figure 4) or crossing the fault, fault tends to slip as SCU pass its limit (1).

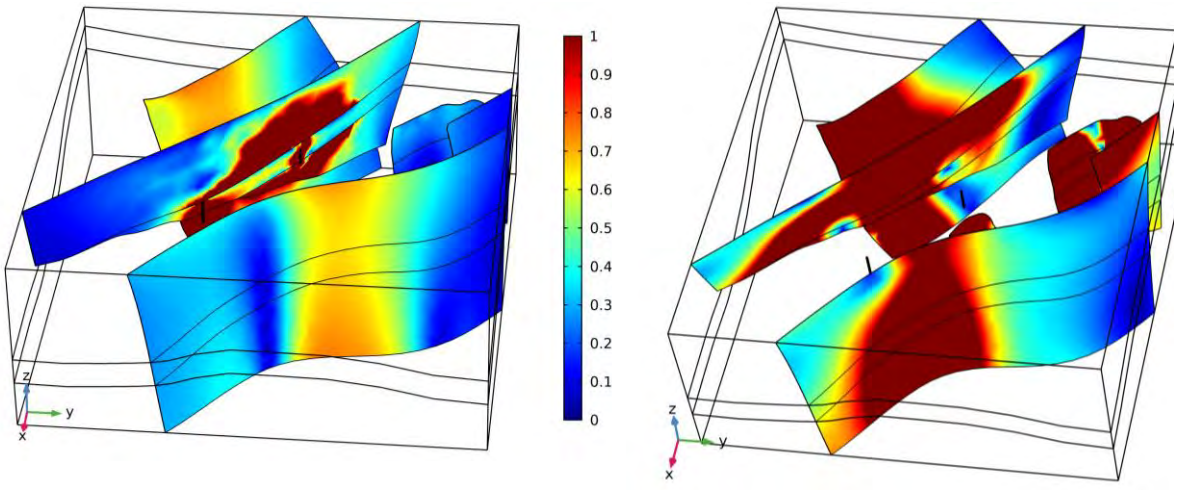


Figure 4. SCU propagation on Faults. Left: wells are crossing fault 4. Right: wells are close by fault 4 (~200m) [Case specifications: well distance=800m, Reservoir permeability=0.05mD, flowrate=50kg/s, injection temperature=50 °C]

For low to high permeability reservoirs (e.g. bigger than 5mD) the combination of well location and flowrate is an important indicator for fault stability and lifetime. Figure 5 shows 4 scenario in which all the physical and operational parameters are the same only well location relative to faults is changing. As it is expected as we get farther from faults the operational effect (change of pressure due to injection and production) of the faults and hence variation of the stress field decreases. Therefore the areal coverage of SCU>1 and hence the chance of fault slip become less.

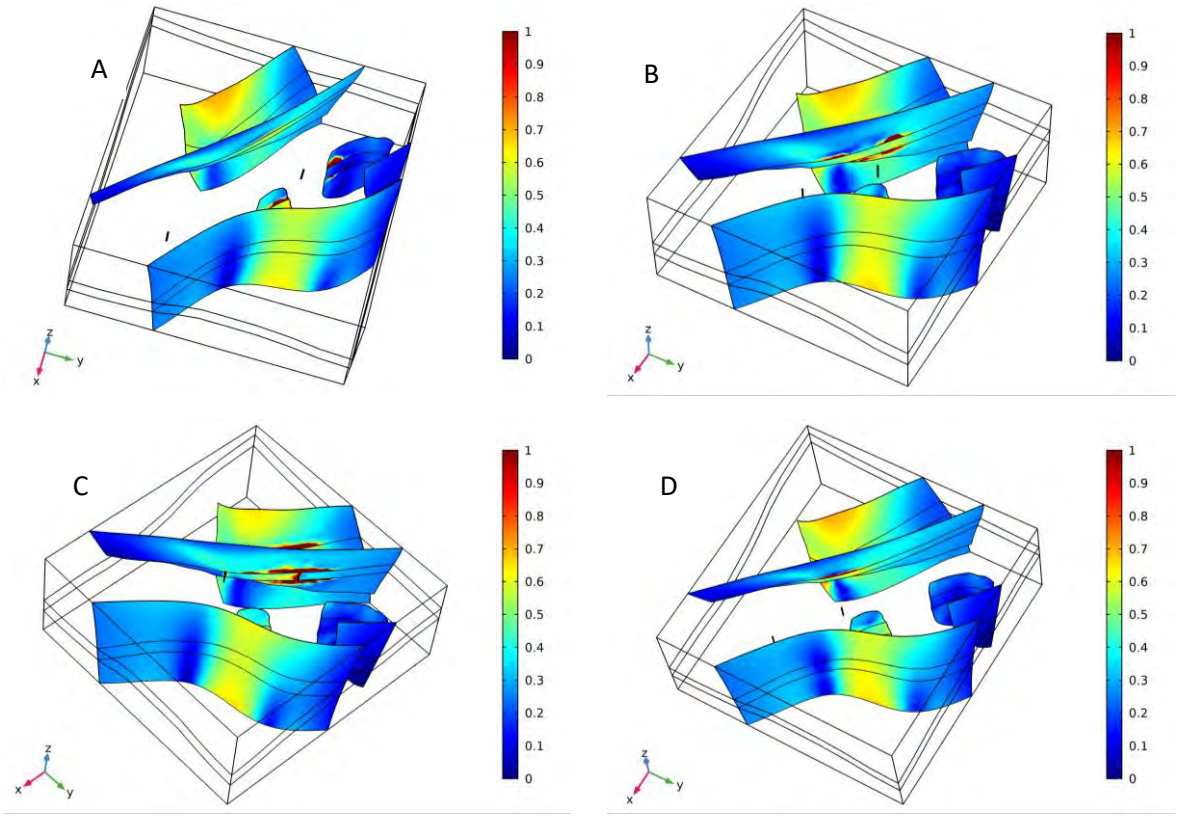


Figure 5. SCU distribution over fault surface for a realisation with Kres=50mD and Q=100 kg/s. Well placement between 4 case. as: A) in the middle (M), B) near fault4 (NF), C) on fault4 (F), D) tuned middle (MM)

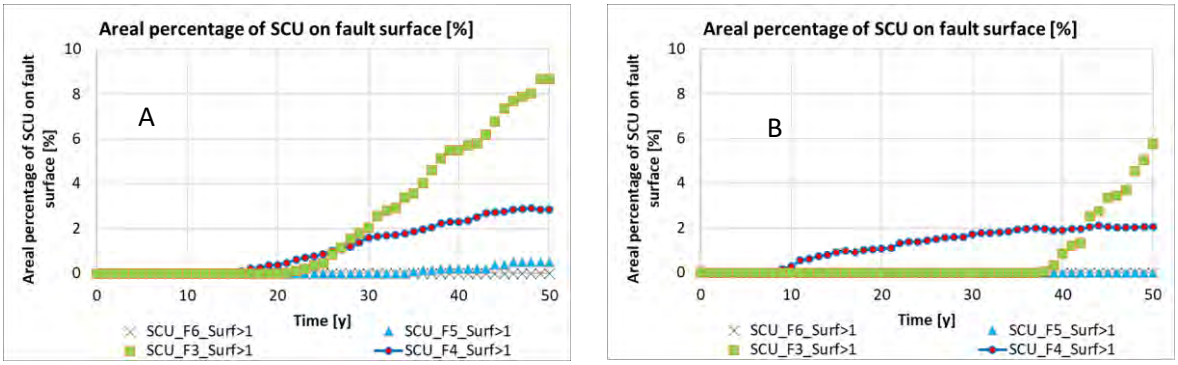

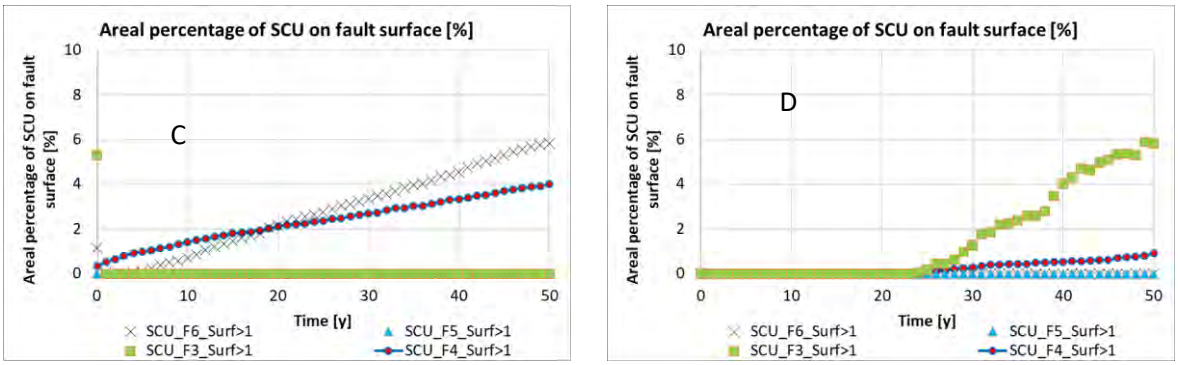


Figure 6. Areal percentage of SCU>1 over different fault surfaces for a realisation with Kres=50mD and Q=100 kg/s. Well placement differs between 4 cases. as: A) in the middle (M), B) near fault4 (NF), C) on fault4 (F), D) tuned middle (MM)

### 2.4.2. Flow rate

Figure 7 demonstrates that for the same reservoir and same well arrangements, as the flow rate increases the SCU and the areal coverage of SCU>1 over the fault surface are also increasing. Figure 8 and Figure 9 are showing the same concept in time. Bottomhole pressure at injection and production wells and breakthrough curves of these cases are demonstrated on Figure 10.

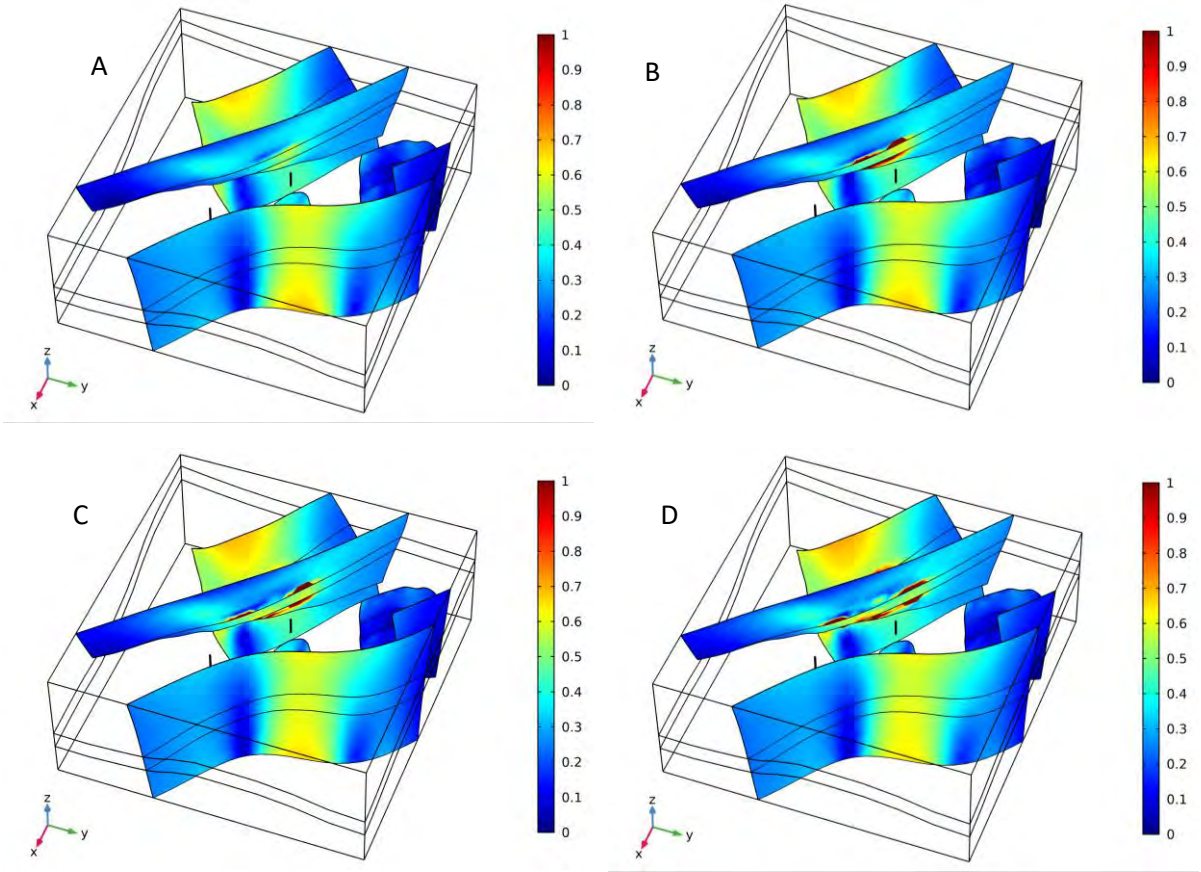


Figure 7. SCU distribution over fault surface for a realisation with Kres=50mD and wells are located close to the fault 4. Injection and production flow rate differs between 4 cases. A) Q=20 kg/s, B) Q=50 kg/s, C) Q=100 kg/s, D) Q=150 kg/s

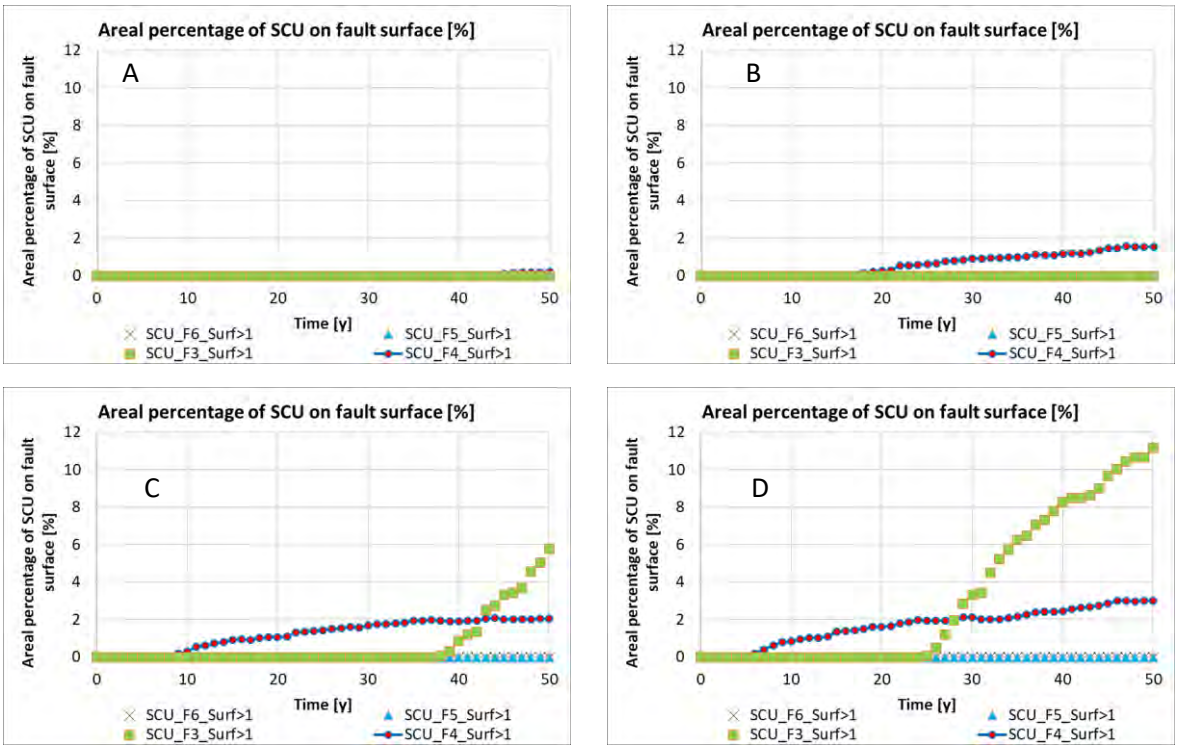


Figure 8. Areal percentage of SCU>1 over different fault surfaces for a realisation with Kres=50mD and wells are located close to the fault 4. Injection and production flow rate differs between 4 cases. A) Q=20 kg/s, B) Q=50 kg/s, C) Q=100 kg/s, D) Q=150 kg/s

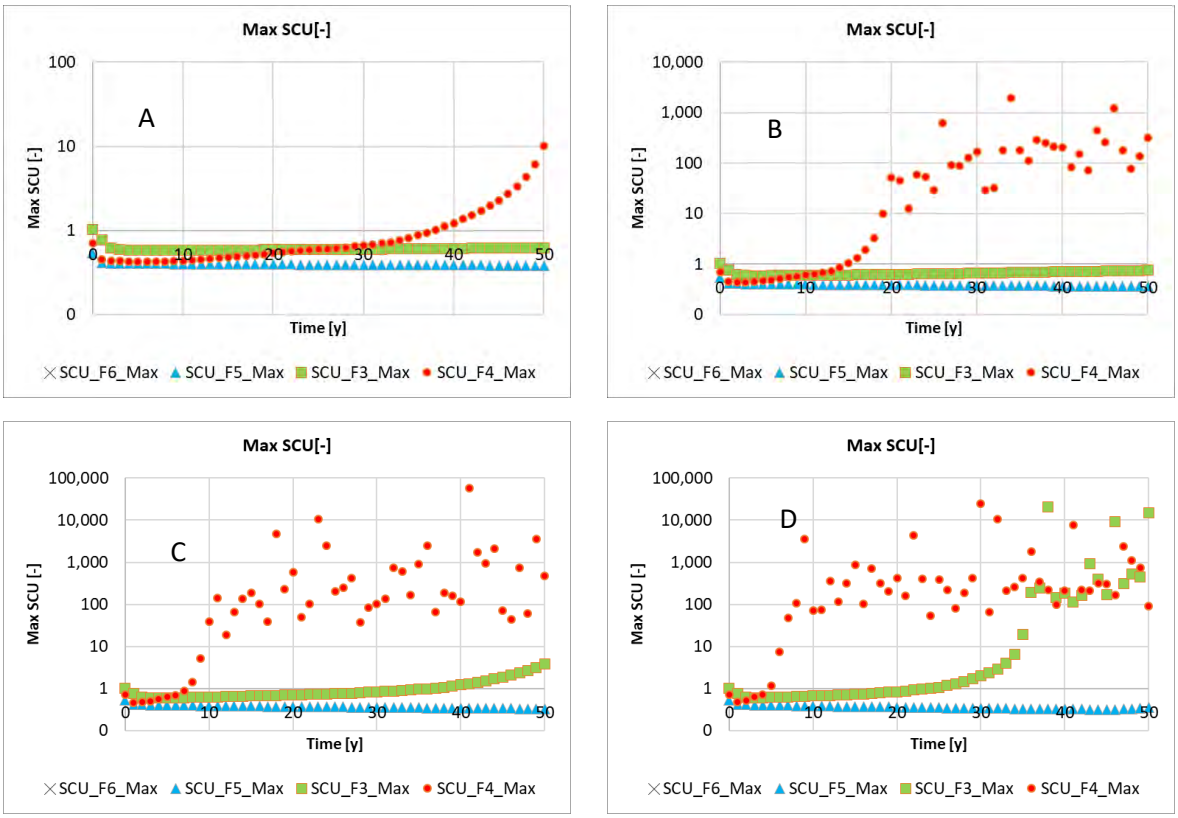


Figure 9. Maximum value of SCU over different fault surfaces for a realisation with Kres=50mD and wells are located close to the fault 4. Injection and production flow rate differs between 4 cases. A) Q=20 kg/s, B) Q=50 kg/s, C) Q=100 kg/s, D) Q=150 kg/s

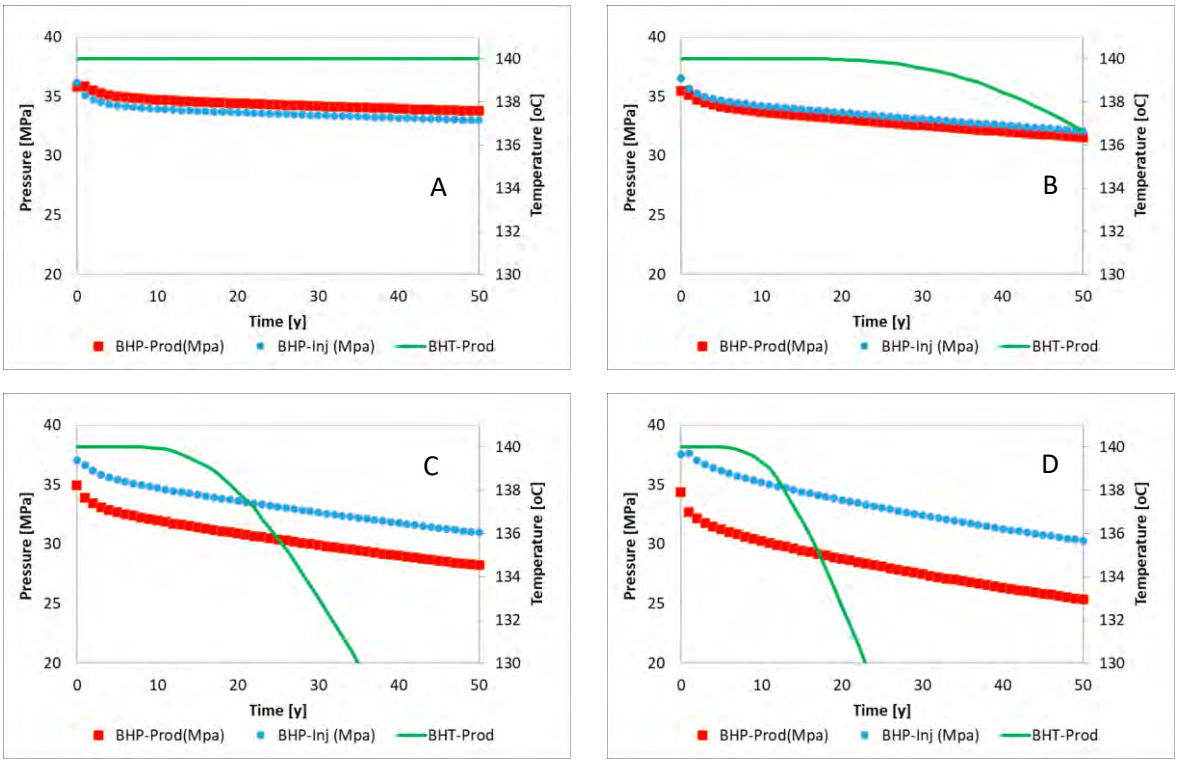


Figure 10. Bottomhole pressure at injection(blue) and production well(red) and breakthrough curve (green) for a realisation with Kres=50mD and wells are located close to the fault 4. Injection and production flow rate differs between 4 cases. A) Q=20 kg/s, B) Q=50 kg/s, C) Q=100 kg/s, D) Q=150 kg/s

### 2.4.3. Reservoir permeability

Figure 11, shows that for the same well distance and well locations, lower reservoir permeability cause higher SCU areal percentage over fault surface. In other words, for low permeability reservoirs the chance of instability in faults is higher than a higher permeability reservoir. In addition this figure demonstrate that higher flowrates always leads to higher SCU areal percentage, due to more disturbance of pressure and hence stress field.

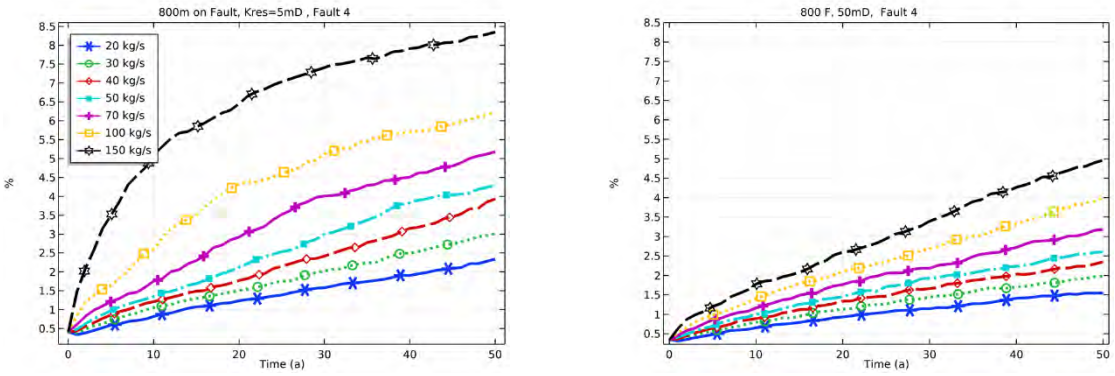


Figure 11. SCU areal percentage over time in 2 realisations (left: reservoir permeability =5 mD, left: reservoir permeability =50 mD)

### 2.4.4. Injection temperature

Injection of cold fluid into the reservoir cool down the reservoir and induce thermal stresses (Gholizadeh Doonechaly et al., 2016). As ΔT (reservoir temperature-injection temperature) become higher, meaning that colder fluid is injected into reservoir, the stress perturbance become higher and therefore the SCU on faults increases.

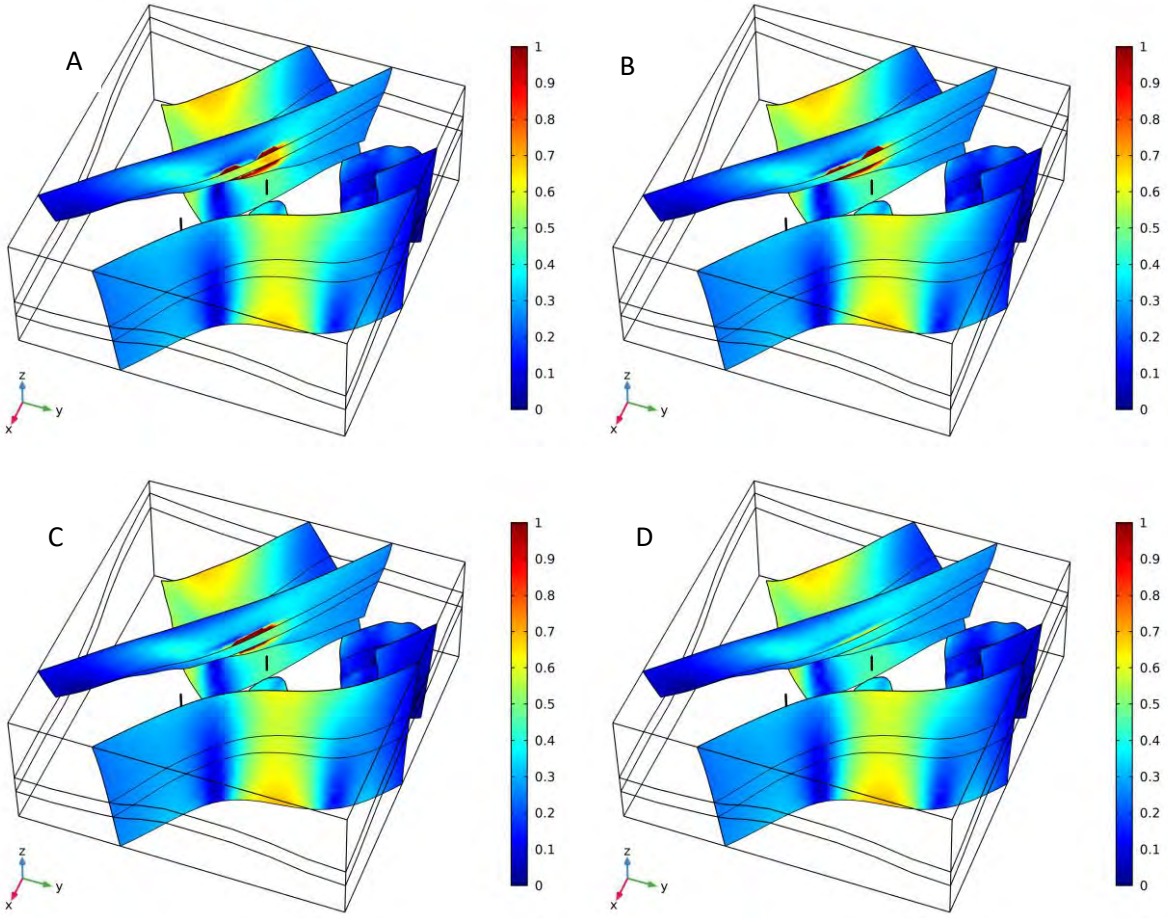


Figure 12. SCU distribution over fault surface for a realisation with Kres=50mD and wells are located close to the fault 4. Injection temperature differs between 4 cases. A) Tinj=20 °C, B) Tinj=50 °C, C) Tinj=80 °C, D) Q= Tinj=110 °C

### 2.4.5. Fault thickness

A sensitivity analysis conducted on fault thickness. The results show that this parameter doesnot have major impact on fault instability. Figure 13 shows the areal percentage of SCU>1 on fault surfaces for the case when both wells are located close to fault 4 (at about 200m distance). A, B,C, and D show the results where fault thickness alters to 10m, 20m, 40m, and 60m, the variation of areal coverage of SCU>1 is insignificant in all cases.

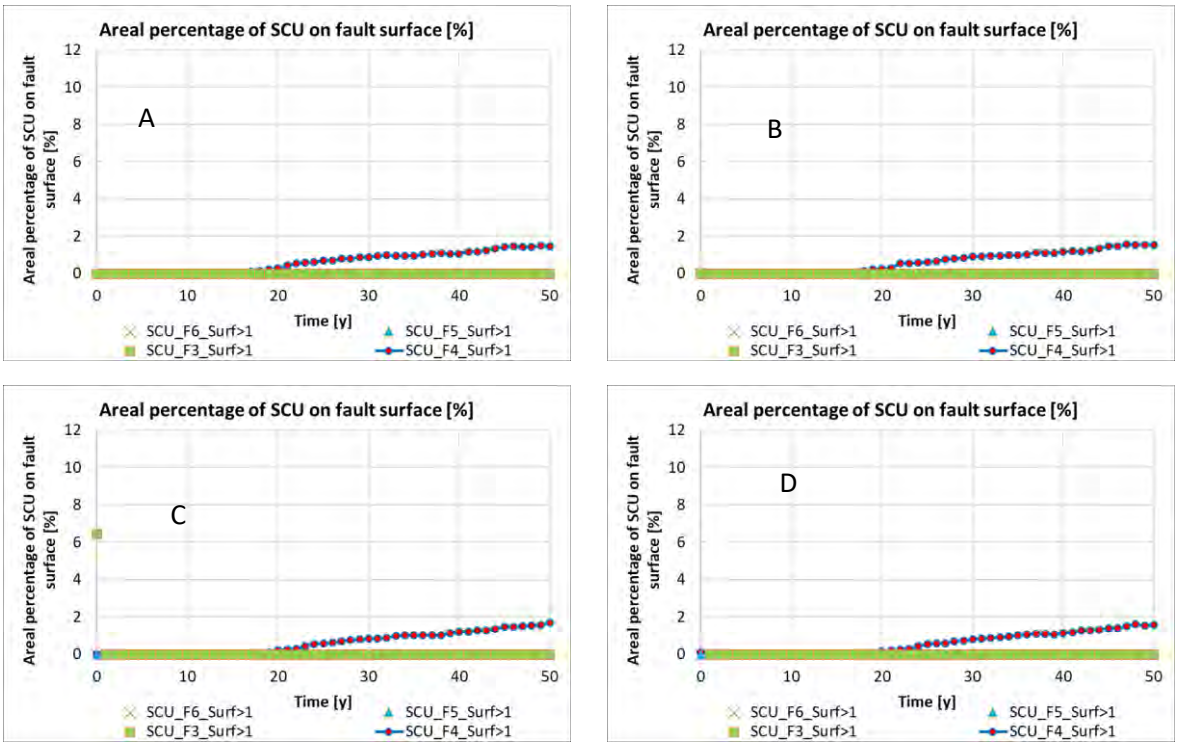


Figure 13. Areal percentage of SCU>1 over different fault surfaces for a realisation with Kres=50mD and wells are located close to the fault 4. Fault thickness differs between 4 cases. A) Fthickness=10m, B) Fthickness=20m, C) Fthickness=40m, D) Fthickness=60m

## 2.5 Selected scenarios

Looking to the conducted sensitivities, it can be concluded that the injection-production flow rate and well location in combination with reservoir permeability has major impact on the instability of the faults. Therefore for the further economic analysis only realisations with variation in reservoir permeability, injection-production flow rate, and well location have been considered. Therefore out of 209 scenarios only 47 were chosen for further economic analysis. The list is presented in Table 1.

Table 1. Cases that will be analysed in economic model

| Case number | Well distance [m] | Well location | Reservoir permeability [mD] | Flow rate [kg/s] | Injection temperature [oC] |
|---|---|---|---|---|---|
| 1 | 1500 | middle of the faults | 50 | 20 | 50 |
| 2 | 1500 | middle of the faults | 50 | 30 | 50 |
| 3 | 1500 | middle of the faults | 50 | 40 | 50 |
| 4 | 1500 | middle of the faults | 50 | 50 | 50 |
| 5 | 1500 | middle of the faults | 50 | 100 | 50 |
| 6 | 1400 | middle of the faults | 50 | 40 | 50 |
| 7 | 1400 | middle of the faults | 50 | 50 | 50 |
| 8 | 1500 | middle of the faults | 50 | 100 | 50 |
| 9 | 1500 | middle of the faults | 500 | 20 | 50 |
| 10 | 1500 | middle of the faults | 500 | 40 | 50 |
| 11 | 1500 | middle of the faults | 500 | 50 | 50 |
| 12 | 1500 | middle of the faults | 500 | 70 | 50 |
| 13 | 1500 | middle of the faults | 500 | 100 | 50 |
| 14 | 1500 | middle of the faults | 500 | 150 | 50 |
| 15 | 800 | middle of the faults (3&4) | 50 | 20 | 50 |
| 16 | 800 | middle of the faults (3&4) | 50 | 30 | 50 |
| 17 | 800 | middle of the faults (3&4) | 50 | 40 | 50 |
| 18 | 800 | middle of the faults (3&4) | 50 | 50 | 50 |

| | | | | | |
|---|---|---|---|---|---|
| 19 | 800 | middle of the faults (3&4) | 50 | 100 | 50 |
| 20 | 800 | Near fault 4 | 50 | 20 | 50 |
| 21 | 800 | Near fault 4 | 50 | 30 | 50 |
| 22 | 800 | Near fault 4 | 50 | 40 | 50 |
| 23 | 800 | Near fault 4 | 50 | 50 | 50 |
| 24 | 800 | Near fault 4 | 50 | 70 | 50 |
| 25 | 800 | Near fault 4 | 50 | 100 | 50 |
| 26 | 800 | Near fault 4 | 50 | 150 | 50 |
| 27 | 800 | Near fault 4 | 5 | 20 | 50 |
| 28 | 800 | Near fault 4 | 5 | 30 | 50 |
| 29 | 800 | Near fault 4 | 5 | 40 | 50 |
| 30 | 800 | Near fault 4 | 5 | 50 | 50 |
| 31 | 800 | Near fault 4 | 5 | 70 | 50 |
| 32 | 800 | Near fault 4 | 5 | 100 | 50 |
| 33 | 800 | Near fault 4 | 5 | 150 | 50 |
| 34 | 800 | on fault 4 | 50 | 20 | 50 |
| 35 | 800 | on fault 4 | 50 | 30 | 50 |
| 36 | 800 | on fault 4 | 50 | 40 | 50 |
| 37 | 800 | on fault 4 | 50 | 50 | 50 |
| 38 | 800 | on fault 4 | 50 | 70 | 50 |
| 39 | 800 | on fault 4 | 50 | 100 | 50 |
| 40 | 800 | on fault 4 | 50 | 150 | 50 |
| 41 | 800 | on fault 4 | 5 | 20 | 50 |
| 42 | 800 | on fault 4 | 5 | 30 | 50 |
| 43 | 800 | on fault 4 | 5 | 40 | 50 |
| 44 | 800 | on fault 4 | 5 | 50 | 50 |
| 45 | 800 | on fault 4 | 5 | 70 | 50 |
| 46 | 800 | on fault 4 | 5 | 100 | 50 |
| 47 | 800 | on fault 4 | 5 | 150 | 50 |

# 3. Economic model

## 3.1 General description of the model

The economic model post-processes simulation runs, performed by the COMSOL THM coupled reservoir simulator, to optimize the position of the injection and production wells, the injection rate and temperature of a geothermal doublet in reservoirs with a primary matrix permeability.

*Objective function*

The delivered workbook computes the objective function to be maximized for a faulted geothermal reservoir. The workbook imports the reservoir performance time-series as computed by a coupled THM reservoir simulator. In this WP6, the COMSOL simulator has been used (version 5.4).

Optimizing the objective function includes setting a geomechanical constraint, SCU (Shear Capacity Utilisation, explained in section 2.3), on a fault's surface area (mainly applicable to those faults that are more vulnerable to seismic events due to their comparatively large length). The objective function is either:

- MAX [ NPV | areal % tolerance of SCU>1 in fault 4, 5 and 6 < tolerance], or:
- MAX [ Discounted cumulative heat-sales | areal % tolerance of SCU>1 < tolerance].

By computing the value of the selected objective function for each decision alternative, the "best" decision alternative can be identified in a sensitivity analysis.

*Operating the workbook*

- For each decision-alternative, complete the yellow cells in worksheet 'Input'!
- Import the tabular results of a coupled THM reservoir simulator into worksheet 'Imported time-series'!
- Inspect worksheet 'KPI'!, and notably the NPV value
- Do a sensitivity analysis with varying well configurations and production/injection rates. Select the alternative with the highest value for the objective function.

Note that the analysis can also be done stochastically by defining probability density functions for (some of) the input variables of 'Input'! In that case, it is recommended to compute the mean-NPV, or mean-discounted heat-sales, and compare the decision alternative based on this quantity.

## 3.2 Pump power calculation

The pressure calculation of the production well and of the ESP power required is as follows (note: HE = Heat Exchanger; ESP = Electrical Submersible Pump, i.e. the pump hanging in the production well; FTHP = Flowing Tubing Head Pressure):

- The pressures upstream of the HE are governed by the HE operating pressure (user input)
- $P_{operating\ HE} + {}^{1}/_{2} \times \Delta P_{HE} + \Delta P_{flowline+choke} = FTHP_{prod}$. This is the required FTHP to be delivered by the ESP.
- The ESP (the production pump) has to yield the negative pressure from the simulator + the required $FTHP_{prod}$.

The pressure calculation of the injector and of the injection pump power required is as follows:

- The pressures downstream of the HE are governed by the HE operating pressure (user input)
- $P_{operating\ HE} - {}^{1}/_{2} \times \Delta P_{HE} - \Delta P_{flowline} + \Delta P_{inj\ pump} = FTHP_{inj}$ . This is the required FTHP to be delivered by the injection pump.

## 3.3 Optimization

We have opted for a trial and error method of optimization, where the reservoir simulation is done separately from the economic analysis, rather than in an integrated way with an objective function that triggers a new search in the parameter space (such as a gradient method). In our method, the reservoir parameters (reservoir permeability, $k_v/k_h$ ratio and skin factor) and decision alternatives (well location, well spacing, production/injection rate and reinjection temperature) have been combined with different reservoir permeability realisations, resulted in 209 scenarios, from which 47 has been chosen for further economic analysis.

All 47 selected scenarios were then imported in a separate economic evaluation XL workbook and processed for economic KPIs (decision metrics) under a range of assumptions. The runs are reported in the Appendix.

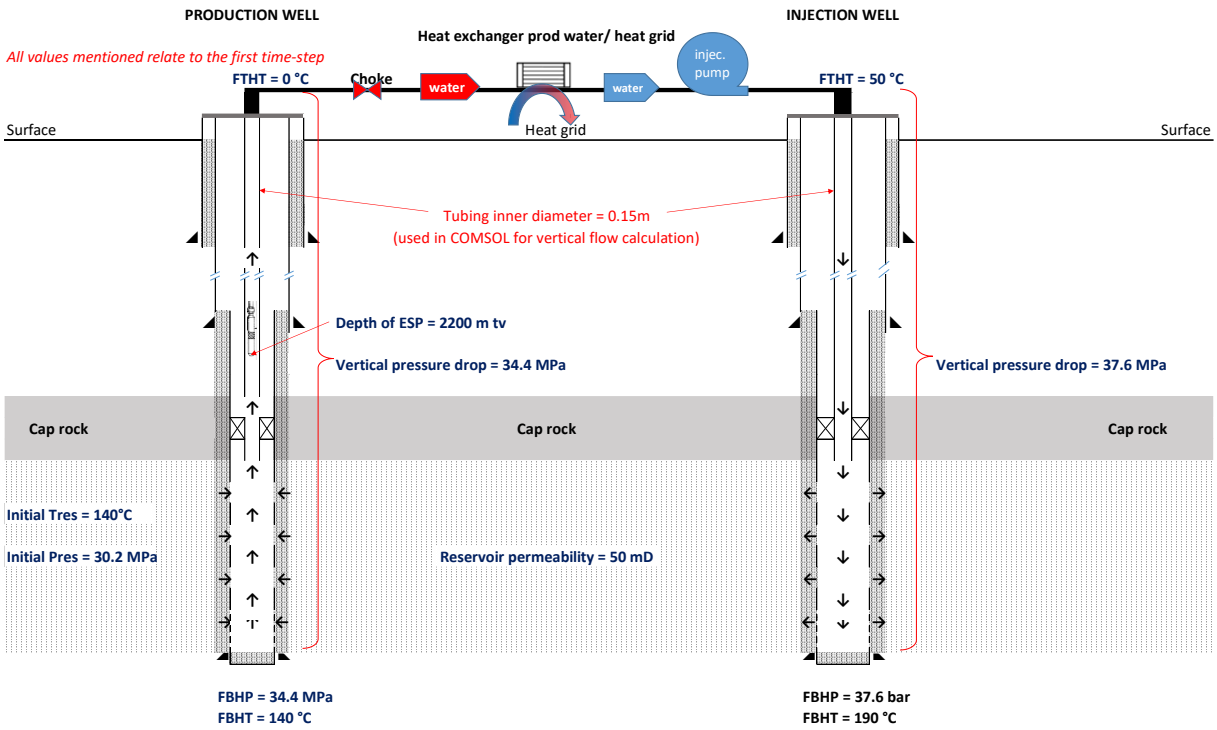


Figure 14. Lay-out of Westland Trias geothermal doublet

The economic model post-processes the COMSOL results by computing heat sales vs. time (conditional on a user-specified maximum number of sequential years that the net cashflow is allowed to be negative, and conditional on a minimum number of injection / production years), by computing the revenue, cash-out and net cashflow. It also computes some physical output, such as the total number of years that the geomechanical constraint tolerance limit has been violated on the main faults of the Westland structure (and which year was the first to violate this tolerance value). It also computes the total heat sold to the market (in GWh), and compares this to the total electrical energy used to drive the Electrical Submersible Pump (ESP) in the producer, and to drive the injection pump just upstream of the injector.

The objective function used for selecting the viable options was as follows:

- MAX (EMV | IRR > hurdle rate; nr of yrs that geomechanical stress tolerance in faults 3&4&5 is violated < tolerance nr of yrs).

EMV is the Expected Monetary Value, or the mean of the output NPV distribution. IRR is the Internal Rate of Return. The runs are then compared using this objective function and the viable runs are selected as possible candidates for developing the Westland geothermal doublet. Note that to have a more generic analysis, we have also assumed the formation permeability to be higher than the ones actually tested. This is to understand better the influence of permeability on the economics.

As an example of the economic analysis, one scenarios is presented below. In this scenario, reservoir permeability is 50mD and the wells are located in the middle of the faults, with a distance of 800m between injector and producer. The reinjected water temperature is 50°C at the injector's wellhead and is reinjected at a rate of 100 kg/s. Figure 15 shows the thermal propagation in this reservoir after 30 years of production.

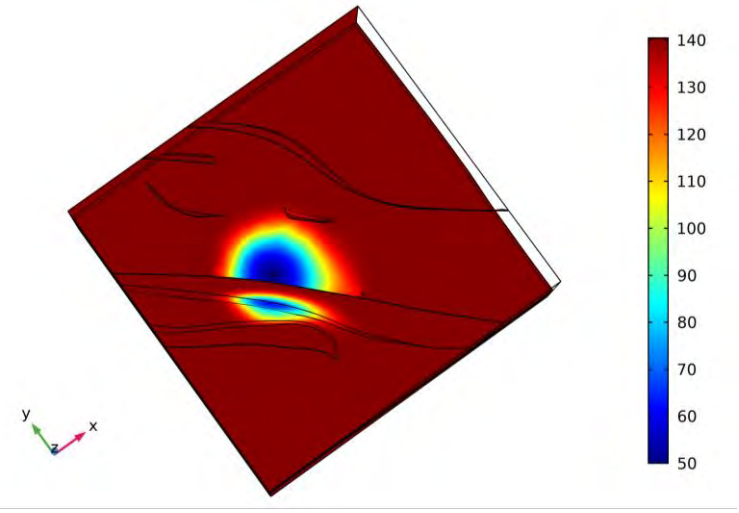


Figure 15. thermal propagation in the reservoir after 30 years of production

The input data for the economic model of this case are given in Table 2 below. It contains some general information on the case, a section for the economic input data (capex, opex, tariffs, subsidies, etc.), and a section for technical data (mainly surface equipment process variables, and an acceptance norm for the SCU>1 areal % of faults). Light yellow cells are required (deterministic) input, and the bright green cells denote required stochastic probability density functions for the uncertain input variables.

Table 2. Input data economic model

| | |
|---|---|
| **Geothermal doublet name** | Westland |
| **Reservoir, formation member** | Vlieland |
| **Doublet & case description** | See comment in cell B6 |
| **Name of case / decision-alternative** | 800MM,50mD,Tinj50,Q100,S-4,Kvh1 |
| **Injection & production rate (kg/s)** | 100 & 100 |
| **Evaluation period (first to last year)** | 0 to 39 |
| **Simulation data imported from file** | 20200217_DESTRESS_SIMULATON_COMSOL.xlsx |
| **Author economic workbook & affiliation** | Christian Bos (TNO) |
| **Author COMSOL data & affiliation** | Sanaz Saeid (TUDelft) |
| **Date** | 20/02/2020 |

| **Cost, tariff, planning data** | **Unit** | **Value** |
|---|---|---|
| | | |
| | | |
| | | |
| Reference year for discounting | year | 0 |
| Discount rate | - | 10% |
| Heat sales tariff | €/kWh | 0.026 |
| | | |
| Pump energy costs (electricity) | €/kWh | 0.29 |
| Flow lines capex | million € | 0.50 |
| Heat exchanger capex | million € | 0.25 |
| Production well drill&compl capex | million € | 19.14 |
| Injection well drill&compl capex | million € | 13.59 |
| Production pump capex | million € | 0.25 |
| Injection pump capex | million € | 0.25 |
| Other capex | million € | 1.00 |
| Subsidies capex | million € | 1.42 |
| O&M fixed opex | million €/yr | 1.25 |
| Variable opex other than lifting costs | €/kg | 0.043 |
| Subsidy per unit heat sales | €/kWh sales | 0.003 |
| Economic stopping criterion: #yrs@NCF<0 | years | 3 |
| Minimum number of inj/prod years | years | 6 |
| Capex multiplier | - | 0.97 |
| Fixed opex multiplier | - | 0.93 |
| | | |
| | | |

| **Technical data** | **Unit** | **Value** |
|---|---|---|
| FBHP (initial) of producer | MPa | 35.1 |
| FBHT (initial) of producer | °C | 140.0 |
| Producer initial vertical ΔP FTHP - FBHP | MPa | 32.8 |
| Producer initial vertical ΔT FTHT - FBHT | °C | 0.0 |
| ΔP wellhead producer to heat exchanger, incl ΔP choke | MPa | 1.4 |
| ΔT wellhead producer to heat exchanger | °C | 8.0 |
| Operating pressure of heat exchanger | MPa | 0.6 |
| ΔP across heat exchanger | MPa | 0.6 |
| ΔT across heat exchanger ($T_{inlet}$ - $T_{outlet}$ of Heat Exchanger) | °C | 90.0 |
| ΔP heat exchanger to wellhead injector | MPa | 0.4 |
| ΔT heat exchanger to wellhead injector | °C | 0.0 |
| Injector ΔP FTHP - FBHP | MPa | 37.8 |
| Injector ΔT FTHT - FBHT | °C | |
| Depth of pump in production well | m tv | 2200.0 |
| Specific gravity of formation water | kg/m3 | 1020.0 |
| Pump efficiency of ESP and injection pump | % | 65.0% |
| Thermal efficiency of heat exchanger | - | 95% |
| Production well top of perforations | m tv | 2965.0 |
| Injection well top of perforations | m tv | 2970.0 |
| Initial reservoir pressure | MPa | 30.2 |
| Tubing inner diameter | m | 0.15 |
| Initial reservoir temperature | °C | 140.0 |
| Reservoir permeability | mD | 50.0 |
| Distance between injector/producer at top reservoir | m | 1400 |
| Geomech. / seismicity SCU>1 areal fault% tolerance | % | 2.0 |

Some values and thresholds in this table are extracted from Daniilidis et al., 2017 and van Dongen, 2019. In Figure 16 below, the computed yearly heat sales time-series is presented, including the electrical pump energy required to produce (hot) and reinject (cold) the formation water.

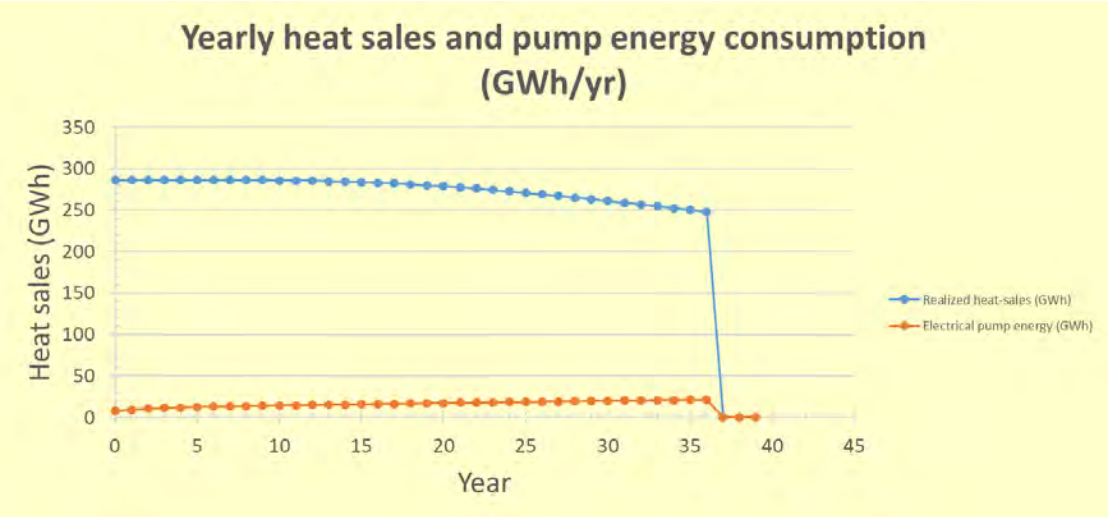


Figure 16. Example of economic model output: heat-sales and pump energy consumption

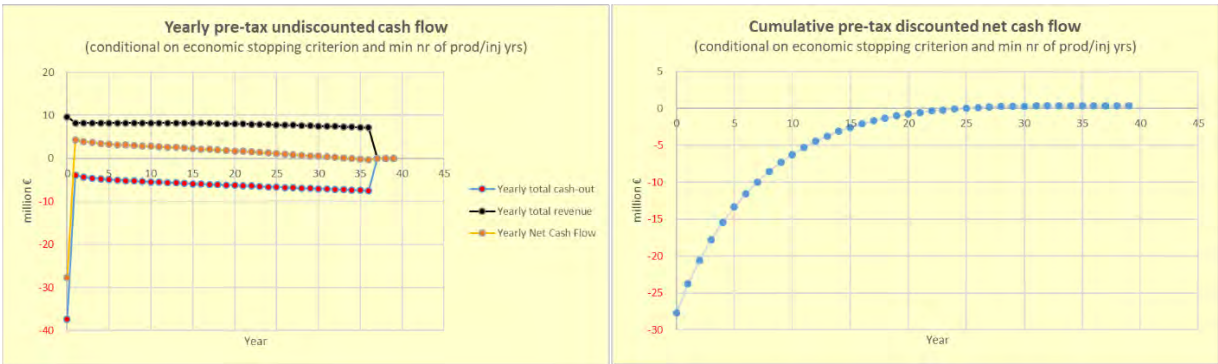


Figure 17. Example of economic model output: yearly and cumulative net cash flows

Table 3. Economic model Key Performance Indicators

| Key Performance Indicators of case Westland; 800MM,50mD,Tinj50,Q100,S-4,Kvh1<br>Case description: See comment in cell B6; Injection rate: 100 & 100 kg/s. Evaluation period 40 years<br>Heat-sales price = € 0.025552034036513 4/kWh; subsidy = € 0.003265778638080 59/kWh heat sales<br>Discount rate = 10% | | | |
|---|---|---|---|
| **KPI** | **Value** | **Unit** | **Comment** |
| **Realized cumulative water production over full evaluation period** | **1.17E+05** | 10^6 kg | Constrained by economic field close-in criterion (3yrs@NCF<0 \| ≥6 yrs production&injection) |
| **Ultimate heat sales over full evaluation period, undiscounted** | **10193** | GWh | Constrained by economic field close-in criterion (3yrs@NCF<0 \| ≥6 yrs production&injection) |
| **Ultimate heat sales over full evaluation period, discounted** | **3026** | GWh | Constrained by economic field close-in criterion (3yrs@NCF<0 \| ≥6 yrs production&injection) |
| **Pre-tax NPV (ref yr 0; disc rate 10%) at end of evaluation period** | **0.3** | M€ | Constrained by economic field close-in criterion (3yrs@NCF<0 \| ≥6 yrs production&injection) |
| **Pre-tax IRR** (if NPV<0, the IRR is set to -100%) | **10.2%** | % | Capital efficiency measure |
| **Pre-tax VIR** (Value Investment Ratio = NPV / PV(capex) | **0.01** | ratio | Capital efficiency measure |
| **Maximum exposure** (discounted = undiscounted as all capex in yr 0) | **-27.68** | M€ | As all capex is spent in 1st yr of evaluation, the max exposure will occur in that yr |
| **Pay-out time, undiscounted (pre-tax)** | **8** | yrs | |
| **Pay-out time, discounted (pre-tax)** | **25** | yrs | |
| **Cumulative capex + opex (undiscounted)** | **278.8** | M€ | |
| **Cumulative capex + opex (discounted)** | **88.9** | M€ | |
| **UTC** (Unit Technical Cost: costs and produced heat-sales volumes undiscounted) | **0.0274** | €/kWh | |
| **LCOH** (Levelised Cost Of Heat: costs and produced heat-sales volumes discounted) | **0.0294** | €/kWh | |
| **Year of closing-in the geothermal doublet** | **Year 37** | | |
| **Total nr of years that tolerance of areal % @SCU>1 of fault#3 is violated** | **7** | yrs | Assumed areal % tolerance of fault with SCU>1 = 2%. 1st yr of violation: Year 33 |
| **Total nr of years that tolerance of areal % @SCU>1 of fault#4 is violated** | **0** | yrs | Assumed areal % tolerance of fault with SCU>1 = 2%. 1st yr of violation: Tolerance not violated over full evaluation period |
| **Total nr of years that tolerance of areal % @SCU>1 of fault#5 is violated** | **0** | yrs | Assumed areal % tolerance of fault with SCU>1 = 2%. 1st yr of violation: Tolerance not violated over full evaluation period |

As the model has been coded in Microsoft Excel, it can be combined with Crystal Ball, a statistical XL plug-in. This allows uncertain input variables to be sampled by the Monte Carlo process and output histograms of KPIs and probabilistic time-series to be generated. Also, sensitivity analyses can be easily done to determine which uncertain input variables contribute most to the uncertainty in some output

KPI. This may help decision-makers to better understand the top drivers and top risk factors that contribute most to some decision metric (e.g. a KPI). Alternative project definitions, to further improve the project, can then be more easily defined and investigated. In the above table, output histograms are generated for the bright blue cells.

## 4. Business case optimization

To demonstrate the workflow developed in this task, an example is given of a business case optimization, based on alternative project definitions (well locations etc.), and eventually also based on the managerial flexibility one has to intervene and change the operational variables mid-course ("reservoir management", i.e. by changing the injection rate when the risk of fault reactivation starts becoming too high).

As concluded in previous sections, in case of a reservoir permeability that is low relative to the fault permeability, an option is to increase the production by placing the well closer to the faults. The higher hydraulic conductivity of the fault can then be exploited to improve the hydraulic conductivity between the injector and producer. However, locating the wells close to a fault increases the risk that the fault will be reactivated by the changing pressure and temperature fields as a result of the injection or production.

Initially, case 33 was considered, where both wells are crossing fault number 4. In this case, the flowrate is set at 150 kg/s. The predicted areal percentage with a SCU of >1 over the fault's surface (Figure 18) indicates that this case is probably unacceptable in view of the fault reactivation risk (as no clear guidelines exist on this areal % norm, we have assumed 2% as acceptance criterion for the fault's surface area having an SCU above 1). Therefore, it was decided to move the wells further away from the faults (case 26).

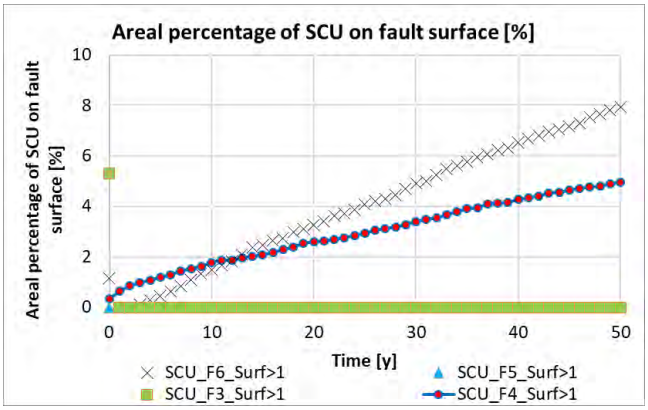


Figure 18. Areal percentage of SCU>1 on fault surface for case 33

The economic analysis of case 26 (see Table 1) is promising, however with its injection production rate of 150 kg/s it shows that the risk of fault reactivation is too high (see also **Fehler! Verweisquelle konnte nicht gefunden werden.**, page **Fehler! Textmarke nicht definiert.**). Hence, it should be investigated whether this case can be further optimised by reducing the injection rate when the risk of fault reactivation start becoming too high. Case 26 shows the following physical evolution of state variables (Figure 19 belowFigure 1):

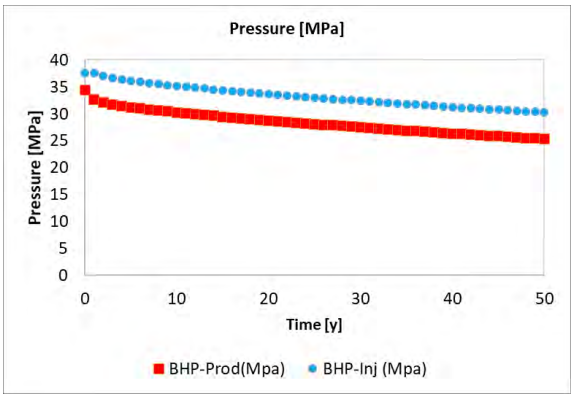


A) Bottomhole injection and production pressure

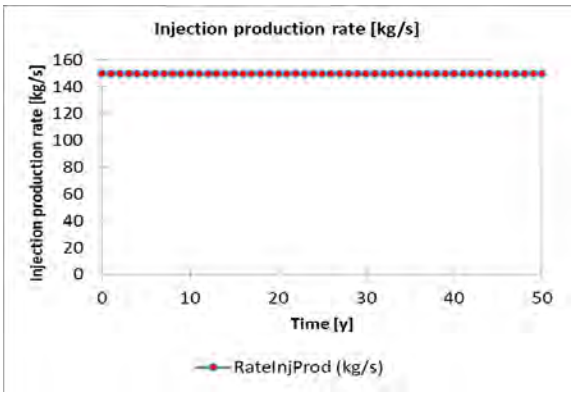


B) Injection-production flow rate

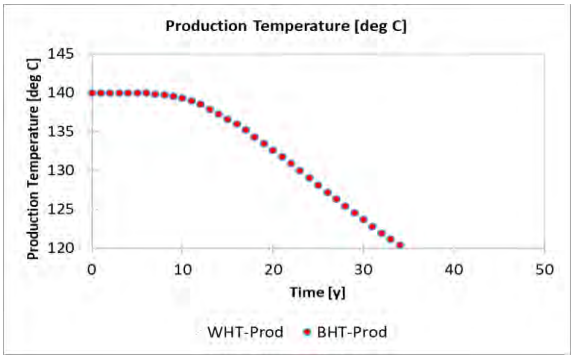


C) Production temperature

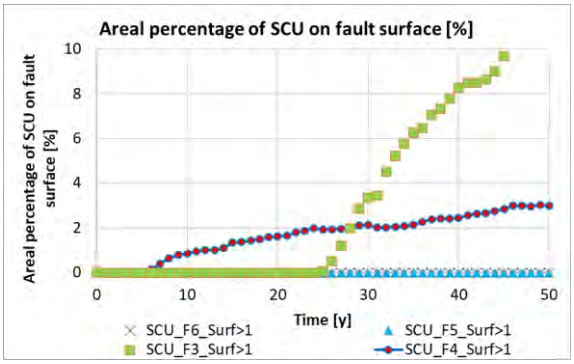


D) Areal percentage of SCU>1 on fault surface

Figure 19. Reservoir modelling response of case 26

When studying case 25, which has a lower flow rate (100 kg/s) than case 26 (150 kg/s), one can observe that it is safer than case 26 regarding the fault reactivation risk (Figure 20). From an economic point of view, it is however less attractive (EMV of case 25 = € 14.5 million, with 72% of stochastic realization having an NPV>0, vs. EMV of case 26 = € 35.6 million, with 85% of stochastic realization having an NPV>0; see **Fehler! Verweisquelle konnte nicht gefunden werden.**, page **Fehler! Textmarke nicht definiert.**).

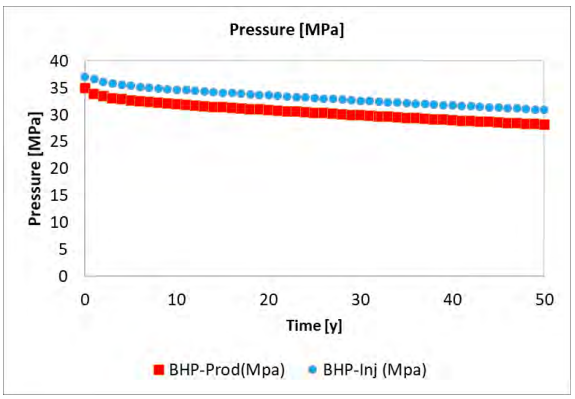


A) Bottomhole injection and production pressure

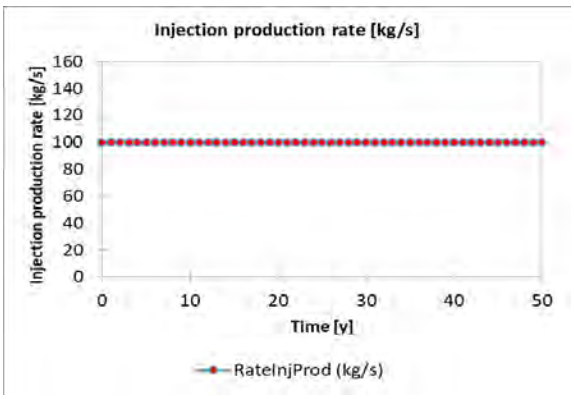


B) Injection-production flow rate

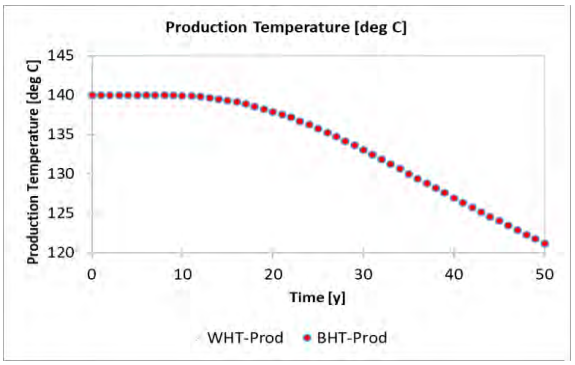


C) Production temperature

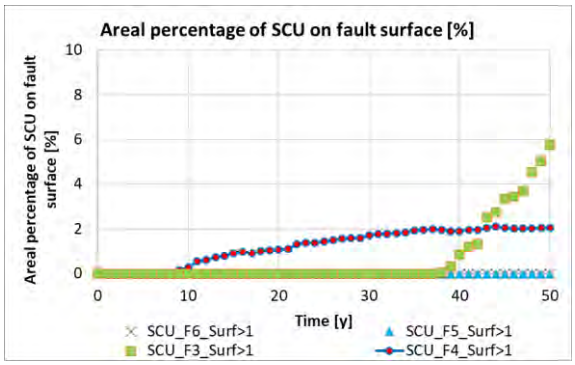


D) Areal percentage of SCU>1 on fault surface

Figure 20. Reservoir modelling response of case 25

Combining both cases 25 and 26 gives a better business case. In this combined case, the reservoir starts with a 150 kg/s injection and production rate until year 10, when the production temperature starts to drop from 140°C. From year 10 onwards, the flowrate is reduced to 100 kg/s. With this reservoir management strategy, the temperature drop over the next 30 years (an economic evaluation period of 40 years was assumed in the model) is only 10°C, compared to a 20°C temperature drop in case 26). And importantly, the fault reactivation risk constraint is fully honoured until the end of the evaluation period.

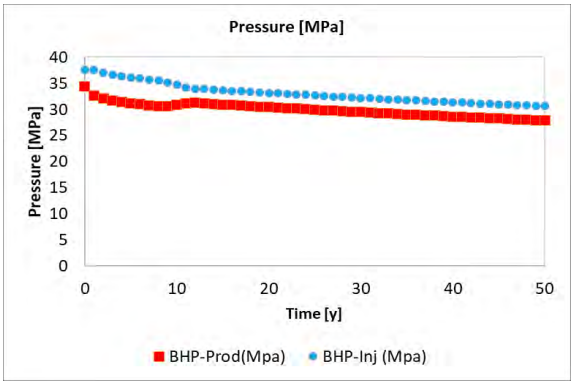


A) Bottomhole injection and production pressure

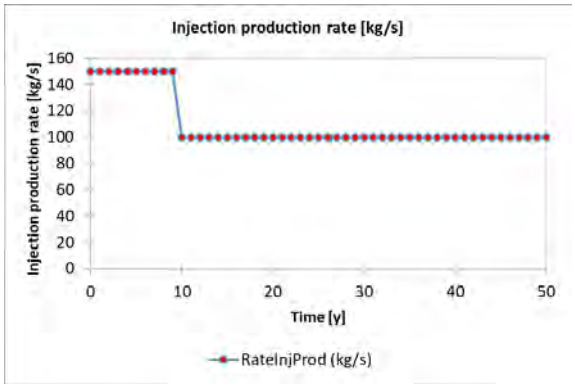


B) Injection-production flow rate

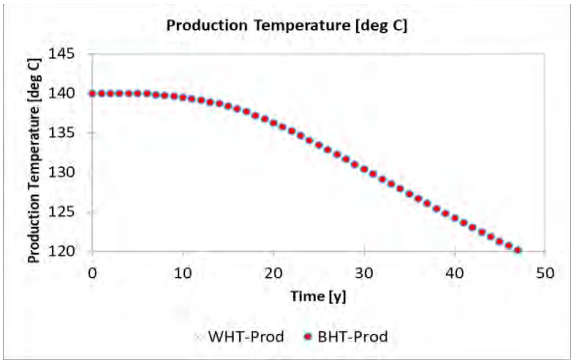


C) Production temperature

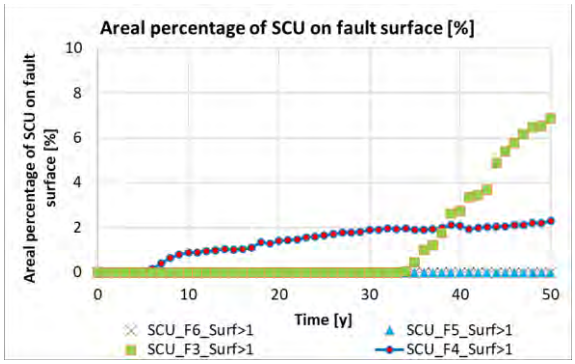


D) Areal percentage of SCU>1 on fault surface

Figure 21. Reservoir modelling response of optimised case

The combined cases 25 and 26, as described above, thus satisfy the fault reactivation risk constraint and yield much better economics than case 25:

Table 4. Economics of cases 25, 26 and optimized case 25+26

| Case | EMV (€ million) | % of stochastic realization having an NPV>0 |
|---|---|---|
| 25 | 14.5 | 72 |
| 26 | 35.6 | 85 |
| 25+26 | 30.3 | 83 |

The resulting pre-tax NPV histogram of the combined, optimized case 25+26 is displayed below:

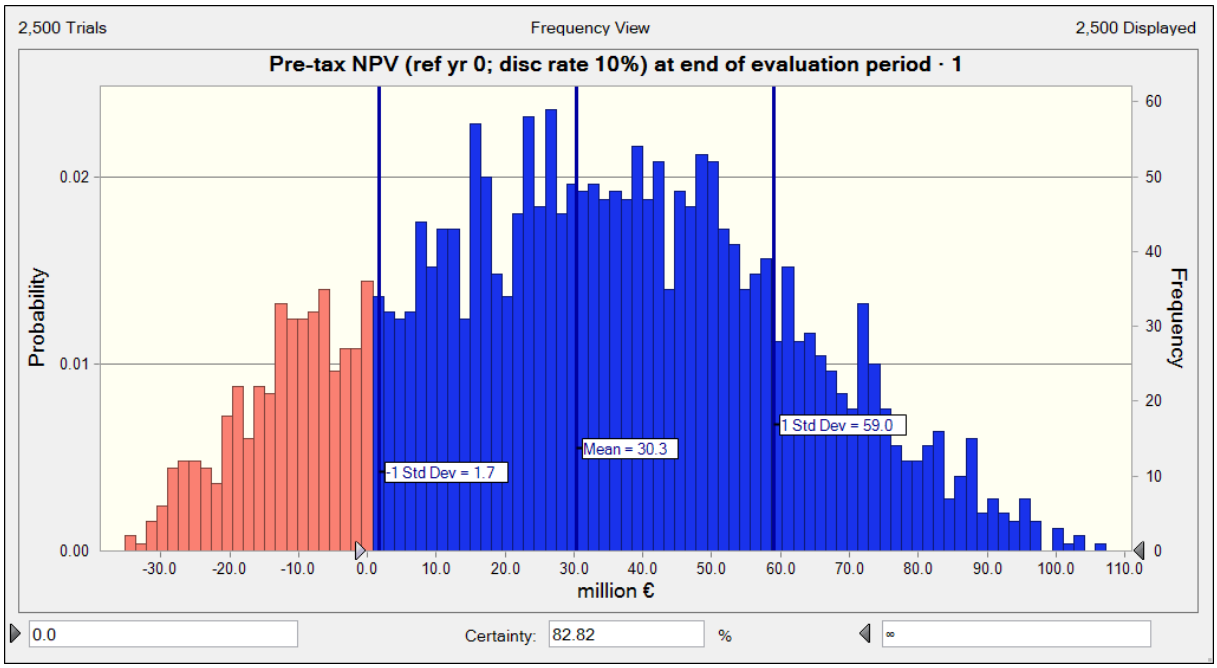


Figure 22. Pre-tax NPV histogram of optimized case 25+26

The resulting Levelised Cost Of Heat (LCOH) histogram of the combined, optimized case 25+26 is next:

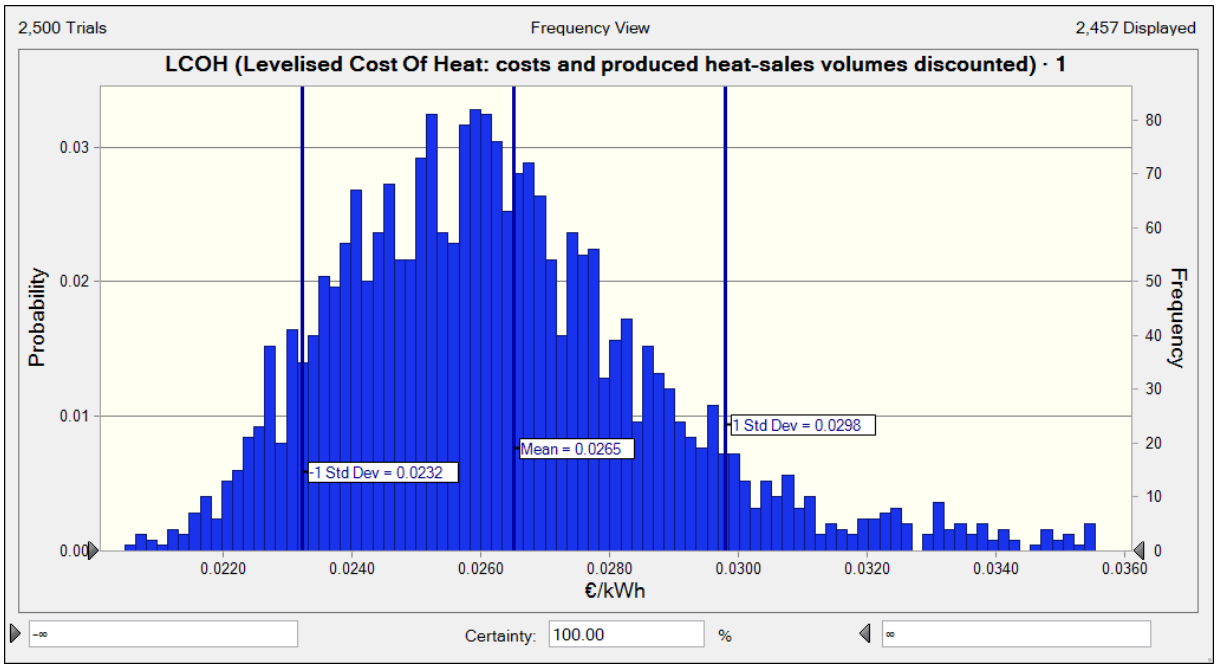


Figure 23. LCOH histogram of optimized case 25+26

And the pre-tax NPV sensitivity diagram is also given below:

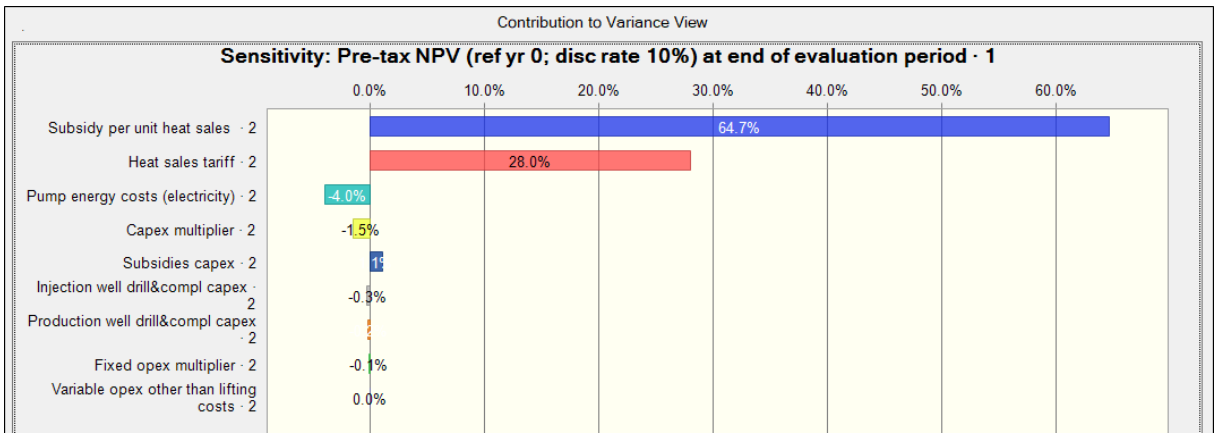


Figure 24. Sensitivity analysis of optimized case 25+26 (contribution to NPV variance)

As can be seen in the sensitivity analysis, the uncertain input variables having the most impact on the economics are the ones related to the revenue stream from the heat sales (heat sales tariff, and subsidies on heat sales).

One of the Monte Carlo stochastic realizations of the optimized combined case 25+26 is displayed below:

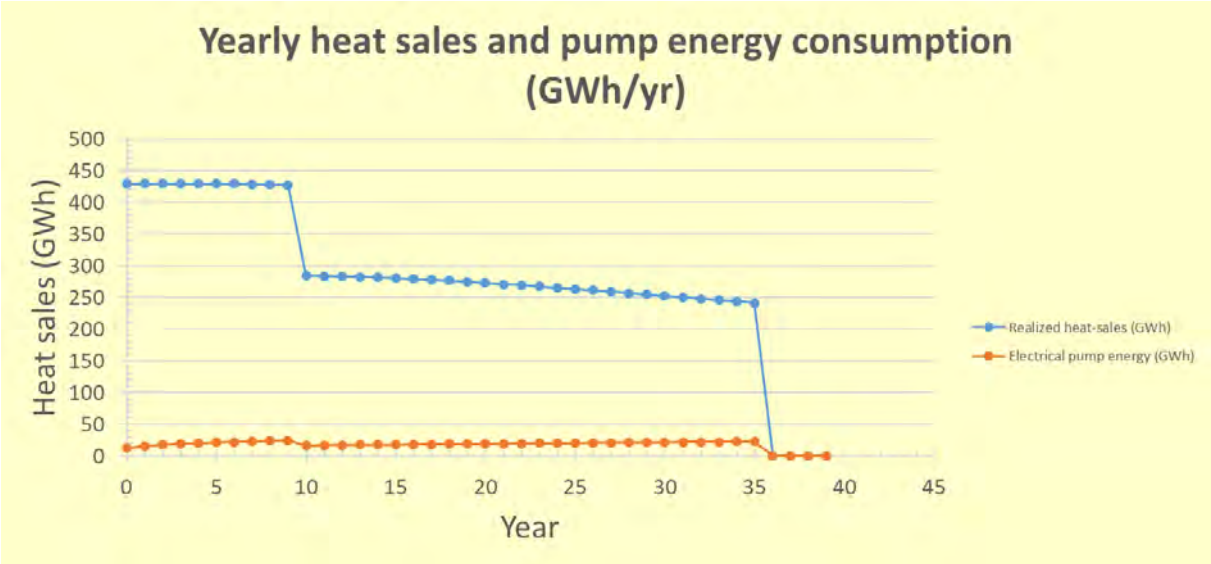


Figure 25. Yearly heat sales and pump energy consumption for one stochastic realization of optimized case

In this optimized case (combination of cases 25+26), it can be clearly seen how the heat sales and required pump energy vary in time (Figure 25). The step changes in year 10 are conspicuous.

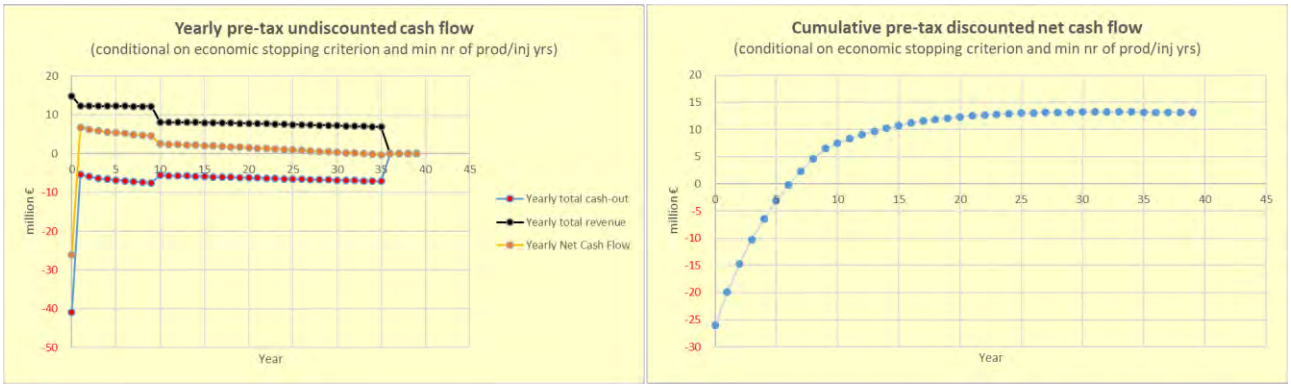


Figure 26. Optimized case: yearly and cumulative cashflows for one stochastic realization

In the yearly cashflow of Figure 26, it can be seen how the field close-in date due to the economic stopping criterion (a maximum of three years with a negative net cashflow is allowed) is delayed by tilting the slope of the NCF vs. time. The economic life-time of the geothermal doublet is highly sensitive to the combination of gradually decreasing revenue and gradually increasing opex (i.e. pumping costs). Slightly improving either the revenue decline and/or the opex trend may extend the field's life for many years.

The KPIs of the above stochastic realization of the optimized case are given in the next table:

Table 5. Optimized case: Key Performance Indicators of one stochastic realization

| KPI | Value | Unit |
|---|---|---|
| **Realized cumulative water production over full evaluation period** | **1.29E+05** | 10^6 kg |
| **Ultimate heat sales over full evaluation period, undiscounted** | **11215** | GWh |
| **Ultimate heat sales over full evaluation period, discounted** | **3967** | GWh |
| **Pre-tax NPV (ref yr 0; disc rate 10%) at end of evaluation period** | **13.2** | M€ |
| **Pre-tax IRR** (if NPV<0, the IRR is set to -100%) | **19.2%** | % |
| **Pre-tax VIR** (Value Investment Ratio = NPV / PV(capex) | **0.37** | ratio |
| **Maximum exposure** (discounted = undiscounted as all capex in yr 0) | **-25.98** | M€ |
| **Pay-out time, undiscounted (pre-tax)** | **5** | yrs |
| **Pay-out time, discounted (pre-tax)** | **7** | yrs |
| **Cumulative capex + opex (undiscounted)** | **296.2** | M€ |
| **Cumulative capex + opex (discounted)** | **103.0** | M€ |
| **UTC** (Unit Technical Cost: costs and produced heat-sales volumes undiscounted) | **0.0264** | €/kWh |
| **LCOH** (Levelised Cost Of Heat: costs and produced heat-sales volumes discounted) | **0.0260** | €/kWh |
| **Year of closing-in the geothermal doublet** | **Year 36** | |
| **Total nr of years that tolerance of areal % @SCU>1 of fault#3 is violated** | **1** | yrs |
| **Total nr of years that tolerance of areal % @SCU>1 of fault#4 is violated** | **1** | yrs |
| **Total nr of years that tolerance of areal % @SCU>1 of fault#5 is violated** | **0** | yrs |

# 5. Conclusions

Some first conclusions of the techno-economic modelling and sensitivity analysis are:

- The main operational parameter that affects the economic viability in EGS systems is the flow rate. The pump energy required to obtain the desired rate has a secondary effect on economics (note that the maximum possible flow rate is obviously limited by a realistic minimum for the flowing bottomhole pressure).
- However, as the flowrate may increase the instability of the faults, a geomechanical constraint has to be imposed by computing the fault slip tendency as a function of the pressure and temperature fields, and maximizing the fault's surface that is exposed to stresses above the bearing shear stress.
- When the reservoir permeability is very low (e.g. <0.1 - 1 mD) the case will not be economic because realistic flowrates will be too low (both the injection and production pressures are technically limited). But also the increasing pump power costs negatively affect the economics.
- For Trias Westland (in all permeability realisations, and given the assumptions for the various economic parameters) a flow rate of at least 100 kg/s is required to have an business case. However, not all >100 kg/s cases will meet the condition of fault reactivation risk tolerance.
- The uncertainty in the NPV of case 25 is caused mainly by the uncertainty in the subsidy per unit heat-sales, and the heat-sales tariff, as in all high-rate cases. Other uncertainties are not significant.
- The lower the rate, the more sensitive the NPV uncertainty is due to the uncertainty in capex and capex subsidy. The reason is that due to a negative net cashflow the field will be closed-in relatively soon and that the capex cannot be recovered. Lower capex and/or capex subsidies then become relatively more important.
- The higher the rate, the more sensitive the NPV uncertainty is due to the uncertainty in heat-sales tariff and heat-sales subsidy.

- The uncertainty in the pumping costs can become significant but will never reach more than 8% contribution to the NPV variance (in the high-rate economic cases). However, the date of closing in the field will be sensitive to the pumping costs (as can be seen e.g. in Figure 16).

# 6. Recommendations

In this DESTRESS work Package, we have demonstrated a methodology to optimize a geothermal doublet under the constraint of a fault reactivation risk tolerance. To render the methodology more generic, some assumptions both in the reservoir model and economic model may be reviewed. This will however not change the validity of the overall methodology presented, but will enable more specific adjustments to be made per individual case.

The model should be verified for the economic input variables and be calibrated to local conditions and market values, notably costs and tariffs.

Another recommendation would be to redefine and adjust the areal percentage of the SCU>1 constraint, based on the acceptable seismic magnitude in each region (e.g. different countries have different norms). Also, the areal % tolerance norm (fault area with a SCY>1) may be a function of fault geometry, fault length and depth. This has not yet been investigated.

The proposed methodology in this report is based on comparing a series of hand-picked decision alternatives, rather than these alternatives being selected by some mathematical optimization scheme that uses, for example, a gradient method to define new combinations of well positions, re-injection temperature and injection/production rates. Ongoing research projects focus on this geothermal doublet well positioning optimization using mathematical optimization schemes. It would be interesting to compare our method with the methods of those other research projects.

# 7. References

Al-Khoury, R., 2011. Computational Modeling of Shallow Geothermal Systems, First. ed. CRC Press.

Churchill, S.W., 1977. Friction-factor equation spans all fluid-flow regimes. Chem. Eng. 84, 91–92.

COMSOL Multiphysics, 2017. COMSOL 5.3a Pipe Flow Module user's guide.

Daniilidis, A., Alpsoy, B., Herber, R., 2017. Impact of technical and economic uncertainties on the economic performance of a deep geothermal heat system. Renew. Energy 114, 805–816. https://doi.org/10.1016/j.renene.2017.07.090

Gholizadeh Doonechaly, N., Abdel Azim, R.R., Rahman, S.S., 2016. A Study of Permeability Changes Due to Cold Fluid Circulation in Fractured Geothermal Reservoirs. Groundwater 54, 325–335. https://doi.org/10.1111/gwat.12365

Haaland, S.E., 1983. Simple and Explicit Formulas for the Friction Factor in Turbulent Pipe Flow. J. Fluids Eng. 105, 89–90.

Jeanne, P., Rutqvist, J., Dobson, P.F., Walters, M., Hartline, C., Garcia, J., 2014. The impacts of mechanical stress transfers caused by hydromechanical and thermal processes on fault stability during hydraulic stimulation in a deep geothermal reservoir. Int. J. Rock Mech. Min. Sci. 72, 149–163. https://doi.org/10.1016/j.ijrmms.2014.09.005

Lepillier, B., Daniilidis, A., Doonechaly Gholizadeh, N., Bruna, P.O., Kummerow, J., Bruhn, D., 2019. A fracture flow permeability and stress dependency simulation applied to multi-reservoirs, multi-production scenarios analysis. Geotherm. Energy 7, 1–16. https://doi.org/10.1186/s40517-019-0141-8

Lin, S., Kwok, C.C.K., Li, R.-Y., Chen, Z.-H., Chen, Z.-Y., 1991. Local frictional pressure drop during vaporization of R-12 through capillary tubes. Int. J. Multiph. Flow 17, 95–102. https://doi.org/10.1016/0301-9322(91)90072-B

Livescu, S., Durlofsky, L.J., Aziz, K., Ginestra, J.C., 2010. A fully-coupled thermal multiphase wellbore flow model for use in reservoir simulation. J. Pet. Sci. Eng. 71, 138–146. https://doi.org/10.1016/J.PETROL.2009.11.022

Magnenet Vincentand Fond, C. and G.A. and S.J., 2014. Two-dimensional THM modelling of the large scale natural hydrothermal circulation at Soultz-sous-Forêts. Geotherm. Energy 2, 17. https://doi.org/10.1186/s40517-014-0017-x

Saeid, S., Al-Khoury, R., Barends, F., 2013. An efficient computational model for deep low-enthalpy geothermal systems. Comput. Geosci. 51, 400–409. https://doi.org/10.1016/j.cageo.2012.08.019

Saeid, S., Al-Khoury, R., Nick, H.M., Hicks, M.A., 2015. A prototype design model for deep low-enthalpy hydrothermal systems. Renew. Energy 77, 408–422. https://doi.org/http://dx.doi.org/10.1016/j.renene.2014.12.018

van Dongen, B., 2019. The economic potential of deep, direct use geothermal systems in the Netherlands.

Wassing, B.B.T., Buijze, L., Ter Heege, J.H., Orlic, B., Osinga, S., 2017. The impact of viscoelastic

caprock on fault reactivation and fault rupture in producing gas fields. 51st US Rock Mech. / Geomech. Symp. 2017 2, 1325–1337.

Zoback, M.D., Gorelick, S.M., 2012. Earthquake triggering and large-scale geologic storage of carbon dioxide. Proc. Natl. Acad. Sci. U. S. A. 109, 10164–10168. https://doi.org/10.1073/pnas.1202473109

*http://www.triaswestland.nl/*. (n.d.)

# 8. APPENDIX – Results of economic modelling and optimization

## 8.1 Introduction

A *case* is a combination of geological assumptions and decision alternatives.

Each case is tested for its compliance to a user-defined tolerance value for the maximum areal % of fault 3, 4 and 5 that is allowed to have a SCU value of >1. In many cases, this tolerance value is violated. The KPIs also indicate for how many years of the evaluation period of 40 years this tolerance norm has been violated, and flags the first year that this norm is violated in the simulation.

In total, 47 cases have been simulated and reported using COMSOL. All COMSOL *cases* have been imported into the economic XL model. Their economic performance is reported below. For each case, the same basic economic data are used, with some of the economic input data modelled stochastically (see table below: the cells coloured bright green). These stochastic economic data have been assigned a particular stochastic distribution each (pdf = probability density function). A Monte Carlo XL plug-in programme has been used to compute the case's output distribution for a series of selected KPIs (Key Performance Indicators). This allows also a sensitivity analysis to be done, in order to understand better which uncertain input variables contribute most to the uncertainty in some output-KPI.

## 8.2 Economic data model input all cases

The deterministic input values are indicated in the yellow cells below and have been selected as follows. Note that most input values would still need further verification / calibration.

**Model input - Scalar input variables - Case: Westland; 1500M,50mD,Tinj50,Q100,S-4,Kvh1**

| | |
|---|---|
| Geothermal doublet name | Westland |
| Reservoir, formation member | Vlieland |
| Doublet & case description | See comment in cell B6 |
| Name of case / decision-alternative | 1500M,50mD,Tinj50,Q100,S-4,Kvh1 |
| Injection & production rate (kg/s) | 100 & 100 |
| Evaluation period (first to last year) | 0 to 39 |
| Simulation data imported from file | 20200217_DESTRESS_SIMULATON_COMSOL.xlsx |
| Author economic workbook & affiliation | Christian Bos (TNO) |
| Author COMSOL data & affiliation | Sanaz Saeid (TUDelft) |
| Date | 20/02/2020 |

| Cost, tariff, planning data | Unit | Value |
|---|---|---|
| | | |
| | | |
| | | |
| Reference year for discounting | year | 0 |
| Discount rate | - | 10% |
| Heat sales tariff | €/kWh | 0.022 |
| | | |
| Pump energy costs (electricity) | €/kWh | 0.25 |
| Flow lines capex | million € | 0.50 |
| Heat exchanger capex | million € | 0.25 |
| Production well drill&compl capex | million € | 16.00 |
| Injection well drill&compl capex | million € | 16.00 |
| Production pump capex | million € | 0.25 |
| Injection pump capex | million € | 0.25 |
| Other capex | million € | 1.00 |
| Subsidies capex | million € | 5.00 |
| O&M fixed opex | million €/yr | 1.25 |
| Variable opex other than lifting costs | €/kg | 0.040 |
| Subsidy per unit heat sales | €/kWh sales | 0.000 |
| Economic stopping criterion: #yrs@NCF<0 | years | 3 |
| Minimum number of inj/prod years | years | 6 |
| Capex multiplier | - | 1.00 |
| Fixed opex multiplier | - | 1.00 |
| | | |
| | | |

| Technical data | Unit | Value |
|---|---|---|
| FBHP (initial) of producer | MPa | 35.1 |
| FBHT (initial) of producer | °C | 140.0 |
| Producer initial vertical ΔP FTHP - FBHP | MPa | 32.8 |
| Producer initial vertical ΔT FTHT - FBHT | °C | 0.0 |
| ΔP wellhead producer to heat exchanger, incl ΔP choke | MPa | 1.4 |
| ΔT wellhead producer to heat exchanger | °C | 8.0 |
| Operating pressure of heat exchanger | MPa | 0.6 |
| ΔP across heat exchanger | MPa | 0.6 |
| ΔT across heat exchanger ($T_{inlet}$ - $T_{outlet}$ of Heat Exchanger) | °C | 90.0 |
| ΔP heat exchanger to wellhead injector | MPa | 0.4 |
| ΔT heat exchanger to wellhead injector | °C | 0.0 |
| Injector ΔP FTHP - FBHP | MPa | 37.8 |
| Injector ΔT FTHT - FBHT | °C | |
| Depth of pump in production well | m tv | 2200.0 |
| Specific gravity of formation water | kg/m3 | 1020.0 |
| Pump efficiency of ESP and injection pump | % | 65.0% |
| Thermal efficiency of heat exchanger | - | 95% |
| Production well top of perforations | m tv | 2965.0 |
| Injection well top of perforations | m tv | 2970.0 |
| Initial reservoir pressure | MPa | 30.2 |
| Tubing inner diameter | m | 0.15 |
| Initial reservoir temperature | °C | 140.0 |
| Reservoir permeability | mD | 50.0 |
| Distance between injector/producer at top reservoir | m | 1400 |
| Geomech. / seismicity SCU>1 areal fault% tolerance | % | 2.0 |

| Legend | |
|---|---|
| Input variable (deterministic) | |
| Input: stochastic input variable (CB-pdf) | |
| Input: decision (CB) / deterministic assumption | |
| Output: calculated deterministic result | |
| Output: CB 'Forecast', CB-histogram | |
| Special, see comment | |
| Imported value from 'reservoir simulation' worksheet | |
| Value for display only, not for calculation purposes | |
| *Note: CB = Crystal Ball* | |
| *Note: filling-in cells with this colour is required:* | |
| *If no value is filled in, zero or blank will be assumed* | |
| to be extracted from case name (DecAltName) | |
| to be extracted from case name (DecAltName) | |

The stochastic input values are indicated in the bright green cells above and have been selected as follows. Note that all stochastic input variables have been assumed uncorrelated. For the units of the input variable distributions, see the table above.

*Assumption: Variable opex other than lifting costs · 2* *Cell: C32*

Uniform distribution with parameters:

| | |
|---|---|
| Minimum | 0.030 |
| Maximum | 0.050 |

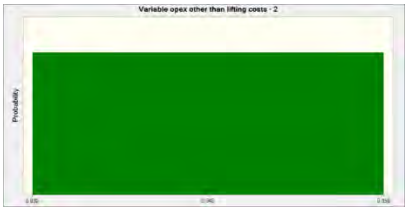


*Cell: C33*

*Assumption: Subsidy per unit heat sales · 2*

Uniform distribution with parameters:

| | |
|---|---|
| Minimum | 0.000 |
| Maximum | 0.020 |


*Cell: C30*

*Assumption: Subsidies capex · 2*

Uniform distribution with parameters:

| | |
|---|---|
| Minimum | 0.00 |
| Maximum | 10.00 |

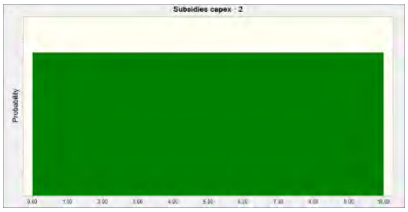


*Cell: C22*

*Assumption: Pump energy costs (electricity) · 2*

Uniform distribution with parameters:

| | |
|---|---|
| Minimum | 0.20 |
| Maximum | 0.30 |

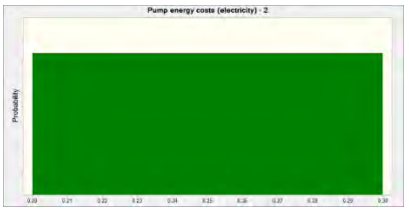


*Cell: C25*

*Assumption: Production well drill&compl capex · 2*

Triangular distribution with parameters:

| | |
|---|---|
| Minimum | 12.00 |
| Likeliest | 16.00 |
| Maximum | 20.00 |

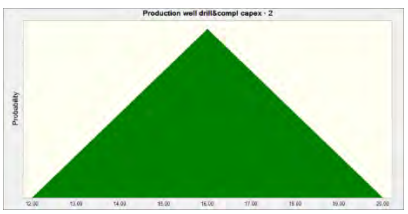


*Cell: C26*

*Assumption: Injection well drill&compl capex · 2*

Triangular distribution with parameters:

| | |
|---|---|
| Minimum | 12.00 |
| Likeliest | 16.00 |
| Maximum | 20.00 |

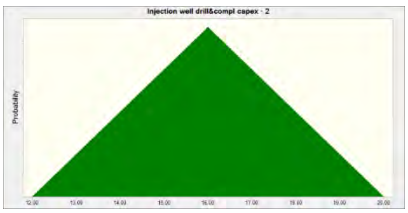


Cell: C20

*Assumption: Heat sales tariff · 2*

Uniform distribution with parameters:

| | |
|---|---|
| Minimum | 0.015 |
| Maximum | 0.029 |

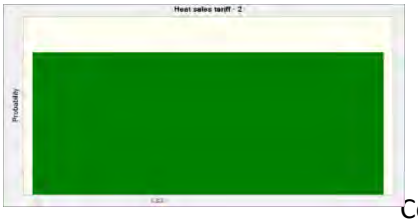


Cell: C36

*Assumption: Capex multiplier · 2*

Triangular distribution with parameters:

| | |
|---|---|
| Minimum | 0.80 |
| Likeliest | 1.00 |
| Maximum | 1.35 |

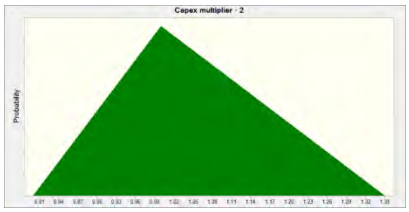


Cell: C37

*Assumption: Fixed opex multiplier · 2*

Triangular distribution with parameters:

| | |
|---|---|
| Minimum | 0.80 |
| Likeliest | 1.00 |
| Maximum | 1.35 |

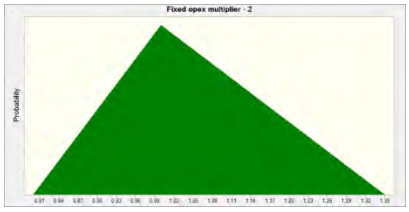


The results of the various cases are described in the sections below.

## Case 1 - 1500M,50mD,Tinj50,Q20,S-4,Kvh1

### Deterministic output using basic economic data

The deterministic KPI-output of case 1 is given in the table below.

**Key Performance Indicators of case Westland; 1500M,50mD,Tinj50,Q20,S-4,Kvh1**

Case description: See comment in cell B6; Injection rate: 20 & 20 kg/s. Evaluation period 40 years
Heat-sales price = € 0.022/kWh; subsidy = € 0/kWh heat sales
Discount rate = 10%

| KPI | Value | Unit | Comment |
|---|---|---|---|
| **Realized cumulative water production over full evaluation period** | 3.79E+03 | 10^6 kg | Constrained by economic field close-in criterion (3yrs@NCF<0 \| ≥6 yrs production&injection) |
| **Ultimate heat sales over full evaluation period, undiscounted** | 330 | GWh | Constrained by economic field close-in criterion (3yrs@NCF<0 \| ≥6 yrs production&injection) |
| **Ultimate heat sales over full evaluation period, discounted** | 263 | GWh | Constrained by economic field close-in criterion (3yrs@NCF<0 \| ≥6 yrs production&injection) |
| **Pre-tax NPV (ref yr 0; disc rate 10%) at end of evaluation period** | -32.3 | M€ | Constrained by economic field close-in criterion (3yrs@NCF<0 \| ≥6 yrs production&injection) |
| **Pre-tax IRR** (if NPV<0, the IRR is set to -100%) | -100.0% | % | Capital efficiency measure |
| **Pre-tax VIR** (Value Investment Ratio = NPV / PV(capex) | -0.94 | ratio | Capital efficiency measure |
| **Maximum exposure** (discounted = undiscounted as all capex in yr 0) | -33.13 | M€ | As all capex is spent in 1st yr of evaluation, the max exposure will occur in that yr |
| **Pay-out time, undiscounted (pre-tax)** | No pay-out | yrs | |
| **Pay-out time, discounted (pre-tax)** | No pay-out | yrs | |
| **Cumulative capex + opex (undiscounted)** | 114.1 | M€ | |
| **Cumulative capex + opex (discounted)** | 55.0 | M€ | |
| **UTC** (Unit Technical Cost: costs and produced heat-sales volumes undiscounted) | 0.3461 | €/kWh | |
| **LCOH** (Levelised Cost Of Heat: costs and produced heat-sales volumes discounted) | 0.2088 | €/kWh | |
| **Year of closing-in the geothermal doublet** | Year 6 | | |
| **Total nr of years that tolerance of areal % @SCU>1 of fault#3 is violated** | 0 | yrs | Assumed areal % tolerance of fault with SCU>1 = 2%. 1st yr of violation: Tolerance not violated over full evaluation period |
| **Total nr of years that tolerance of areal % @SCU>1 of fault#4 is violated** | 0 | yrs | Assumed areal % tolerance of fault with SCU>1 = 2%. 1st yr of violation: Tolerance not violated over full evaluation period |
| **Total nr of years that tolerance of areal % @SCU>1 of fault#5 is violated** | 0 | yrs | Assumed areal % tolerance of fault with SCU>1 = 2%. 1st yr of violation: Tolerance not violated over full evaluation period |

## Probabilistic output

The probabilistic KPI-output of case 1 is given in the graphs below. Although computed, the statistical moments and the percentiles are not reported here. The pre-tax NPV is distributed as follows:

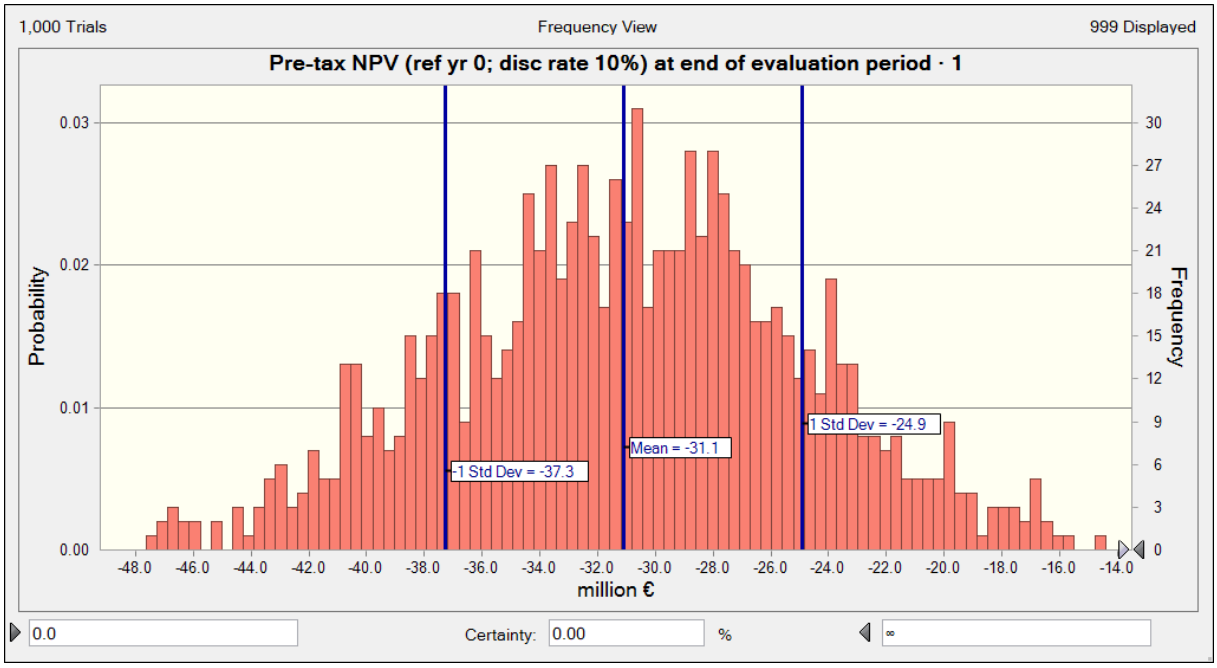


The maximum exposure is distributed as follows:

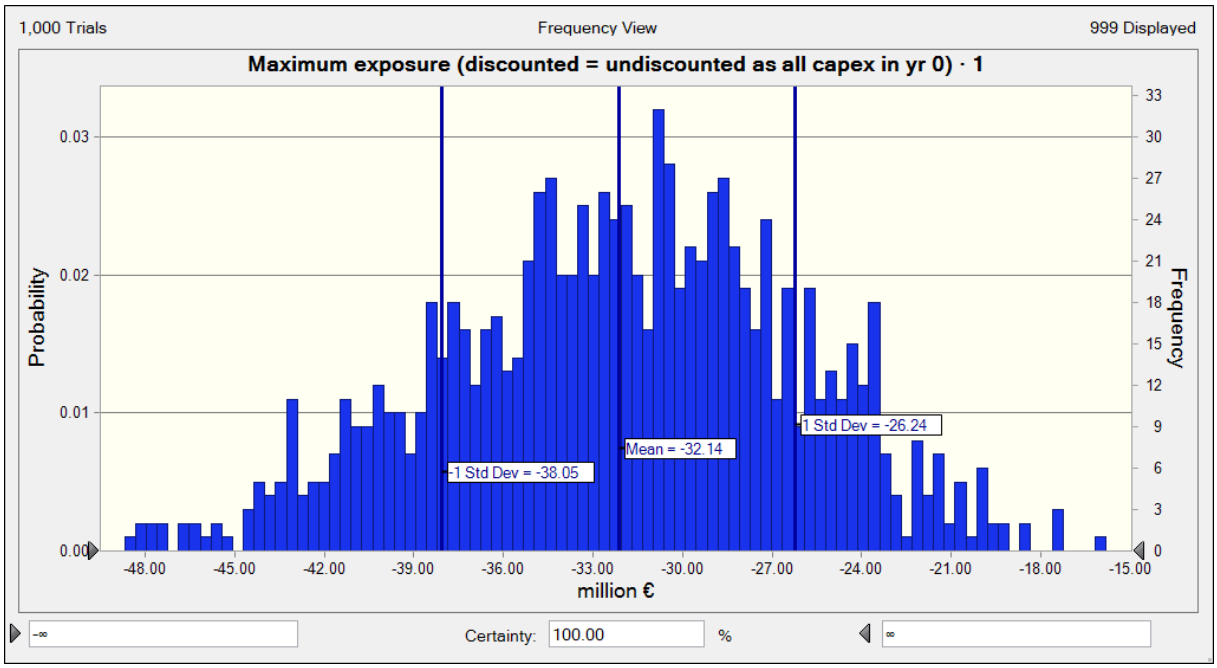


The Levelised Cost of Heat is distributed as follows:

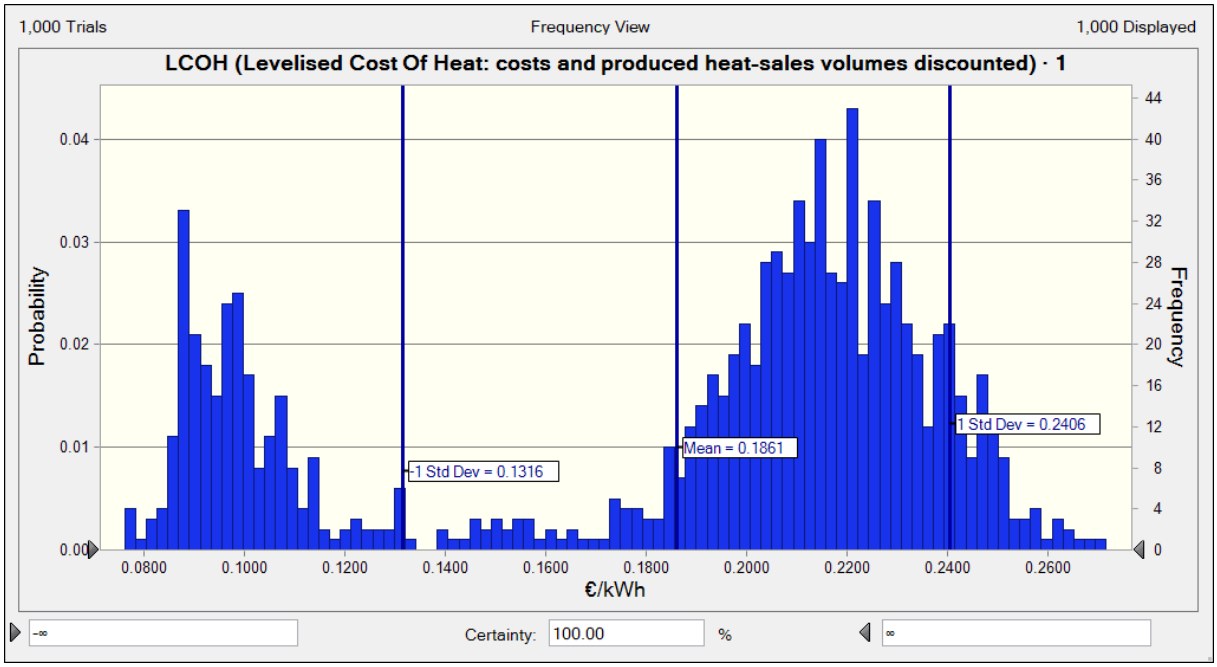


The above bimodal output distribution for the Levelized Cost Of Heat stems from the selection of the economic stopping criteria (i.e. a minimum of 6 years injection and production; after this period, close-in the geothermal doublet as soon as 3 consecutive years with a negative net cashflow have been observed).

## Sensitivity analysis

The contribution to variance of the NPV stems from the uncertainties in the following stochastic input variables:

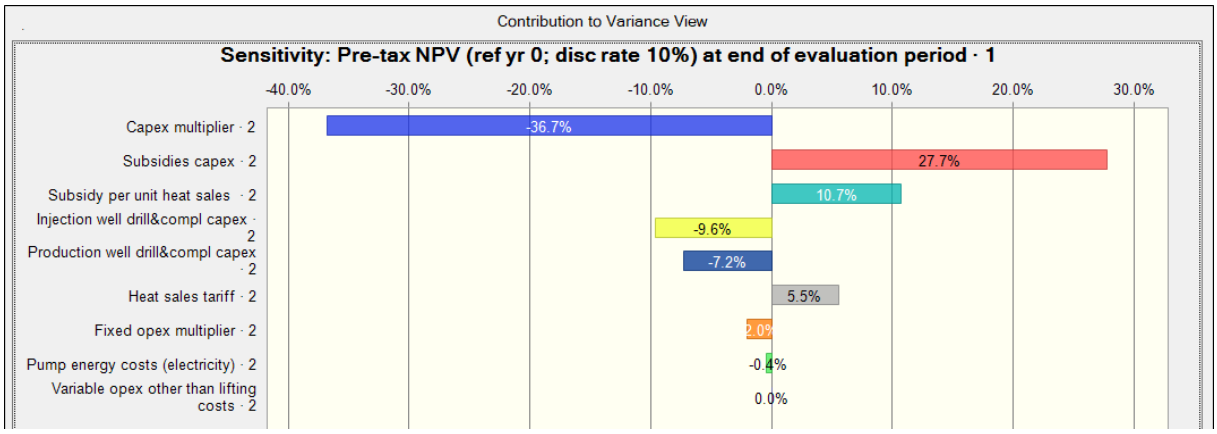


## Case 2 - 1500M,50mD,Tinj50,Q30,S-4,Kvh1

### Deterministic output using basic economic data

The deterministic KPI-output of case 1 is given in the table below.

**Key Performance Indicators of case Westland; 1500M,50mD,Tinj50,Q30,S-4,Kvh1**

Case description: See comment in cell B6; injection rate: 30 & 30 kg/s. Evaluation period 40 years
Heat-sales price = € 0.022/kWh; subsidy = € 0/kWh heat sales
Discount rate = 10%

| KPI | Value | Unit | Comment |
|---|---|---|---|
| **Realized cumulative water production over full evaluation period** | **5.68E+03** | 10^6 kg | Constrained by economic field close-in criterion (3yrs@NCF<0 \| ≥6 yrs production&injection) |
| **Ultimate heat sales over full evaluation period, undiscounted** | **505** | GWh | Constrained by economic field close-in criterion (3yrs@NCF<0 \| ≥6 yrs production&injection) |
| **Ultimate heat sales over full evaluation period, discounted** | **403** | GWh | Constrained by economic field close-in criterion (3yrs@NCF<0 \| ≥6 yrs production&injection) |
| **Pre-tax NPV (ref yr 0; disc rate 10%) at end of evaluation period** | **-30.7** | M€ | Constrained by economic field close-in criterion (3yrs@NCF<0 \| ≥6 yrs production&injection) |
| **Pre-tax IRR** (if NPV<0, the IRR is set to -100%) | **-100.0%** | % | Capital efficiency measure |
| **Pre-tax VIR** (Value Investment Ratio = NPV / PV(capex) | **-0.90** | ratio | Capital efficiency measure |
| **Maximum exposure** (discounted = undiscounted as all capex in yr 0) | **-31.14** | M€ | As all capex is spent in 1st yr of evaluation, the max exposure will occur in that yr |
| **Pay-out time, undiscounted (pre-tax)** | **No pay-out** | yrs | |
| **Pay-out time, discounted (pre-tax)** | **No pay-out** | yrs | |
| **Cumulative capex + opex (undiscounted)** | **130.8** | M€ | |
| **Cumulative capex + opex (discounted)** | **58.8** | M€ | |
| **UTC** (Unit Technical Cost: costs and produced heat-sales volumes undiscounted) | **0.2591** | €/kWh | |
| **LCOH** (Levelised Cost Of Heat: costs and produced heat-sales volumes discounted) | **0.1459** | €/kWh | |
| **Year of closing-in the geothermal doublet** | **Year 6** | | |
| **Total nr of years that tolerance of areal % @SCU>1 of fault#3 is violated** | **0** | yrs | Assumed areal % tolerance of fault with SCU>1 = 2%. 1st yr of violation: Tolerance not violated over full evaluation period |
| **Total nr of years that tolerance of areal % @SCU>1 of fault#4 is violated** | **0** | yrs | Assumed areal % tolerance of fault with SCU>1 = 2%. 1st yr of violation: Tolerance not violated over full evaluation period |
| **Total nr of years that tolerance of areal % @SCU>1 of fault#5 is violated** | **0** | yrs | Assumed areal % tolerance of fault with SCU>1 = 2%. 1st yr of violation: Tolerance not violated over full evaluation period |

### Probabilistic output

The probabilistic KPI-output of case 1 is given in the graphs below. Although computed, the statistical moments and the percentiles are not reported here. The pre-tax NPV is distributed as follows:

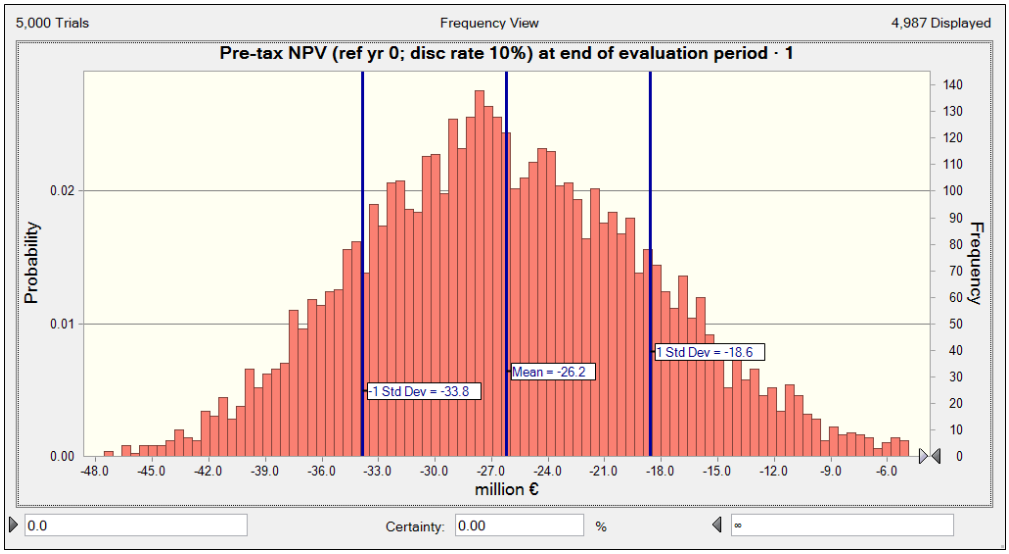

The maximum exposure is distributed as follows:

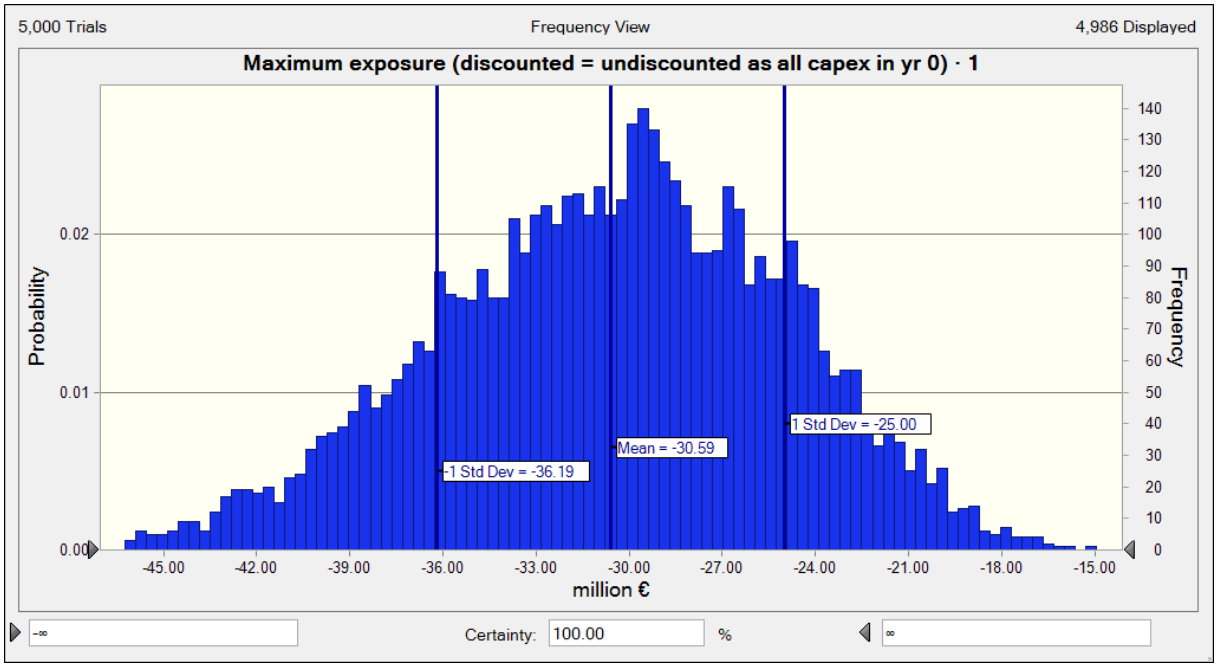


The Levelised Cost of Heat is distributed as follows:

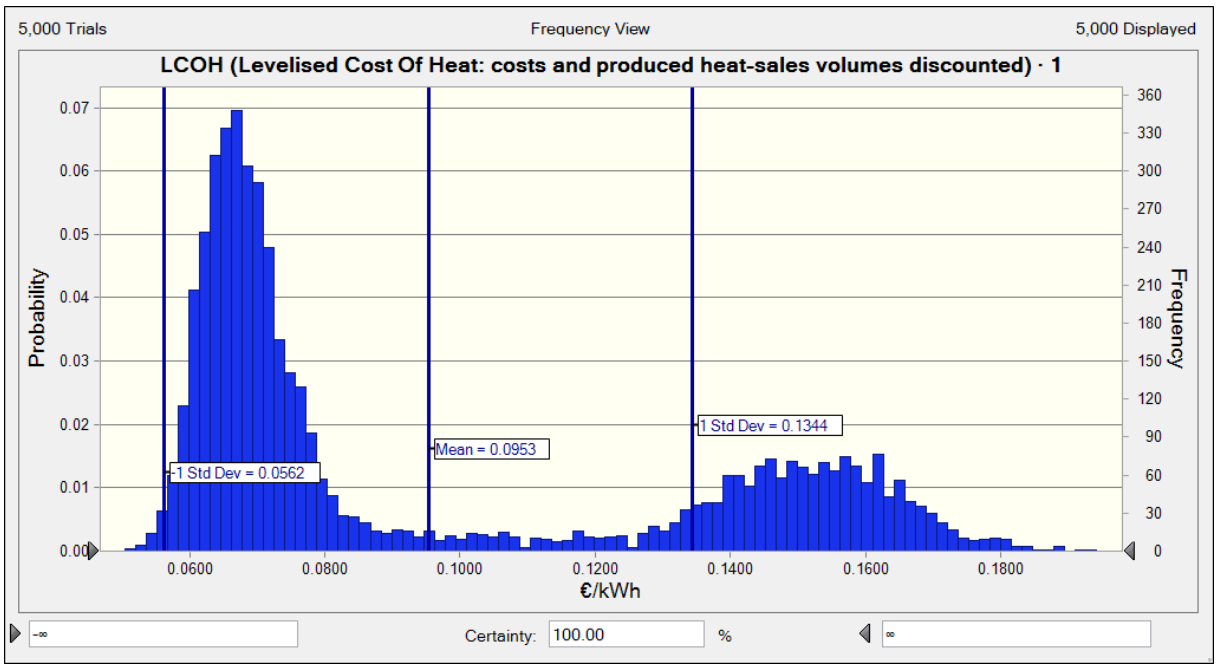


Interestingly, this yields a bimodal output distribution, which is caused by the economic cut-off criteria of the model.

## Sensitivity analysis

The contribution to variance of the NPV stems from the uncertainties in the following stochastic input variables:

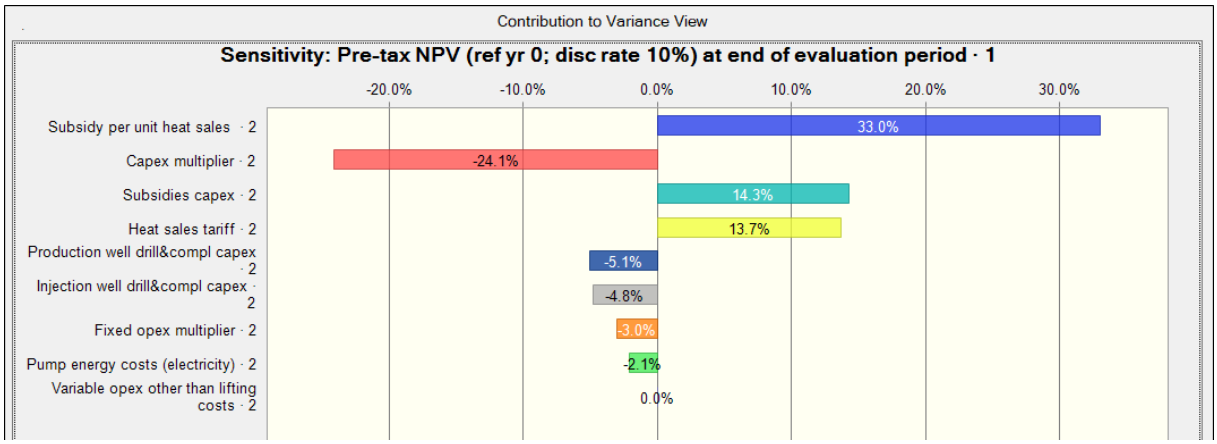


## Case 3 - 1500M,50mD,Tinj50,Q40,S-4,Kvh1

### Deterministic output using basic economic data

The deterministic KPI-output of case 1 is given in the table below.

**Key Performance Indicators of case Westland; 1500M,50mD,Tinj50,Q40,S-4,Kvh1**

Case description: See comment in cell B6; Injection rate; 40 & 40 kg/s. Evaluation period 40 years
Heat-sales price = € 0.022/kWh; subsidy = € 0/kWh heat sales
Discount rate = 10%

| KPI | Value | Unit | Comment |
|---|---|---|---|
| **Realized cumulative water production over full evaluation period** | **7.57E+03** | 10^6 kg | Constrained by economic field close-in criterion (3yrs@NCF<0 \| ≥6 yrs production&injection) |
| **Ultimate heat sales over full evaluation period, undiscounted** | **679** | GWh | Constrained by economic field close-in criterion (3yrs@NCF<0 \| ≥6 yrs production&injection) |
| **Ultimate heat sales over full evaluation period, discounted** | **542** | GWh | Constrained by economic field close-in criterion (3yrs@NCF<0 \| ≥6 yrs production&injection) |
| **Pre-tax NPV (ref yr 0; disc rate 10%) at end of evaluation period** | **-29.1** | M€ | Constrained by economic field close-in criterion (3yrs@NCF<0 \| ≥6 yrs production&injection) |
| **Pre-tax IRR** (if NPV<0, the IRR is set to -100%) | **-100.0%** | % | Capital efficiency measure |
| **Pre-tax VIR** (Value Investment Ratio = NPV / PV(capex) | **-0.85** | ratio | Capital efficiency measure |
| **Maximum exposure** (discounted = undiscounted as all capex in yr 0) | **-29.23** | M€ | As all capex is spent in 1st yr of evaluation, the max exposure will occur in that yr |
| **Pay-out time, undiscounted (pre-tax)** | **No pay-out** | yrs | |
| **Pay-out time, discounted (pre-tax)** | **No pay-out** | yrs | |
| **Cumulative capex + opex (undiscounted)** | **148.7** | M€ | |
| **Cumulative capex + opex (discounted)** | **62.9** | M€ | |
| **UTC** (Unit Technical Cost: costs and produced heat-sales volumes undiscounted) | **0.2191** | €/kWh | |
| **LCOH** (Levelised Cost Of Heat: costs and produced heat-sales volumes discounted) | **0.1160** | €/kWh | |
| **Year of closing-in the geothermal doublet** | **Year 6** | | |
| **Total nr of years that tolerance of areal % @SCU>1 of fault#3 is violated** | **0** | yrs | Assumed areal % tolerance of fault with SCU>1 = 2%. 1st yr of violation: Tolerance not violated over full evaluation period |
| **Total nr of years that tolerance of areal % @SCU>1 of fault#4 is violated** | **0** | yrs | Assumed areal % tolerance of fault with SCU>1 = 2%. 1st yr of violation: Tolerance not violated over full evaluation period |
| **Total nr of years that tolerance of areal % @SCU>1 of fault#5 is violated** | **0** | yrs | Assumed areal % tolerance of fault with SCU>1 = 2%. 1st yr of violation: Tolerance not violated over full evaluation period |

### Probabilistic output

The probabilistic KPI-output of case 1 is given in the graphs below. Although computed, the statistical moments and the percentiles are not reported here. The pre-tax NPV is distributed as follows:

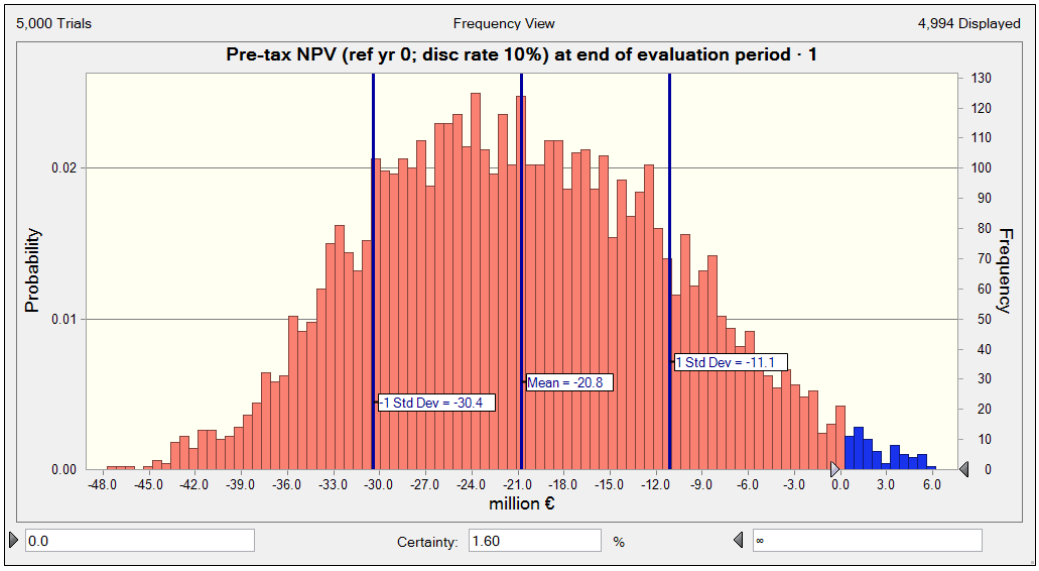

The maximum exposure is distributed as follows:

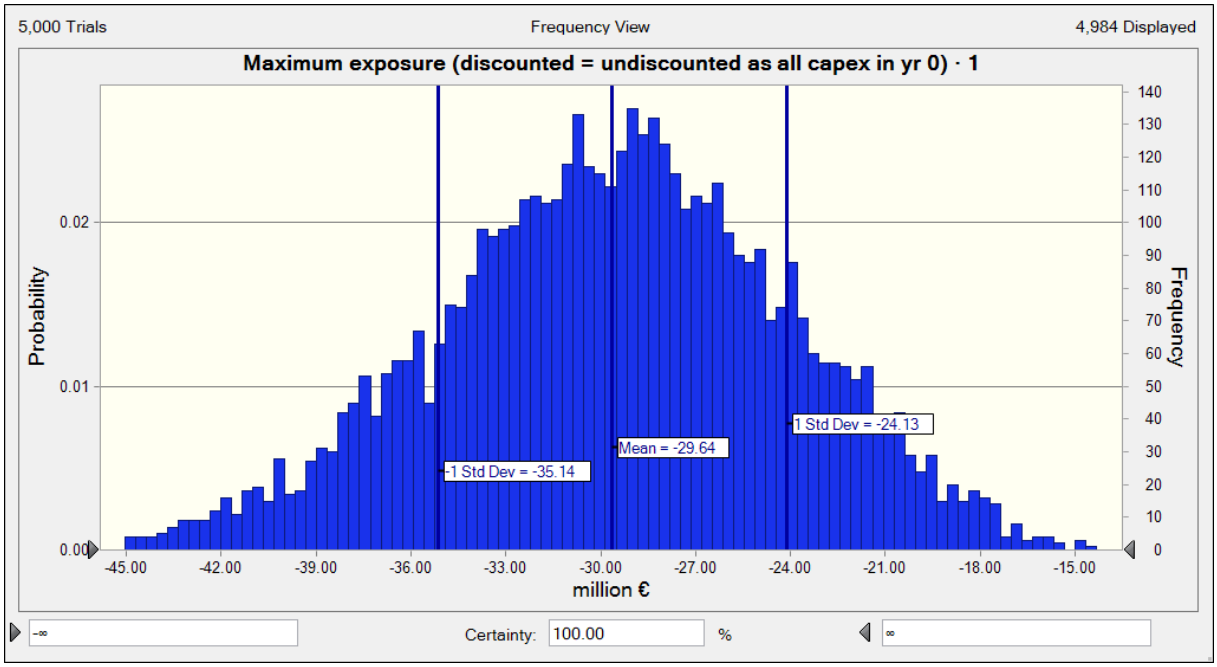


The Levelised Cost of Heat is distributed as follows:

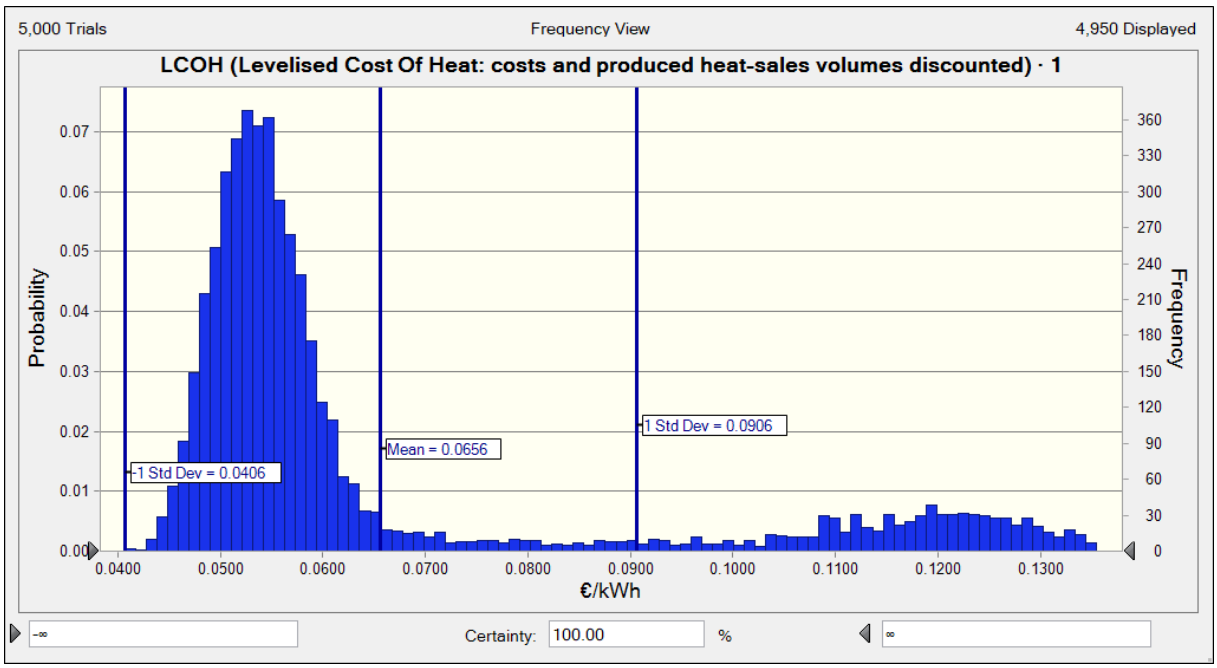


## Sensitivity analysis

The contribution to variance of the NPV stems from the uncertainties in the following stochastic input variables:

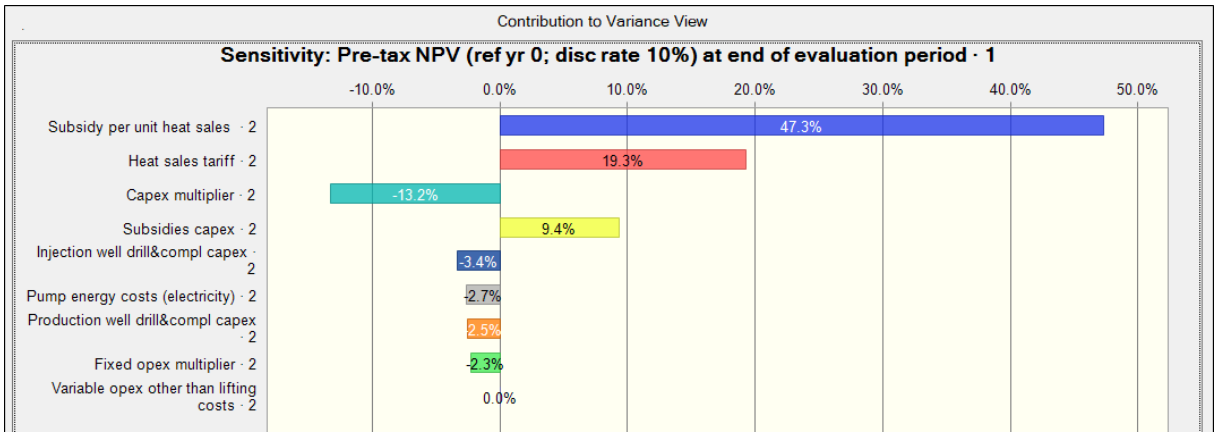


## Case 4 - 1500M,50mD,Tinj50,Q50,S-4,Kvh1

### Deterministic output using basic economic data

The deterministic KPI-output of case 1 is given in the table below.

**Key Performance Indicators of case Westland; 1500M,50mD,Tinj50,Q50,S-4,Kvh1**

Case description: See comment in cell B6; Injection rate: 50 & 50 kg/s. Evaluation period 40 years
Heat-sales price = € 0.022/kWh; subsidy = € 0/kWh heat sales
Discount rate = 10%

| KPI | Value | Unit | Comment |
|---|---|---|---|
| **Realized cumulative water production over full evaluation period** | 1.74E+04 | 10^6 kg | Constrained by economic field close-in criterion (3yrs@NCF<0 \| ≥6 yrs production&injection) |
| **Ultimate heat sales over full evaluation period, undiscounted** | 1562 | GWh | Constrained by economic field close-in criterion (3yrs@NCF<0 \| ≥6 yrs production&injection) |
| **Ultimate heat sales over full evaluation period, discounted** | 1015 | GWh | Constrained by economic field close-in criterion (3yrs@NCF<0 \| ≥6 yrs production&injection) |
| **Pre-tax NPV (ref yr 0; disc rate 10%) at end of evaluation period** | -27.6 | M€ | Constrained by economic field close-in criterion (3yrs@NCF<0 \| ≥6 yrs production&injection) |
| **Pre-tax IRR** (if NPV<0, the IRR is set to -100%) | -100.0% | % | Capital efficiency measure |
| **Pre-tax VIR** (Value Investment Ratio = NPV / PV(capex) | -0.81 | ratio | Capital efficiency measure |
| **Maximum exposure** (discounted = undiscounted as all capex in yr 0) | -28.41 | M€ | As all capex is spent in 1st yr of evaluation, the max exposure will occur in that yr |
| **Pay-out time, undiscounted (pre-tax)** | No pay-out | yrs | |
| **Pay-out time, discounted (pre-tax)** | No pay-out | yrs | |
| **Cumulative capex + opex (undiscounted)** | 167.9 | M€ | |
| **Cumulative capex + opex (discounted)** | 67.1 | M€ | |
| **UTC** (Unit Technical Cost: costs and produced heat-sales volumes undiscounted) | 0.1075 | €/kWh | |
| **LCOH** (Levelised Cost Of Heat: costs and produced heat-sales volumes discounted) | 0.0661 | €/kWh | |
| **Year of closing-in the geothermal doublet** | Year 11 | | |
| **Total nr of years that tolerance of areal % @SCU>1 of fault#3 is violated** | 0 | yrs | Assumed areal % tolerance of fault with SCU>1 = 2%. 1st yr of violation: Tolerance not violated over full evaluation period |
| **Total nr of years that tolerance of areal % @SCU>1 of fault#4 is violated** | 0 | yrs | Assumed areal % tolerance of fault with SCU>1 = 2%. 1st yr of violation: Tolerance not violated over full evaluation period |
| **Total nr of years that tolerance of areal % @SCU>1 of fault#5 is violated** | 0 | yrs | Assumed areal % tolerance of fault with SCU>1 = 2%. 1st yr of violation: Tolerance not violated over full evaluation period |

### Probabilistic output

The probabilistic KPI-output of case 1 is given in the graphs below. Although computed, the statistical moments and the percentiles are not reported here. The pre-tax NPV is distributed as follows:

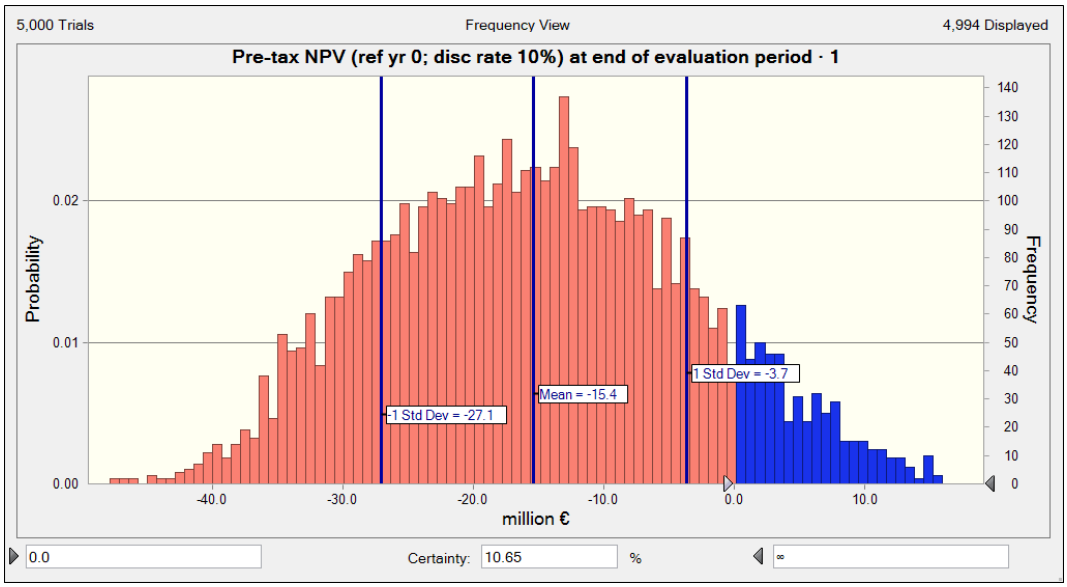

The maximum exposure is distributed as follows:

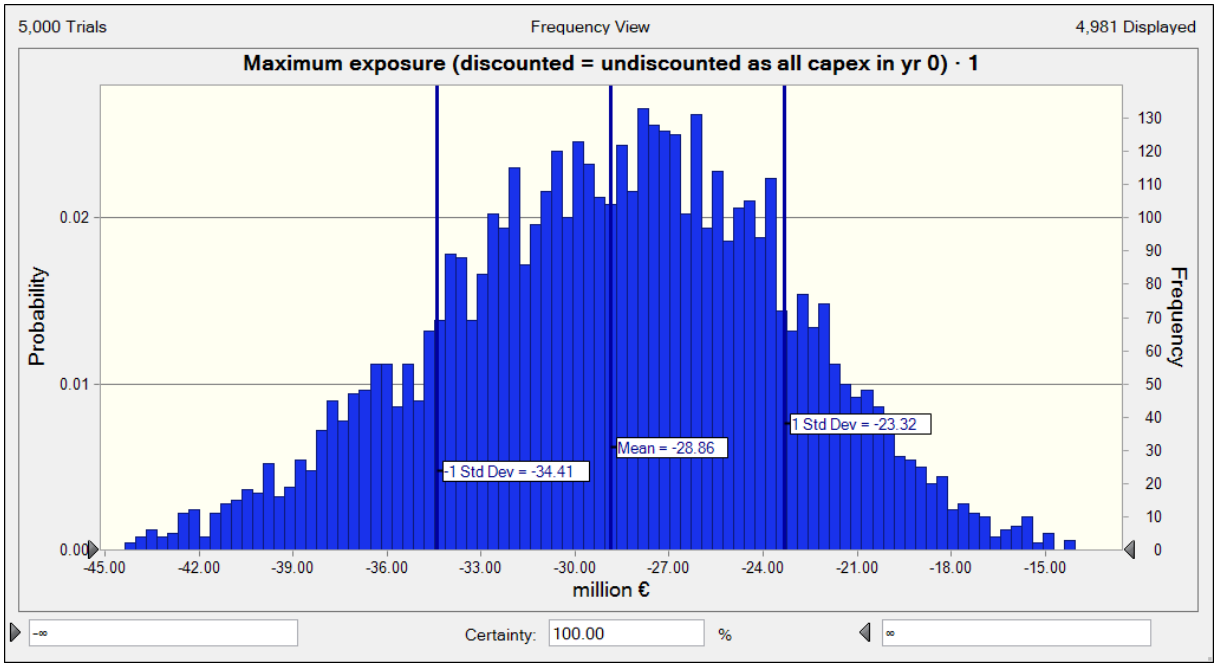


The Levelised Cost of Heat is distributed as follows:

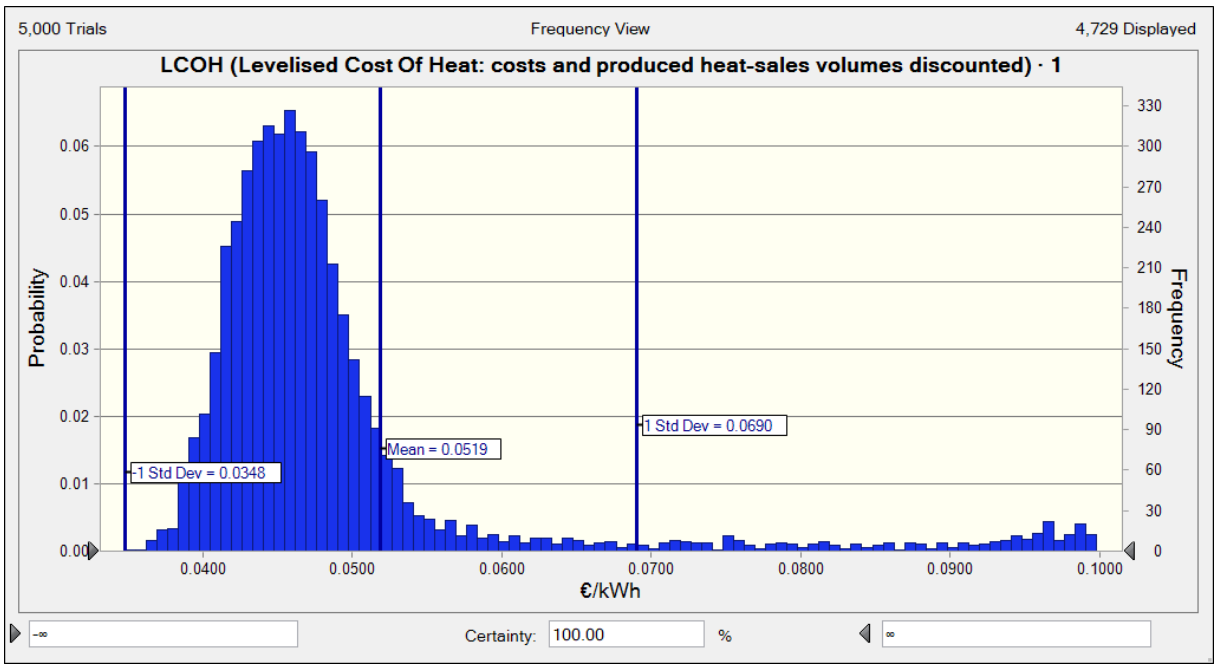


## Sensitivity analysis

The contribution to variance of the NPV stems from the uncertainties in the following stochastic input variables:

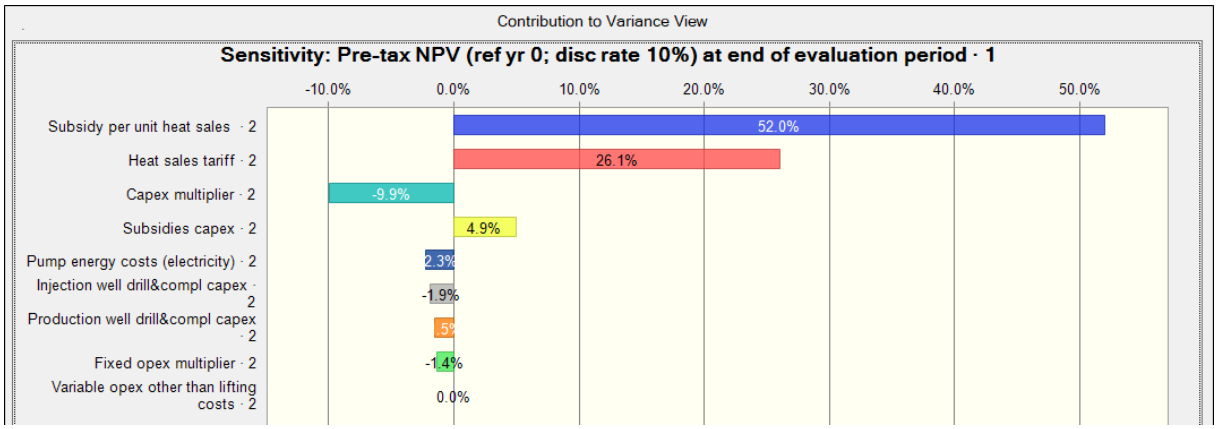


## Case 5 - 1500M,50mD,Tinj50,Q100,S-4,Kvh1

Deterministic output using basic economic data

The deterministic KPI-output of case 1 is given in the table below.

**Key Performance Indicators of case Westland; 1500M,50mD,Tinj50,Q100,S-4,Kvh1**

Case description: See comment in cell B6; Injection rate: 100 & 100 kg/s. Evaluation period 40 years
Heat-sales price = € 0.022/kWh; subsidy = € 0/kWh heat sales
Discount rate = 10%

| KPI | Value | Unit | Comment |
|---|---|---|---|
| **Realized cumulative water production over full evaluation period** | **7.26E+04** | 10^6 kg | Constrained by economic field close-in criterion (3yrs@NCF<0 \| ≥6 yrs production&injection) |
| **Ultimate heat sales over full evaluation period, undiscounted** | **6580** | GWh | Constrained by economic field close-in criterion (3yrs@NCF<0 \| ≥6 yrs production&injection) |
| **Ultimate heat sales over full evaluation period, discounted** | **2796** | GWh | Constrained by economic field close-in criterion (3yrs@NCF<0 \| ≥6 yrs production&injection) |
| **Pre-tax NPV (ref yr 0; disc rate 10%) at end of evaluation period** | **-17.3** | M€ | Constrained by economic field close-in criterion (3yrs@NCF<0 \| ≥6 yrs production&injection) |
| **Pre-tax IRR** (if NPV<0, the IRR is set to -100%) | **-100.0%** | % | Capital efficiency measure |
| **Pre-tax VIR** (Value Investment Ratio = NPV / PV(capex) | **-0.51** | ratio | Capital efficiency measure |
| **Maximum exposure** (discounted = undiscounted as all capex in yr 0) | **-26.28** | M€ | As all capex is spent in 1st yr of evaluation, the max exposure will occur in that yr |
| **Pay-out time, undiscounted (pre-tax)** | **No pay-out** | yrs | |
| **Pay-out time, discounted (pre-tax)** | **No pay-out** | yrs | |
| **Cumulative capex + opex (undiscounted)** | **281.0** | M€ | |
| **Cumulative capex + opex (discounted)** | **90.6** | M€ | |
| **UTC** (Unit Technical Cost: costs and produced heat-sales volumes undiscounted) | **0.0427** | €/kWh | |
| **LCOH** (Levelised Cost Of Heat: costs and produced heat-sales volumes discounted) | **0.0324** | €/kWh | |
| **Year of closing-in the geothermal doublet** | **Year 23** | | |
| **Total nr of years that tolerance of areal % @SCU>1 of fault#3 is violated** | **15** | yrs | Assumed areal % tolerance of fault with SCU>1 = 2%. 1st yr of violation: Year 25 |
| **Total nr of years that tolerance of areal % @SCU>1 of fault#4 is violated** | **0** | yrs | Assumed areal % tolerance of fault with SCU>1 = 2%. 1st yr of violation: Tolerance not violated over full evaluation period |
| **Total nr of years that tolerance of areal % @SCU>1 of fault#5 is violated** | **0** | yrs | Assumed areal % tolerance of fault with SCU>1 = 2%. 1st yr of violation: Tolerance not violated over full evaluation period |

Probabilistic output

The probabilistic KPI-output of case 1 is given in the graphs below. Although computed, the statistical moments and the percentiles are not reported here. The pre-tax NPV is distributed as follows.

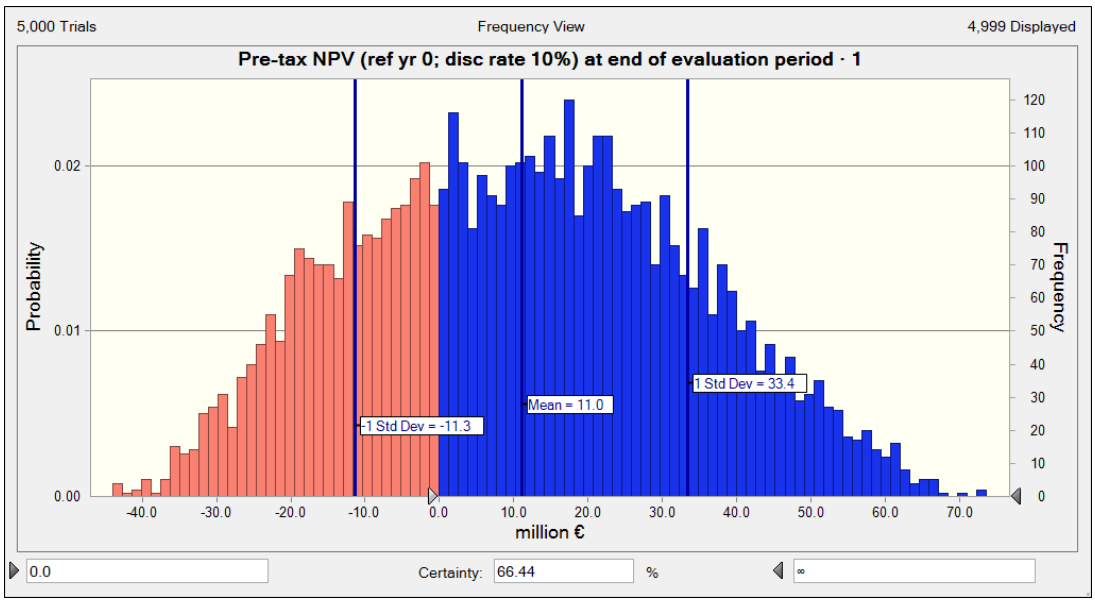

The maximum exposure is distributed as follows:

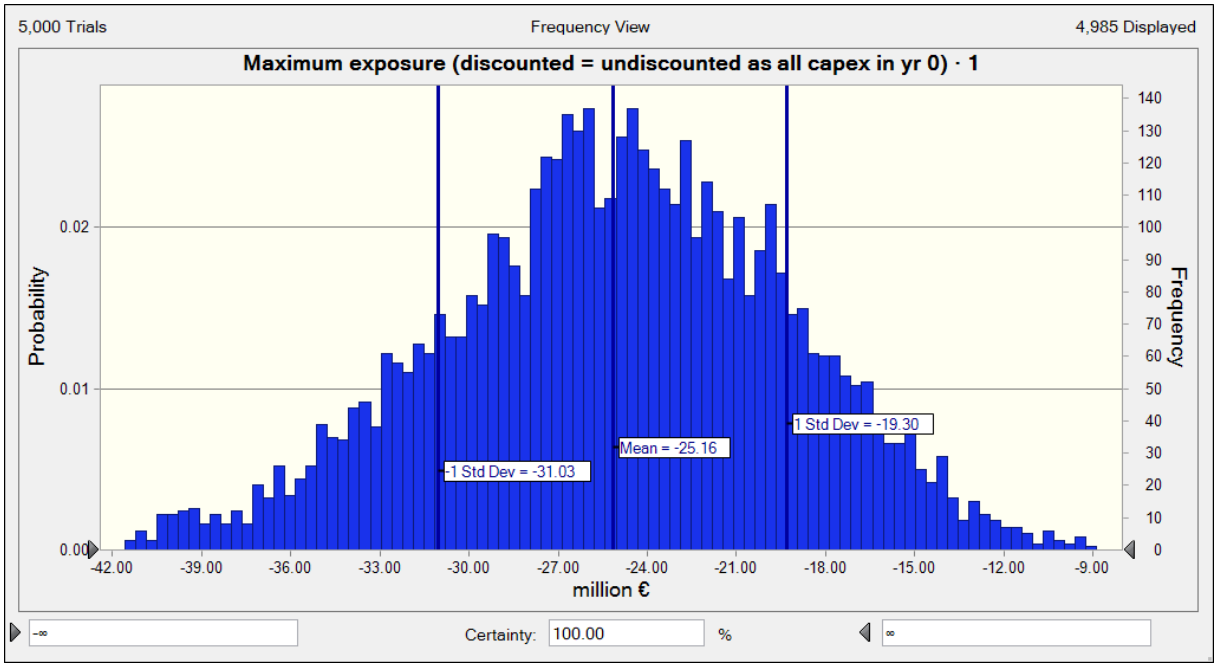


The Levelised Cost of Heat is distributed as follows:

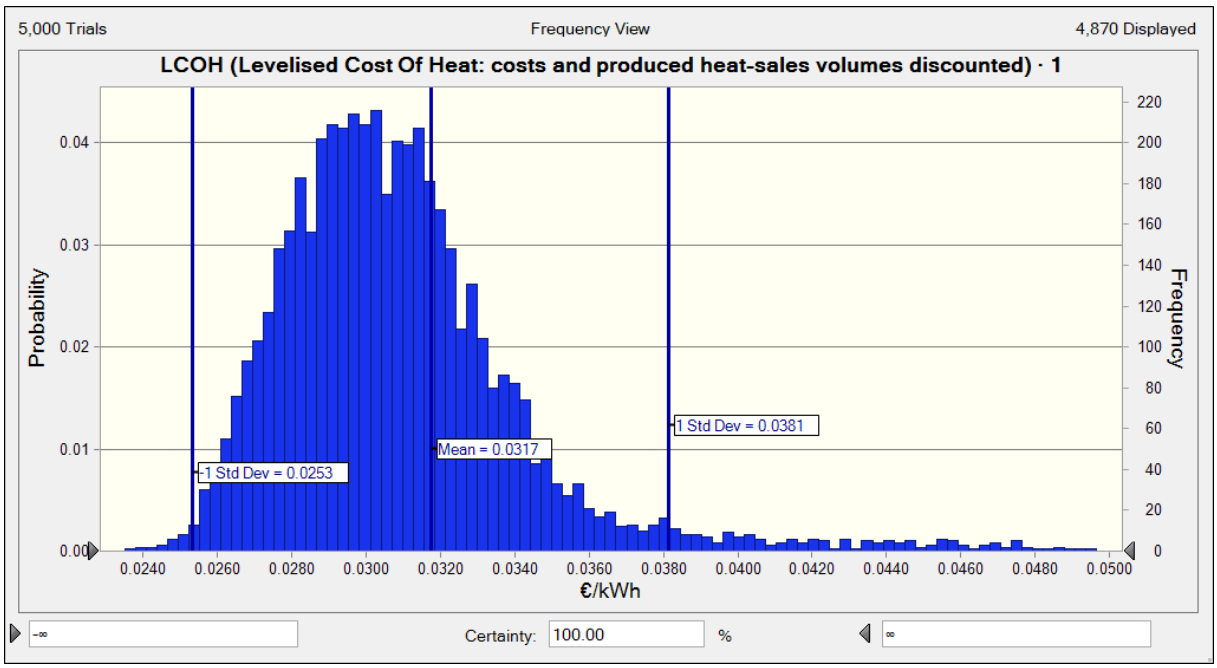


## Sensitivity analysis

The contribution to variance of the NPV stems from the uncertainties in the following stochastic input variables:

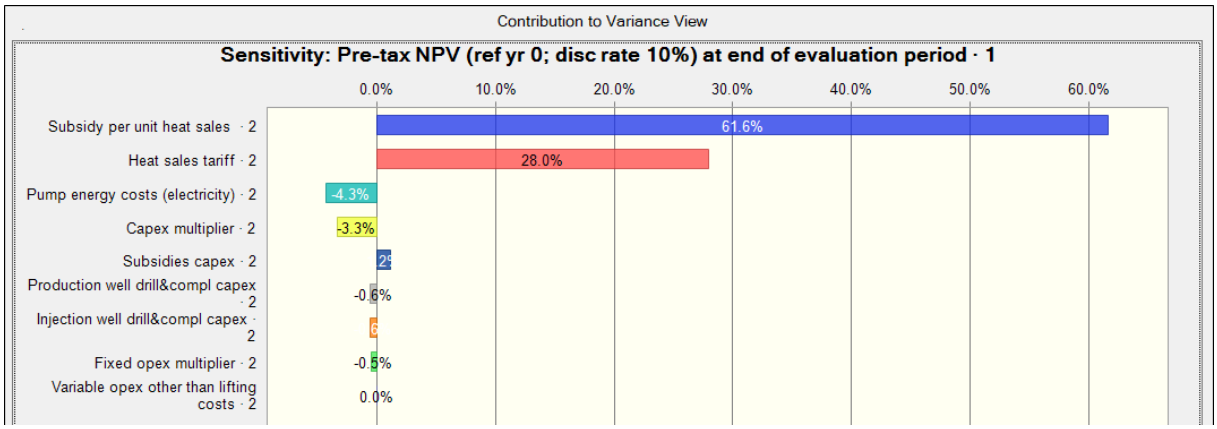


## Case 6 - 1400MM,50mD,Tinj50,Q40,S-4,Kvh1

Deterministic output using basic economic data

The deterministic KPI-output of case 1 is given in the table below.

**Key Performance Indicators of case Westland; 1400MM,50mD,Tinj50,Q40,S-4,Kvh1**

Case description: See comment in cell B6; Injection rate; 40 & 40 kg/s. Evaluation period 40 years
Heat-sales price = € 0.022/kWh; subsidy = € 0/kWh heat sales
Discount rate = 10%

| KPI | Value | Unit | Comment |
|---|---|---|---|
| **Realized cumulative water production over full evaluation period** | **7.57E+03** | 10^6 kg | Constrained by economic field close-in criterion (3yrs@NCF<0 \| ≥6 yrs production&injection) |
| **Ultimate heat sales over full evaluation period, undiscounted** | **679** | GWh | Constrained by economic field close-in criterion (3yrs@NCF<0 \| ≥6 yrs production&injection) |
| **Ultimate heat sales over full evaluation period, discounted** | **542** | GWh | Constrained by economic field close-in criterion (3yrs@NCF<0 \| ≥6 yrs production&injection) |
| **Pre-tax NPV (ref yr 0; disc rate 10%) at end of evaluation period** | **-29.0** | M€ | Constrained by economic field close-in criterion (3yrs@NCF<0 \| ≥6 yrs production&injection) |
| **Pre-tax IRR** (if NPV<0, the IRR is set to -100%) | **-100.0%** | % | Capital efficiency measure |
| **Pre-tax VIR** (Value Investment Ratio = NPV / PV(capex) | **-0.85** | ratio | Capital efficiency measure |
| **Maximum exposure** (discounted = undiscounted as all capex in yr 0) | **-29.05** | M€ | As all capex is spent in 1st yr of evaluation, the max exposure will occur in that yr |
| **Pay-out time, undiscounted (pre-tax)** | **No pay-out** | yrs | |
| **Pay-out time, discounted (pre-tax)** | **No pay-out** | yrs | |
| **Cumulative capex + opex (undiscounted)** | **147.4** | M€ | |
| **Cumulative capex + opex (discounted)** | **62.5** | M€ | |
| **UTC** (Unit Technical Cost: costs and produced heat-sales volumes undiscounted) | **0.2171** | €/kWh | |
| **LCOH** (Levelised Cost Of Heat: costs and produced heat-sales volumes discounted) | **0.1154** | €/kWh | |
| **Year of closing-in the geothermal doublet** | **Year 6** | | |
| **Total nr of years that tolerance of areal % @SCU>1 of fault#3 is violated** | **0** | yrs | Assumed areal % tolerance of fault with SCU>1 = 2%. 1st yr of violation: Tolerance not violated over full evaluation period |
| **Total nr of years that tolerance of areal % @SCU>1 of fault#4 is violated** | **0** | yrs | Assumed areal % tolerance of fault with SCU>1 = 2%. 1st yr of violation: Tolerance not violated over full evaluation period |
| **Total nr of years that tolerance of areal % @SCU>1 of fault#5 is violated** | **0** | yrs | Assumed areal % tolerance of fault with SCU>1 = 2%. 1st yr of violation: Tolerance not violated over full evaluation period |

Probabilistic output

The probabilistic KPI-output of case 1 is given in the graphs below. Although computed, the statistical moments and the percentiles are not reported here. The pre-tax NPV is distributed as follows:

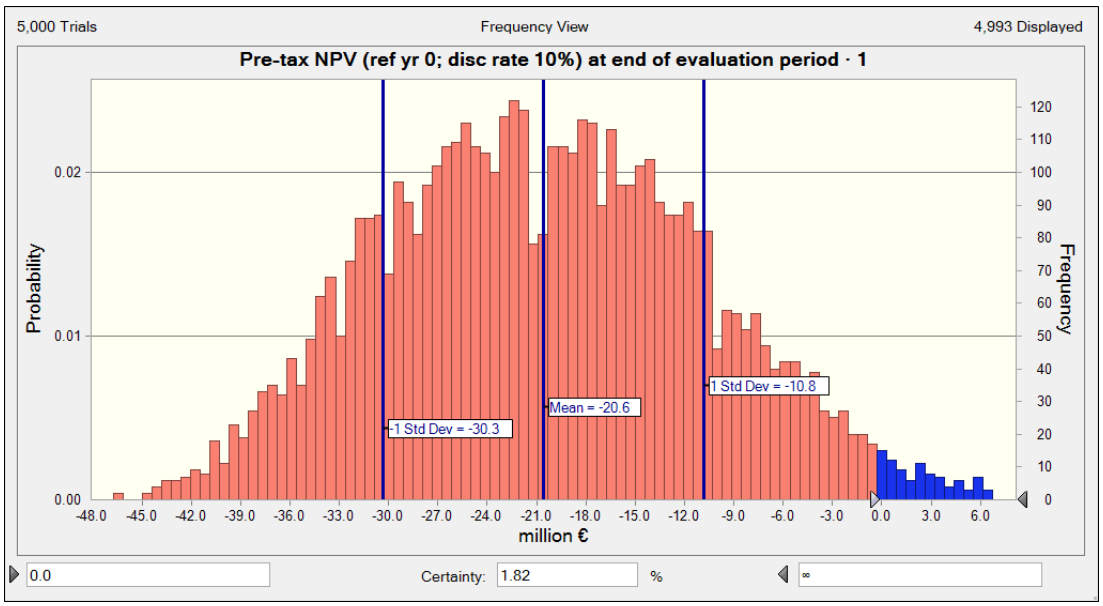

The maximum exposure is distributed as follows:

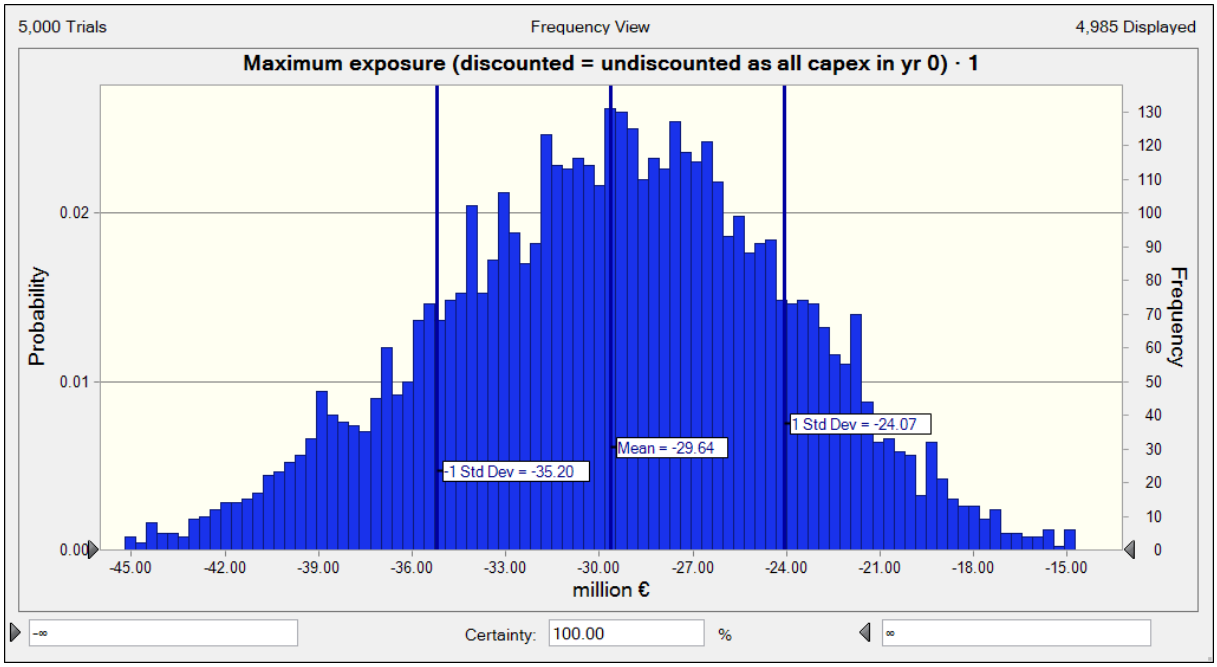


The Levelised Cost of Heat is distributed as follows:

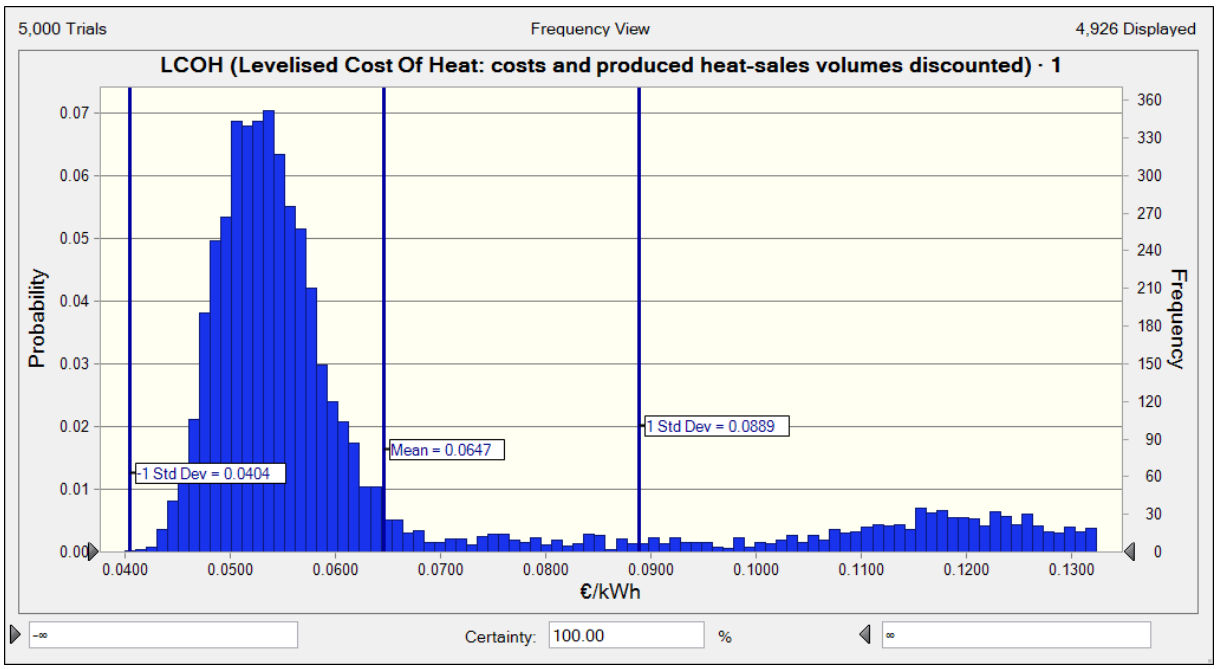


## Sensitivity analysis

The contribution to variance of the NPV stems from the uncertainties in the following stochastic input variables:

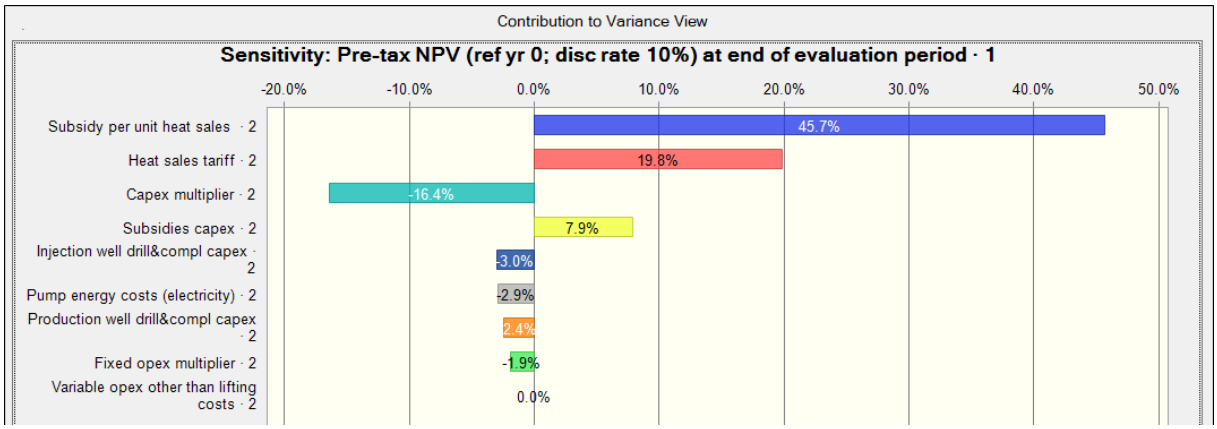


Note: Rather than continuing displaying the various economic performance histograms for the subsequent cases, it was decided to summarize all cases in a joint sensitivity table, allowing a more easy comparison between the cases. The above histograms however give an impression of what economic and technical detail can be computed and used for optimization purposes.

The sensitivity table for all cases is displayed on the following page.

# Key Performance Indicator comparison of Westland geothermal doublet cases

General assumptions: Evaluation period 40 years. Discount rate 10 %

| Nr | Case | Deterministic: fault3 nr yrs@areal tol SCU>1 | | Deterministic: fault4 nr yrs@areal tol SCU>1 | | Deterministic: fault5 nr yrs@areal tol SCU>1 | | Deterministic: year of C/I doublet (\|min 6 & 3 yrs NCF<0 ) | Probabilistic: Mean NPV (million €) | Probabilistic: probability of NPV>0 (%) | Probabilistic: mean LCOH (€ / kWh) | Probabilistic: sensitivity analysis, contr to NPV variance from subs/unit heat sales (%) | Probabilistic: sensitivity analysis, contr to NPV variance from heat sales tariff (%) | Probabilistic: sensitivity analysis, contr to NPV variance from capex multiplier (%) | Probabilistic: sensitivity analysis, contr to NPV variance from capex subsidy (%) | Probabilistic: sensitivity analysis, contr to NPV variance from pump energy costs (%) | Probabilistic: sensitivity analysis, contr to NPV variance from drillex prod well (%) | Probabilistic: sensitivity analysis, contr to NPV variance from drillex inj well (%) |
|---|---|---|---|---|---|---|---|---|---|---|---|---|---|---|---|---|---|---|
| | | F3 Σ yrs | F3 1st yr | F4 Σ yrs | F4 1st yr | F5 Σ yrs | F5 1st yr | C/I yrs | EMV (10^6 €) | $P_{NPV>0}$ (%) | mean LCOH (€ / kWh) | contr to NPV var from subs/unit heat sales (%) | contr to NPV var from heat sales tariff (%) | contr to NPV var from capex multiplier (%) | contr to NPV var from capex subsidy (%) | contr to NPV var from pump energy costs (%) | contr to NPV var from drillex prod well (%) | contr to NPV var from drillex inj well (%) |
| 1 | 1500M,50mD,Tinj50,Q20,S-4,Kvh1 | 0 | NA | 0 | NA | 0 | NA | 6 | -31.1 | 0.0 | 0.1861 | 10.7 | 5.5 | -36.7 | 27.7 | -0.4 | -7.2 | -9.4 |
| 2 | 1500M,50mD,Tinj50,Q30,S-4,Kvh1 | 0 | NA | 0 | NA | 0 | NA | 6 | -30.7 | 0.0 | 0.0953 | 33.0 | 13.7 | -24.1 | 14.3 | -2.1 | -5.1 | -4.8 |
| 3 | 1500M,50mD,Tinj50,Q40,S-4,Kvh1 | 0 | NA | 0 | NA | 0 | NA | 6 | -20.8 | 1.6 | 0.0656 | 47.3 | 19.3 | -13.2 | 9.4 | -2.7 | -2.5 | -3.4 |
| 4 | 1500M,50mD,Tinj50,Q50,S-4,Kvh1 | 0 | NA | 0 | NA | 0 | NA | 11 | -15.4 | 10.7 | 0.0519 | 52.0 | 26.1 | -9.9 | 4.9 | -2.3 | -1.5 | -1.9 |
| 5 | 1500M,50mD,Tinj50,Q100,S-4,Kvh1 | 15 | 25 | 0 | NA | 0 | NA | 23 | 11.0 | 66.4 | 0.0317 | 61.6 | 28.0 | -3.3 | 2.0 | -4.3 | -0.6 | -0.6 |
| 6 | 1400MM,50mD,Tinj50,Q40,S-4,Kvh1 | 0 | NA | 0 | NA | 0 | NA | 6 | -20.6 | 1.8 | 0.0647 | 45.7 | 19.8 | -16.4 | 7.9 | -2.9 | -2.4 | -3.0 |
| 7 | 1400MM,50mD,Tinj50,Q50,S-4,Kvh1 | 0 | NA | 0 | NA | 0 | NA | 12 | -14.7 | 12.4 | 0.0511 | 54.0 | 23.4 | -10.3 | 4.2 | -2.3 | -1.1 | -3.1 |
| 8 | 1400MM,50mD,Tinj50,Q100,S-4,Kvh1 | 10 | 30 | 3 | 37 | 0 | NA | 24 | 11.4 | 67.7 | 0.0314 | 62.7 | 27.5 | -3.0 | 2.0 | -2.7 | -0.6 | -1.0 |
| 9 | 1500M,500mD,Tinj50,Q20,S-4,Kvh1 | 0 | NA | 0 | NA | 0 | NA | 6 | -31.3 | 0.0 | 0.1824 | 8.3 | 4.6 | -45.4 | 22.6 | -0.5 | -8.1 | -8.5 |
| 10 | 1500M,500mD,Tinj50,Q40,S-4,Kvh1 | 0 | NA | 0 | NA | 10 | 30 | 6 | -20.5 | 2.1 | 0.0645 | 45.5 | 20.3 | -15.4 | 9.1 | -2.0 | -3.2 | -3.1 |
| 11 | 1500M,500mD,Tinj50,Q50,S-4,Kvh1 | 0 | NA | 0 | NA | 0 | NA | 11 | -15.2 | 10.6 | 0.0512 | 52.4 | 23.6 | -9.8 | 5.2 | -2.4 | -2.4 | -2.7 |
| 12 | 1500M,500mD,Tinj50,Q70,S-4,Kvh1 | 1 | 39 | 0 | NA | 0 | NA | 22 | -3.9 | 40.5 | 0.0388 | 56.7 | 28.9 | -5.5 | 2.3 | -3.0 | -0.7 | -1.4 |
| 13 | 1500M,500mD,Tinj50,Q100,S-4,Kvh1 | 12 | 28 | 0 | NA | 0 | NA | 24 | 10.8 | 67.3 | 0.0318 | 61.4 | 29.1 | -1.5 | 3.4 | -2.8 | -0.1 | -0.6 |
| 14 | 1500M,500mD,Tinj50,Q150,S-4,Kvh1 | 22 | 18 | 0 | NA | 4 | 35 | 21 | 33.7 | 82.4 | 0.0271 | 63.2 | 27.8 | -1.4 | 1.0 | -5.1 | -0.5 | -0.8 |
| 15 | 800MM,50mD,Tinj50,Q20,S-4,Kvh1 | 0 | NA | 0 | NA | 0 | NA | 6 | -30.7 | 0.0 | 0.1693 | 11.0 | 6.0 | -42.3 | 23.9 | -0.9 | -5.7 | -7.2 |
| 16 | 800MM,50mD,Tinj50,Q30,S-4,Kvh1 | 0 | NA | 0 | NA | 0 | NA | 6 | -25.2 | 0.0 | 0.0846 | 34.1 | 14.8 | -23.3 | 13.3 | -1.5 | -5.2 | -6.4 |
| 17 | 800MM,50mD,Tinj50,Q40,S-4,Kvh1 | 0 | NA | 0 | NA | 0 | NA | 11 | -18.7 | 2.8 | 0.0587 | 50.7 | 19.4 | -13.1 | 7.9 | -1.5 | -2.5 | -3.3 |
| 18 | 800MM,50mD,Tinj50,Q50,S-4,Kvh1 | 0 | NA | 0 | NA | 0 | NA | 25 | -12.1 | 16.7 | 0.0466 | 54.1 | 24.6 | -9.4 | 4.9 | -1.8 | -2.4 | -1.3 |
| 19 | 800MM,50mD,Tinj50,Q100,S-4,Kvh1 | 7 | 33 | 0 | NA | 0 | NA | 28 | 16.0 | 73.4 | 0.0293 | 61.6 | 29.9 | -2.3 | 0.6 | -2.2 | -0.5 | -1.0 |
| 20 | 800NF,50mD,Tinj50,Q20,S-4,Kvh1 | 0 | NA | 0 | NA | 0 | NA | 6 | -31.0 | 0.0 | 0.1765 | 12.0 | 5.5 | -40.7 | 23.5 | -0.7 | -7.8 | -8.0 |
| 21 | 800NF,50mD,Tinj50,Q30,S-4,Kvh1 | 0 | NA | 0 | NA | 0 | NA | 6 | -25.5 | 0.0 | 0.0887 | 34.2 | 15.4 | -25.1 | 12.2 | -1.7 | -5.4 | -4.1 |
| 22 | 800NF,50mD,Tinj50,Q40,S-4,Kvh1 | 0 | NA | 0 | NA | 0 | NA | 8 | -19.9 | 2.4 | 0.0615 | 49.4 | 20.8 | -12.0 | 9.0 | -1.3 | -3.5 | -3.2 |
| 23 | 800NF,50mD,Tinj50,Q50,S-4,Kvh1 | 0 | NA | 0 | NA | 0 | NA | 19 | -13.7 | 13.7 | 0.0489 | 53.2 | 24.7 | -9.5 | 4.7 | -2.0 | -1.7 | -2.9 |
| 24 | 800NF,50mD,Tinj50,Q70,S-4,Kvh1 | 0 | NA | 0 | NA | 0 | NA | 28 | -1.9 | 45.3 | 0.0369 | 56.9 | 27.3 | -7.2 | 2.9 | -2.8 | -1.4 | -0.7 |
| 25 | 800NF,50mD,Tinj50,Q100,S-4,Kvh1 | 0 | NA | 0 | NA | 0 | NA | 26 | 14.5 | 71.8 | 0.0301 | 61.5 | 28.8 | -2.9 | 0.8 | -2.9 | -0.8 | -1.0 |
| 26 | 800NF,50mD,Tinj50,Q150,S-4,Kvh1 | 11 | 29 | 11 | 29 | 0 | NA | 21 | 35.6 | 84.7 | 0.0266 | 66.3 | 28.6 | -1.0 | 0.4 | -2.9 | -0.2 | -0.3 |
| 27 | 800NF,5mD,Tinj50,Q20,S-4,Kvh1 | 0 | NA | 0 | NA | 0 | NA | 6 | -31.0 | 0.0 | 0.1786 | 8.8 | 3.9 | -43.1 | 25.2 | -0.4 | -8.0 | -8.5 |
| 28 | 800NF,5mD,Tinj50,Q30,S-4,Kvh1 | 0 | NA | 0 | NA | 0 | NA | 6 | -25.5 | 0.0 | 0.0884 | 32.6 | 13.1 | -23.4 | 17.4 | -1.2 | -4.7 | -4.9 |
| 29 | 800NF,5mD,Tinj50,Q40,S-4,Kvh1 | 0 | NA | 0 | NA | 0 | NA | 7 | -19.8 | 2.2 | 0.0620 | 45.7 | 21.0 | -15.4 | 6.8 | -1.3 | -3.3 | -4.3 |
| 30 | 800NF,5mD,Tinj50,Q50,S-4,Kvh1 | 0 | NA | 0 | NA | 0 | NA | 17 | -14.2 | 13.6 | 0.0493 | 50.8 | 23.6 | -11.0 | 6.1 | -2.7 | -2.3 | -2.4 |
| 31 | 800NF,5mD,Tinj50,Q70,S-4,Kvh1 | 0 | NA | 0 | NA | 0 | NA | 26 | -2.8 | 42.3 | 0.0375 | 60.0 | 25.2 | -4.7 | 3.2 | -3.8 | -1.5 | -1.0 |
| 32 | 800NF,5mD,Tinj50,Q100,S-4,Kvh1 | 0 | NA | 6 | 34 | 0 | NA | 25 | 12.6 | 69.5 | 0.0365 | 62.4 | 29.3 | -1.8 | 1.0 | -3.5 | -0.6 | -0.6 |
| 33 | 800NF,5mD,Tinj50,Q150,S-4,Kvh1 | 11 | 29 | 17 | 23 | 0 | NA | 20 | 33.1 | 82.8 | 0.0274 | 63.9 | 29.5 | -0.9 | 1.5 | -3.4 | -0.2 | -0.4 |
| 34 | 800F,50mD,Tinj50,Q20,S-4,Kvh1 | 1 | 0 | 0 | NA | 0 | NA | 6 | -31.4 | 0.0 | 0.1847 | 10.7 | 4.6 | -43.1 | 22.4 | -1.1 | -8.7 | -7.1 |
| 35 | 800F,50mD,Tinj50,Q30,S-4,Kvh1 | 1 | 0 | 0 | NA | 0 | NA | 6 | -26.1 | 0.0 | 0.0985 | 32.2 | 14.6 | -25.1 | 13.0 | -2.0 | -4.7 | -6.0 |
| 36 | 800F,50mD,Tinj50,Q40,S-4,Kvh1 | 1 | 0 | 0 | NA | 0 | NA | 6 | -20.6 | 1.7 | 0.0648 | 47.2 | 19.9 | -11.9 | 9.4 | -2.0 | -3.7 | -3.1 |
| 37 | 800F,50mD,Tinj50,Q50,S-4,Kvh1 | 1 | 0 | 7 | 33 | 0 | NA | 11 | -15.1 | 11.6 | 0.0515 | 52.0 | 22.8 | -13.4 | 3.7 | -2.5 | -2.0 | -2.1 |
| 38 | 800F,50mD,Tinj50,Q70,S-4,Kvh1 | 1 | 0 | 15 | 25 | 0 | NA | 22 | -4.2 | 39.8 | 0.0388 | 57.2 | 28.4 | -6.1 | 2.9 | -2.7 | -1.2 | -0.8 |
| 39 | 800F,50mD,Tinj50,Q100,S-4,Kvh1 | 1 | 0 | 21 | 19 | 0 | NA | 23 | 10.6 | 66.7 | 0.0317 | 64.0 | 26.9 | -2.5 | 2.1 | -3.1 | -0.7 | -0.2 |
| 40 | 800F,50mD,Tinj50,Q150,S-4,Kvh1 | 1 | 0 | 26 | 14 | 0 | NA | 19 | 31.8 | 81.3 | 0.0279 | 63.0 | 28.9 | -1.4 | 0.8 | -5.0 | -0.2 | -0.5 |
| 41 | 800F,5mD,Tinj50,Q20,S-4,Kvh1 | 1 | 0 | 0 | NA | 0 | NA | 6 | -31.2 | 0.0 | 0.1866 | 10.1 | 4.1 | -44.9 | 24.1 | -0.2 | -5.2 | -9.1 |
| 42 | 800F,5mD,Tinj50,Q30,S-4,Kvh1 | 1 | 0 | 10 | 30 | 0 | NA | 6 | -26.5 | 0.0 | 0.1377 | 32.5 | 15.1 | -27.4 | 11.5 | -0.8 | -3.5 | -6.5 |
| 43 | 800F,5mD,Tinj50,Q40,S-4,Kvh1 | 1 | 0 | 16 | 24 | 0 | NA | 6 | -21.2 | 1.5 | 0.0676 | 42.9 | 22.2 | -15.3 | 8.2 | -3.4 | -2.9 | -2.4 |
| 44 | 800F,5mD,Tinj50,Q50,S-4,Kvh1 | 1 | 0 | 21 | 19 | 0 | NA | 8 | -16.2 | 9.6 | 0.0540 | 51.0 | 22.8 | 9.8 | 6.4 | -4.0 | -1.9 | -2.4 |
| 45 | 800F,5mD,Tinj50,Q70,S-4,Kvh1 | 1 | 0 | 28 | 12 | 0 | NA | 15 | -7.1 | 32.8 | 0.0417 | 56.1 | 25.8 | -6.9 | 3.5 | -4.3 | -1.7 | -1.2 |
| 46 | 800F,5mD,Tinj50,Q100,S-4,Kvh1 | 1 | 0 | 33 | 7 | 0 | NA | 16 | 5.8 | 58.1 | 0.0351 | 61.7 | 26.9 | -3.1 | 0.9 | -6.2 | -0.9 | 0.0 |
| 47 | 800F,5mD,Tinj50,Q150,S-4,Kvh1 | 1 | 0 | 38 | 2 | 0 | NA | 13 | 20.7 | 72.7 | 0.0329 | 62.3 | 27.1 | -1.0 | 1.1 | -7.8 | -0.5 | -0.2 |

# Imprint

| | |
|---|---|
| Project Lead | GFZ German Research Centre for Geosciences<br>Telegrafenberg<br>14473 Potsdam (Germany)<br>www.gfz-potsdam.de/en/home/ |
| Project Coordinator | Prof. Ernst Huenges<br>huenges@gfz-potsdam.de<br>+49 (0)331/288-1440 |
| Project Manager | Dr. Justyna Ellis<br>ellis@gfz-potsdam.de<br>+49 (0)331/288-1526 |
| Project Website | www.destress-H2020.eu |



## Liability claim



## DESTRESS is co-funded by

National Research Foundation of Korea (NRF)
Korea Institute for Advancement of Technology (KIAT)
Swiss State Secretariat for Education, Research and Innovation (SERI)